Cell biology of cone photoreceptors in the degenerating retina: damage, recovery and rod-dependence

Vicki Chrysostomou

March 2009

A thesis submitted for the degree of Doctor of Philosophy of The Australian National University

I declare that the material contained in this thesis is original and my own work, except where acknowledged in the text, and the material has not been submitted, either in whole or in part, for a degree at this or any other educational institution.

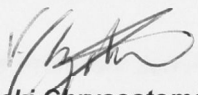

Vicki Chrysostomou

March 2009

Acknowledgements

I would like to express my sincere gratitude to Professor Jonathan Stone, with who it has been a privilege to work with over the past three years. I have progressed immensely as a scientist, and as a person, by watching him at his craft. I have learnt from him how to walk, talk and think like a scientist, and most importantly, how to do so whilst displaying patience, respect and compassion.

I also wish to express my deep appreciation to Dr Krisztina Valter for the selfless donation of her time and resources. She has offered me continual support from the first moment of my research life, which has allowed me unlimited freedom and opportunity in my academic pursuits.

I am indebted to Dr Sally Stowe for the investment of her time in the cone recovery project. Her microscopy and tissue processing expertise, and her assistance with the preparation of the first manuscript, were invaluable.

I am grateful to Dr Nigel Barnett for his assistance in establishing the cone electroretinogram recording protocols.

I am thankful for the sage guidance of Professor Jan Provis, Dr Keely Bumsted O'Brien and Dr Lauren Marotte.

I wish to acknowledge the superior illustrating advice of Sharyn Wragg.

My appreciation extends to the RSBS Plant and Animal Culture staff, particularly Kelly Debono, Lee Philip and Vanessa Barn, for their diligent animal care.

I would like to thank the numerous student colleagues who have shared the PhD journey alongside me. I am especially grateful to Riccardo Natoli, Peter Kozulin, Yuan Zhu, Diana Kirk, Wiebke Ebeling and Ryan Taylor for all the entertainment and camaraderie, both inside and outside of the lab.

Additionally, I wish to give thanks to Gordy Kelly, Rod Horan and all the CIRC regulars for providing friendship, beta and walls, night after night.

Special thanks to Arrin Daley for the ongoing companionship and belay. Our vertical pursuits, above and below ground, over the past three years have been an absolute highlight and have allowed me to approach the scientific workload each week with perspective and a fresh mind.

Lastly, I wish to thank my family; extended and immediate. The few words here cannot possibly do them service. I can only say, again, that I feel grateful every day to have them by my side, showing me unconditional love and support. In particular, I wish to express eternal gratitude to my parents, Anna and Tom Chrysostomou, for their unwavering devotion.

Contents

Abstract

Cone photoreceptors are the light receptive cells of the retina responsible for colour and high acuity vision in daylight. The loss of cone cells and the subsequent deterioration of cone-based vision is a feature of virtually all forms of retinal degeneration even though many causative mutations are in rod-specific genes. The involvement of cone cells in the degenerative process remains a puzzling and poorly understood aspect of retinal disease. This thesis examines the cell biology of cone photoreceptors in the degenerating retina. Observations were made in a transgenic rat model that manifests progressive retinal degeneration similar to that in human autosomal dominant retinitis pigmentosa. Through the use of immunohistochemistry, electron microscopy and electrophysiology, the morphology, function and survival of cones during the course of mutation-driven rod degeneration was assessed. In addition, the modulating effect of light on cone survival and integrity was investigated. Evidence is presented that the stability of cone cells in the degenerative retina is closely linked to the rate of rod damage and death, and that cones have the capacity to self-repair after damage.

CHAPTER 1

Literature Review

1.1 INTRODUCTION

The photoreceptor is a highly specialised and differentiated neuron of the central nervous system, capable of detecting and signalling photons of light. The outcome of this signalling is the perception of vision, the primary sensory system in humans. The structure of the photoreceptor has been conserved throughout the evolution of vertebrates and suggests that they are phylogenically related to the ciliated ependymal cells that line the brain ventricles (Cohen, 1972). Photoreceptors are distinguished morphologically as either rods or cones, but both classes are bipolar cells with photosensitive pigments embedded in a modified cilium (Figure 1.1). As a post-mitotic cell, the photoreceptor does not undergo cell division in the mature retina. Although regeneration of retinal cells in vertebrates is now being acknowledged (Coulombre and Coulombre, 1965; Zhao et al., 1997; Fischer, 2005), photoreceptors are generally considered as irreplaceable, and their death correlates closely with the deterioration of vision. Photoreceptors slowly die throughout the lifetime of an organism as a normal part of the aging process (Gao and Hollyfield, 1992; Curcio et al., 1993; Panda-Jonas et al., 1995). However, in retinal disease, the rate of photoreceptor loss is dramatically accelerated and often culminates in blindness. Physiological and histological investigations of photoreceptor cells, such as those presented in this thesis, allow for an understanding of the function and stability of the photoreceptor and of events involved in their degeneration during disease. Before considering these investigations, it is necessary to review the structure and function of the photoreceptor, and the features of retinal disease.

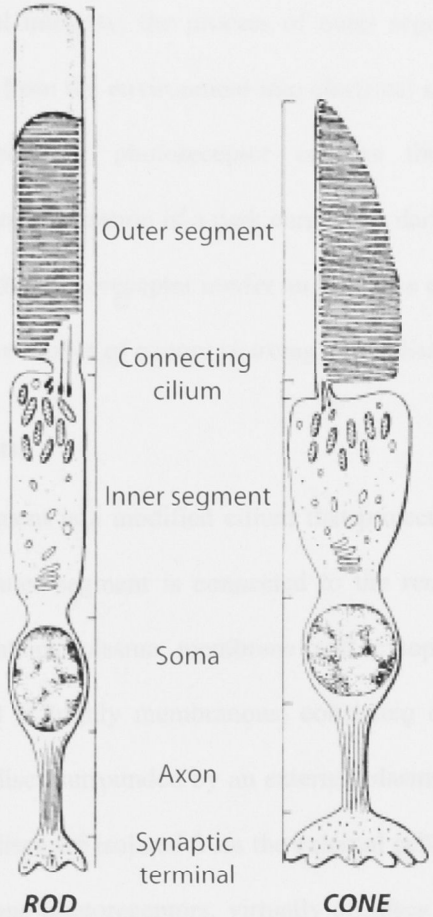

Figure 1.1 Rod and cone photoreceptors consist of six principle regions: an **outer segment** that contains stacks of membranous discs embedded with visual pigments, a narrow **connecting cilium** that contains microtubules and joins the outer segment to the inner segment, an **inner segment** that contains biosynthetic and metabolic machinery, a **soma** that contains the nucleus, an **axon** that extends to the synaptic end of the cell, and a **synaptic terminal** that contains synaptic vesicles filled with neurotransmitter and that makes contact with second order neurons. *Adapted from Lolley and Lee, 1990.*

1.2 SPECIALISATIONS OF THE PHOTORECEPTOR

To fulfil its role as a primary visual cell, the photoreceptor has evolved unique structural and biochemical specialisations. These include the presence of a cell structure capable of absorbing photons of light; the distinctive photoreceptor outer segment. The presence of such a specialised structure demands an equally specialised method of maintaining its morphological and functional integrity; the process of outer segment renewal. Finally, in order to convert light signals from the environment into electrical signals that can be read by the central nervous system, the photoreceptor couples the unique processes of phototransduction (in light) and generation of a dark current (in darkness). The structural and functional specialisations of the photoreceptor confer an immense energy burden on the cell, forcing the need for distinctive modes of energy sourcing and utilisation.

1.2.1 The Outer Segment

The photoreceptor outer segment is a modified cilium that projects from the apical face of the cell (Figure 1.1). The outer segment is connected to the remainder of the cell via a narrow cilium, which maintains plasma membrane and cytoplasmic continuity. Each photoreceptor outer segment is highly membranous, consisting of stacks of hundreds of flattened double-membrane discs surrounded by an external plasma membrane (Figure 1.2). In rod photoreceptors, most discs are isolated from the external cell membrane and thus from the extracellular space. In cone photoreceptors, virtually all discs retain connections to the external cell membrane and thus retain continuity with the extracellular space. The outer segment is the region of the photoreceptor that is specialised for light absorption and transduction (phototransduction). As such, there is a high concentration of enzymes, signalling proteins and light-absorbing visual pigments embedded in the phospholipid bilayer of outer segment discs and aligned along the axis of incoming light.

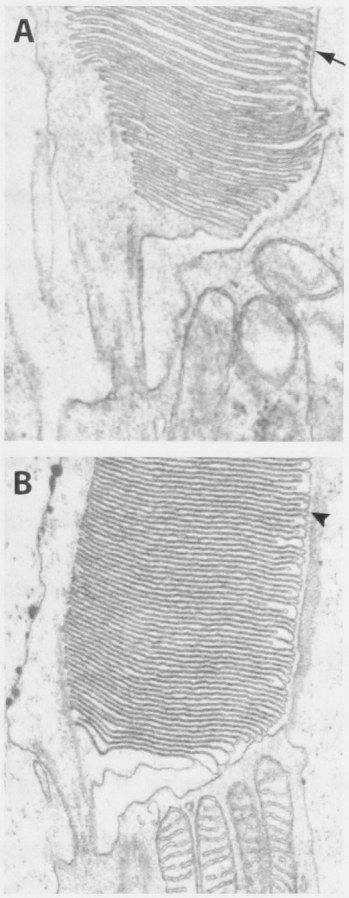

Figure 1.2 The outer segment of rod and cone photoreceptors consists of a stack of membranous discs formed by infolding of the plasma membrane. In rods (**A**) the discs are isolated from the external plasma membrane (*arrow*) while in cones (**B**) the discs remain attached to the external plasma membrane (*arrow head*). Transmission electron micrographs in **A** and **B** show the cilial bases of the outer segments of rhesus monkey rods and cones. *Adapted from Young, 1971.*

1.2.2 Outer Segment Renewal

The photoreceptor outer segment is a dynamic structure that undergoes a constant renewal process. In 1967, Young first described outer segment turnover in the rat by radiolabeling amino acids and watching them "migrate" over time from the basal region of the outer segment to the distal tip, and then disappear. It is now well established that outer segment discs are shed at the distal end and phagocytised by adjacent retinal pigment epithelial (RPE) cells, while nascent disc membrane is synthesised and added at the cilial base. Both rod and cone photoreceptors shed their outer segment discs, though the process is much better understood for rods. It has been shown that rod outer segment renewal is daily and circadian; there is increased shedding after the onset of light and reduced shedding in the dark (Goldman et al., 1980; LaVail, 1980). Complete renewal of a mammalian rod outer segment takes approximately ten days. During the renewal process, disc membrane proteins are continuously replaced but phospholipids are retained by RPE cells and transported back to the inner segment for incorporation into new discs.

To maintain a constant outer segment length, the rate of disc shedding must be matched by disc synthesis. However, it has been shown that disc shedding and synthesis can be independently regulated (LaVail, 1973; Schremser and Williams, 1995), allowing the photoreceptor to alter its outer segment length. This effect is well described in relation to changes in the light environment, where photoreceptors change the length, and thus the rhodopsin content, of their outer segment in order to absorb a constant number of photons per day (Penn and Williams, 1986; Williams et al., 1999). This phenomenon is termed photostasis and is thought to have evolved in response to seasonal variations in daytime light intensity and duration.

The reason for continuous shedding and resynthesis of photoreceptor outer segment discs is unclear but it may be a protective measure against the damaging effects of relentless radiation exposure (Young, 1982), similar to the way in which aged and damaged epithelial

cells of the epidermis or the digestive tract are constantly sloughed and renewed. It has also been suggested that disc renewal may serve as a surrogate antioxidant for glutathione, an important cellular reductant that is absent from the photoreceptor outer segment (Winkler, 2008).

1.2.3 Phototransduction

Phototransduction refers to the sequence of events triggered within photoreceptor cells following the absorption of light. Ultimately, the process leads to modulation of ion channels in the plasma membrane and a change in membrane potential that mediates neurotransmitter release at the synaptic terminal of the photoreceptor. Phototransduction is initiated when visual pigments embedded in the outer segment discs of rods and cones absorb photons of light. All known vertebrate visual pigments consist of an apo-protein, opsin, to which the light-absorbing molecule retinal, the aldehyde form of vitamin A, is attached. Differences in the amino acid sequence of the opsin protein confer different spectral sensitivities of rods and cones (Nathans et al., 1986; Neitz et al., 1991).

Pioneering experiments by Wald and colleagues (1969) showed that the absorption of light by retinal causes a conformational change in the chromophore, from its 11-*cis* to all-*trans* configuration, that subsequently induces a conformational change in opsin. This triggers an amplifying cascade of biochemical events in the outer segment that is well established for rods, but poorly understood for cones (reviewed in Baylor, 1996; Arshavsky et al., 2002; Chen, 2005). Briefly, activated visual pigment stimulates the G-protein transducin, which in turn activates cyclic guanosine monophosphate (cGMP) phosphodiesterase (PDE) and causes the hydrolysis of cGMP to 5'-GMP. The decrease in intracellular cGMP results in the closure of cGMP-gated channels, thereby reducing the influx of sodium ions (Na^+) through these channels and causing the photoreceptor to hyperpolarise. Hyperpolarisation inhibits the release of glutamate at the photoreceptor synapse, thereby completing the conversion of the initial light signal into a neurochemical

event that can be relayed to second order retinal neurons and eventually to the brain. Following excitation by a photon of light, the photoreceptor returns to its dark state through a series of reactions involving inactivation of the visual pigment and other protein components of the visual cascade, and resynthesis of cGMP.

1.2.4 The Dark Current

In darkness, a steady circulating current known as the dark current flows through the photoreceptor cell. The inward component of the dark current enters the photoreceptor outer segment through cGMP-gated channels, kept open in darkness by the binding of cGMP on the cytoplasmic side of the channel. The inward current is carried mainly by Na^+, though calcium and magnesium ions are also involved (Yau and Nakatani, 1984). The outward current is carried largely by potassium ions (K^+) flowing through K^+-selective non-gated channels in the photoreceptor inner segment. Under these conditions, the cell is in a depolarised state and there is constant release of glutamate from the synaptic terminal. Driving the dark current are high densities of ATP-dependent Na^+-K^+ pumps in the photoreceptor inner segment that pump Na^+ out of the cell and K^+ in.

1.2.5 Energy Sourcing

The structural and biochemical specialisations of photoreceptor cells, which subserve their central role in visual signalling, demand a substantial investment of metabolic energy. Maintenance of the dark current requires continuous transport of Na^+ across the photoreceptor inner segment via ATP-dependent Na^+-K^+ pumps. It is estimated that 33% of the retina's total energy consumption is dedicated to this task (Ames et al., 1992). Substantial energy is also required to synthesise the high-energy phosphate bonds involved in the rapid turnover of cGMP as part of the phototransduction cascade. Outer segment renewal, which involves constant shedding and rebuilding of membranous discs, also places a substantial metabolic load on the photoreceptor cell (Ames et al., 1992; Demontis et al., 1997). In

mammals, the complete renewal of rod outer segments every ten days implies that each photoreceptor must synthesise and assemble approximately100 discs per day.

1.2.5.1 The high metabolic activity of photoreceptors

Like other neurons of the central nervous system, photoreceptors use ATP as their energy source, which is generated principally from the catalysis of glucose (Winkler, 1995). Photoreceptors have the ability to metabolise glucose anaerobically via glycolysis or aerobically via oxidative phosphorylation. As predicted by the high energy cost of their specialisations, photoreceptors have much greater glycolytic and oxidative rates than any other retinal neuron. This effect was first shown by Graymore (1959) who measured a doubling of glycolytic and respiratory activity in the isolated rat retina at the time of final photoreceptor differentiation and the onset of photoreceptor function. In support of this work, animals with hereditary or chemically-induced retinal degenerations, in which the photoreceptor population is absent, display a glyoclytic and oxidative rate that is less than half of the normal retina (Graymore and Tansley, 1959; Hopkinson and Kerly, 1959; Graymore, 1960). Furthermore, work with oxygen microelectrodes has shown that photoreceptors consume three to four times more oxygen than any other neuron in the central nervous system (Alder et al., 1990; Braun et al., 1995).

The site of this remarkably high oxidative activity is the photoreceptor inner segment, where dense aggregates of mitochondria almost fill the apical region (Figure 1.3). Intraretinal oxygen profiles show that there is a deep trough in the oxygen partial pressure at the level of the photoreceptor inner segment (Ahmed et al., 1993; Yu et al., 1994; Yu and Cringle, 2001) and mathematical models of intraretinal oxygen consumption confirm that oxygen consumption is dominant at the photoreceptor inner segment (Cringle and Yu, 2002).

1.2.5.2 The ability to switch modes of energy production

A unique interrelationship exists between glycolytic and oxidative metabolism in the retina. Photoreceptors have the ability to upregulate aerobic metabolism in the face of

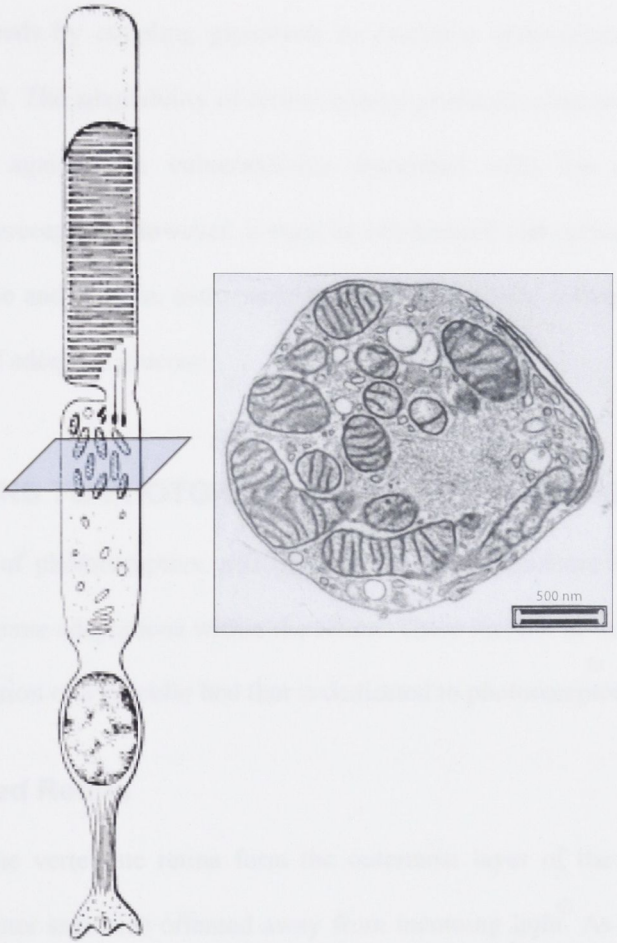

Figure 1.3 The photoreceptor inner segment is a locus of respiratory activity, containing a high concentration of mitochondria and respiratory enzymes. Inset: transmission electron micrograph of a cross-section of a rod inner segment showing dense aggregates of mitochondria. *Adapted from Lolley and Lee, 1990; Drechsler et al., 1987.*

hypoglycaemia or anaerobic metabolism in the face of hypoxia, allowing the cell to maintain a constant stream of energy under adverse conditions. In the absence of oxygen and presence of glucose, the retina can produce 75% of its ATP needs by upregulating glycolysis. Conversely, in the presence of minimal glucose but plentiful oxygen, the retina can produce 85% of its ATP needs by coupling glycolysis to oxidative metabolism (Winkler, 1995; Winkler et al., 1997). The adaptability of retinal energy production has no doubt evolved to provide protection against the vulnerabilities associated with the enormous energy requirement of photoreceptors. However, it must be emphasised that optimal retinal function requires both glucose and oxygen, and conservation of ATP levels during hypoxia depends on the availability of adequate glucose.

1.3 ADAPTATIONS TO PHOTORECEPTOR SPECIALISATIONS

The specialisations of photoreceptors, and the high energy expenditure that they demand, have resulted in extreme adaptations within the retina. These include inversion of the retinal tissue, and the evolution of a vascular bed that is dedicated to photoreceptors.

1.3.1 The Inverted Retina

Photoreceptors of the vertebrate retina form the outermost layer of the tissue, with their sensory ends (the outer segment) oriented away from incoming light. As a consequence of this counterintuitive design, light must pass through all layers of the retina before being captured by the light-receptive outer segment. In biological terms, the vertebrate retina is therefore said to be inverted. This arrangement creates the potential for distortion of the light signal as it passes through the inner retinal layers, and also results in a blind spot in the visual field where ganglion cell axons create a hole in the photoreceptor array in order to exit the retina via the optic nerve. The question arises; what necessitated the evolution of such an unusual design? It can be argued that inversion of the vertebrate retina is an adaptation to the

specialisations of photoreceptors, in particular the structure and function of their outer segments and their very high energy demands.

Fundamental to the inverted retina design is the apposition of photoreceptor outer segments to the RPE. Each RPE cell is in intimate physical contact with multiple photoreceptor outer segments, and there also exists a tight biochemical link. After the absorption of light during phototransduction (Section 1.2.3), visual pigment in the photoreceptor outer segment must be regenerated. Photoreceptors themselves are unable to reisomerise all-*trans* retinal back into 11-*cis* retinal; this task is performed by cells of the RPE (Steinberg, 1985, 1987). Another specialisation of photoreceptors, the shedding of outer segment discs (Section 1.2.2), depends on RPE cells to detect and digest shed outer segment discs, and to recycle essential disc components back to the photoreceptor inner segment. The importance of this task is highlighted in the RCS rat, in which a mutation in an RPE-specific gene renders cells unable to phagocytise shed photoreceptor discs and results in progressive degeneration of photoreceptors (Dowling and Sidman, 1962). Finally, inversion of the retina can be seen as an adaptation to the very high energy demands of photoreceptors (Section 1.2.5.1) as it allows for the presence of a unique nutrient delivery system; the choroid discussed below.

1.3.2 The Choroidal Circulation

To meet their high rates of metabolism, photoreceptors require a continuous supply of glucose and oxygen in large quantities. In the vascular retina of the human, rodent and most other mammals, nutrients are delivered by two circulations; the retinal vasculature and the choroidal vasculature (Figure 1.4). The retinal vasculature originates from the central retinal artery, a branch of the ophthalmic artery, which enters the optic nerve head and divides to form two layers of flat capillary networks that perfuse the inner retinal layers. One capillary network lies adjacent to the ganglion cell layer (the superficial bed) and the second lies at the level of the outer plexiform layer (the deep bed).

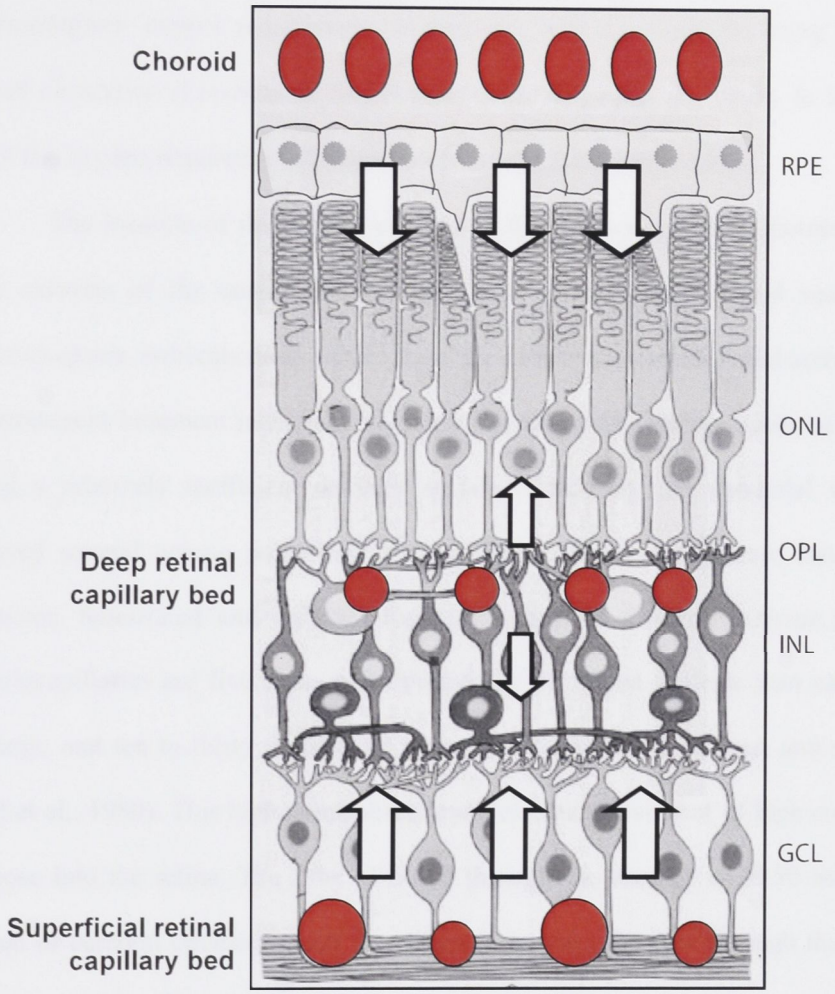

Figure 1.4 Nutrients are delivered to the mammalian retina by two circulations. The outer retina is supplied by vessels of the choroid, which are located external to the RPE. The inner retina is supplied by the retinal vasculature, which forms a deep capillary bed at the OPL and a superficial capillary bed adjacent to the GCL. The *red circles* represent capillaries and the *open arrows* represent the direction of nutirent diffusion from the capillaries. RPE: retinal pigmented epithelium. ONL: outer nuclear layer. OPL: outer plexiform layer. INL: inner nuclear layer. GCL: ganglion cell layer. *Adapted from Bentmann et al., 2005.*

Presumably to prevent the formation of shadows on the light-receptive outer segments, blood vessels are entirely absent from the outer half of the retina. The outer retina, containing the photoreceptor layer, is nourished almost entirely by the choroid, a rich vascular bed located external to the RPE. The choroidal circulation provides 90% of the photoreceptors' oxygen requirements in darkness, with the remainder being supplied by the retinal circulation (Linsenmeier and Braun, 1992; Ahmed et al., 1993). In light conditions, all of the oxygen required by photoreceptors is supplied by the choroid.

The location of the choroid external to the retina means that photoreceptors are the only neurons of the central nervous system to lack intrinsic blood vessels. To reach photoreceptors, nutrients must diffuse from the choroidal circulation and across the RPE and its prominent basement membrane. To meet the substantial energy needs of photoreceptors using a relatively inefficient delivery system (diffusion), the choroidal vasculature has evolved several unique properties. The capillaries of the choroid are unusually large in diameter, fenestrated and crowded together with little connective tissue between them. Choriocapillaries are five times more permeable to plasma proteins than capillaries of the kidneys, and ten to thirty times more permeable than vessels in heart and skeletal muscle (Bill et al., 1980). This high permeability enables rapid movement of high concentrations of glucose into the retina. The flow of blood through the choroid is 40-50 times that of the retinal or cerebral circulation and four times faster than the flow through the kidneys (Alm and Bill, 1972). This arrangement means that the diffusion of nutrients to photoreceptors begins from blood containing near arterial levels of nutrients.

The external location of the choroid and its remarkably high rate of blood flow, the very properties that have evolved to serve the demands of the photoreceptor, also represent a substantial design fault. Because choroidal vessels are physically separated from the cells that they serve, the supply of blood from these vessels remains independent of the photoreceptors' needs (Bill and Sperber, 1990). The inability of choroidal vessels to "autoregulate" in response to local metabolic factors is evidenced by sharp changes in outer

retinal oxygen tension in response to light-dark transitions. In light, when photoreceptor oxygen consumption falls, oxygen tension in the outer retina rises by up to 30 mmHg (Linsenmeier, 1986; Cringle and Yu, 2002), reflecting an unregulated flow of oxygen from the choroid. It is argued that failure of the choroid to autoregulate may contribute to the progression of a range of retinal diseases (Section 1.5.2.3).

1.4 VULNERABILITIES OF THE PHOTORECEPTOR

The previous sections examined the unique design and behaviour of the photoreceptor cell, and the organisation of retinal tissue. The price of the photoreceptors' distinct specialisations is a fragility not seen in any other neuron of the central nervous system. Photoreceptors are exquisitely sensitive to environmental damage, particularly by light, the very stimulus they are built to detect, and by oxygen, the nutrient they depend on for their survival. Above a certain threshold, light causes shortening and disorganisation of photoreceptor outer segments, impairment of photoreceptor function and photoreceptor cell death (Noell et al., 1966). Changes in the local oxygen concentration, either elevations or reductions, are similarly devastating to the photoreceptor, inducing structural and functional damage and cell death (Noell, 1955; Yamada et al., 1999; Wellard et al., 2005). Here, focus is given to the sensitivity of photoreceptors to genetic insults; small changes to the DNA sequence of genes that cause the degeneration of photoreceptors and the blinding group of diseases known as retinitis pigmentosa (RP). The following section considers the roles of genes and the environment in RP, the mechanisms of rod and cone survival during the course of the disease, and the current status of therapeutic interventions.

1.5 RETINITIS PIGMENTOSA

The term retinitis pigmentosa describes a large and diverse group of usually hereditary retinal diseases that cause progressive degeneration of photoreceptors. RP has a prevalence

of 1:4000, affecting an estimated 1.5 million people worldwide, and is the leading cause of inherited blindness in the developed world (Berson, 1993). The first symptoms of RP, usually noted in adolescence, are typically impaired adaptation, night blindness and difficulty with mid-peripheral visual fields (Berson, 1993; Kremmer et al., 1997). With further disease progression, there is a tendency to blue blindness, loss of far-peripheral visual fields and eventually, deterioration of central vision resulting in complete blindness (Berson, 1993). Some RP patients become blind as early as 30 years of age; the majority are legally blind by 60.

1.5.1 Genetics

RP is a heterogeneous disease, because of the wide range of genetic mutations known to cause photoreceptor degeneration (the core pathology of RP), and the large proportion of cases for which there is no family history. In the familial forms, the condition may be transmitted in autosomal dominant, autosomal recessive or X-linked hereditary patterns, and can also occur in syndromes such as Ushers, which involves sensorineural deafness and vestibular dysfunction, and Bardet-Biedl, which involves obesity and mental retardation. In addition, 50% of RP cases are classed as simplex, occurring without predictable Mendelian patterns of inheritance or without any family history of the disease (Jay, 1982; Haim, 1993).

At present, 30 different genes have been linked to RP; 15 in autosomal dominant RP, 13 in autosomal recessive RP, two in X-linked RP, nine in Usher syndrome, 12 in Bardet-Biedl syndrome, and 12 disease loci have been mapped (but not yet identified) for RP or syndromes incorporating RP (www.sph.uth.tmc.edu/Retnet/disease.htm). Both photoreceptor-specific genes and genes expressed in adjacent RPE cells are associated with RP, and there is great diversity in the function and location of the proteins that they encode. Affected proteins include enzymes of the phototransduction cascade (rhodopsin, transducin, arrestin, cGMP-dependent PDE), photoreceptor structural proteins (USH2A, RDS, EYS), transport proteins (TULP1, MYO7A, ABCA4), components of the retinoid cycle (CRALBP,

RPE65), transcription factors (RP31, NRL, RAX2, NR2E3), and enzymes involved in pre-mRNA splicing (RP9, PAP1) (www.sph.uth.tmc.edu/Retnet/disease.htm). Adding to the variety of RP forms, photoreceptor degeneration can be caused by many distinct mutations within a single gene.

Despite the immense genetic heterogeneity of RP, apoptosis of photoreceptors involving endonuclease-mediated DNA fragmentation is the final common pathway that links genotype to phenotype (Chang et al., 1993; Lolley et al., 1994; Portera-Cailliau et al., 1994; Tso et al., 1994). In many cases, the intervening steps from gene mutation to photoreceptor apoptosis remain unclear.

1.5.1.1 Rhodopsin mutations

The first genetic defect to be associated with any form of RP was a mutation in the rhodopsin gene, documented by Dryja and colleagues in 1990 (Dryja et al., 1990b). In a pedigree of patients with autosomal dominant RP, they discovered a substitution of the highly conserved proline at codon 23 with histidine, at the amino terminus of the rhodopsin protein. This mutation is now commonly known as the P23H mutation. Not only was this the first documented mutation in the rhodopsin gene, it was the first description of a mutation in any photoreceptor-specific gene. Since then, 88 different rhodopsin mutations have been linked to RP and account for 20-25% of all cases of autosomal dominant RP in Europe (Bunge et al., 1993), the United Kingdom (Inglehearn et al., 1992) and the USA (Dryja et al., 1990a; Sung et al., 1991). The mechanisms by which mutations in the rhodopsin gene lead to photoreceptor cell death are incompletely understood, although protein misfolding (Sung et al., 1991; Olsson et al., 1992; Roof et al., 1994; Illing et al., 2002) and defective targeting of the protein to the photoreceptor outer segment (Sung et al., 1991; Sung et al., 1994; Tam et al., 2000) have been suggested.

The P23H rhodopsin mutation that Dryja and colleagues first described in 1991 is now known to be the most common mutation associated with autosomal dominant RP in the

North American population (Dryja et al., 1991). Due to the high prevalence of this particular mutation, several P23H transgenic animals have been engineered as a model to study the human disease. In 1992, the first P23H transgenic mouse was developed (Olsson et al., 1992), which was later shown to display a retinal degeneration similar to that in humans with autosomal dominant RP (Naash et al., 1993; Goto et al., 1995). However, the small size of the mouse eye made surgical manipulations difficult and this led to the generation of a larger animal, the P23H transgenic rat (Lewin et al., 1998). The albino P23H rat carries a mutant mouse opsin gene as well as endogenous native opsin genes, and displays a pattern of photoreceptor degeneration common to human autosomal dominant RP (Lewin et al., 1998; Machida et al., 2000).

1.5.2 Cone-Rod Dependence

Many forms of RP display a rod-cone pattern of degeneration. Initially, rod photoreceptors are lost, causing the primary symptoms of night blindness and constriction of the peripheral visual field. As rod degeneration progresses, the viability of cone photoreceptors is compromised, resulting in the loss of day and high acuity vision, the overriding cause of blindness. Even though many of the mutations known to cause RP affect proteins expressed specifically in rods, secondary cone pathology is invariably observed. The progression of the disease suggests that cone survival depends on the presence of rods, and this idea is supported by animal experiments showing the loss of cones in retinas in which rods have been selectively eliminated (Carter-Dawson et al., 1978; Ogilvie et al., 1997). The mechanism of cone-rod dependence is not fully understood although several theories are commonly discussed.

1.5.2.1 Rod-derived protective factor

In 1998, Mohand-Said and colleagues used an in vitro model to search for rod-derived trophic factors that could influence cone survival (Mohand-Said et al., 1998). They found that culturing degenerative mouse retinas (rod-sparse and cone-rich) in the presence of

normal retinas (rod- and cone-rich) resulted in greater numbers of surviving cones compared to degenerative retinas that were cultured with rod-sparse tissue. This finding suggested the presence of a diffusible trophic factor released from retinas with rod cells that acts on retinas with cone cells. Using a similar organ culture technique, the same effect was reported by Streichert and colleagues (1999) who, in addition, found that the survival-promoting activity of cultured rod-rich retinas was diffusible through a filter, heat-labile, and not present in transgenic degenerative retinal cells.

Switching to an in vivo model, Mohand-Said's group performed subretinal transplants of normal mouse rods into degenerative mouse retinas, and found that this rescued cone cells in the recipient retina (Mohand-Said et al., 2000). These experiments did not distinguish between an effect induced by rods themselves and an effect due to interactions with other retinal cells, nor could they determine if cone rescue was due to a diffusible factor or structural protection from toxins. To address the former of these issues, the same group used expression cloning to identify and characterise a protein, which they named rod-derived cone viability factor, that is specifically expressed by photoreceptors and has the effect of rescuing cultured cones (Leveillard et al., 2004).

Despite recent interest in rod-derived protective factors, functional rescue of cones by such a substance has not yet been demonstrated. In addition, proof that a single trophic factor accounts entirely for cone death is lacking (see Punzo and Cepko, 2007). Studies show that a broad spectrum of neuroprotective factors, including CNTF, BNDF, Axokine and FGF-2 (Faktorovich et al., 1990; LaVail et al., 1998; Akimoto et al., 1999; Ali et al., 2000; Okoye et al., 2003), can prevent or delay photoreceptor death.

1.5.2.2 Rod-derived toxin

A second mechanism of cone-rod dependence also involves the release of a diffusible extracellular substance from rods. However, in this case, the factor is toxic to neighbouring cones. Potential toxic agents include the excitatory amino acids glutamate and aspartate

(Ulshafer et al., 1990), and products of apoptosis (Kedzierski et al., 1998), all of which have been detected in high concentrations in degenerating retinas. Rod-induced glutamate toxicity is unlikely to be a significant cause of cone cell death as Müller cells have a high-affinity glutamate uptake system that protects retinal cells from excitotoxicity (Sarantis and Attwell, 1990). Furthermore, several studies have shown that intravitreal injection of high concentrations of glutamate or glutamate analogues causes severe damage to inner retinal neurons but has little effect on photoreceptors (Lucas and Newhouse, 1957; Potts et al., 1960; Sisk and Kuwabara, 1985).

Ripps (2002) proposes an alternative intracellular, rather than extracellular, diffusion pathway in which endogenous intermediates of rod apoptosis pass through gap-junction channels to neighbouring cone cells. In this way, named the "bystander effect", it is suggested that the disease is spread from dying rod cells to healthy cone cells.

1.5.2.3 Oxygen toxicity

An alternative mechanism of cone-rod dependence has been proposed by Stone and colleagues (1999), who suggest an "oxygen toxicity hypothesis." They theorise that any substantial depletion of photoreceptors results in a hyperoxic outer retina because the death of photoreceptors (the major consumers of oxygen in the retina) significantly reduces oxygen consumption. The choroid continues to deliver the same quantity of oxygen due to its poor ability to autoregulate (Section 1.3.2) and as a consequence, the remaining photoreceptors are exposed to high levels of oxygen. It has long been known (Noell, 1955), and commonly reported (Yamada et al., 1999; Wellard et al., 2005; Geller et al., 2006; Natoli et al., 2008), that oxygen is directly and specifically toxic to photoreceptors. The oxygen toxicity hypothesis also establishes a reinforcing effect of hyperoxia on the remaining survivors, with the loss of some photoreceptors further reducing oxygen consumption and resulting in further accumulation of oxygen in the outer retina.

In support of the oxygen toxicity hypothesis, chronic elevation of oxygen tension in the outer retina has been detected in three different animal models of RP, all with different underlying genetic defects. First, the RCS rat, a model of autosomal recessive RP in which a naturally occurring genetic defect expressed in the RPE (MERTK gene) renders the pigmented cells unable to phagocytise shed photoreceptor outer segments (Yu et al., 2000). Second, the P23H-3 transgenic rat, a model of autosomal dominant RP in which there is a point mutation in the rhodopsin gene (Yu et al., 2004). Third, the Abyssinian cat, which has a hereditary retinal degeneration that follows a similar pattern to autosomal recessive RP in humans (Padnick-Silver et al., 2006). In all three of these animals, oxygen consumption is reduced and oxygen tension is elevated in the outer retina at a time when the photoreceptor population is depleted.

Further evidence that the photoreceptor-depleted retina is hyperoxic comes from observations of the retinal vasculature. In the late stages of human RP (Heckenlively, 1988) and in rodent models of RP (Penn et al., 2000), thinning of retinal vessels is seen. This indirectly suggests hyperoxia as oxygen regulates vasoactive factors and excess amounts of the gas are known to cause vasoconstriction. In addition, direct evidence of oxidative damage to cone DNA, proteins and lipids has been shown in the rod-depleted retina of the P23H transgenic pig (Shen et al., 2005).

Also of relevance is the curious finding by Arden (2001) of the absence of diabetic retinopathy in patients with RP. Arden searched worldwide for patients with both RP and diabetes mellitus and, once identified, collected comprehensive data on their ocular and diabetic state including the type of diabetes, degree of diabetic control, type of RP, age of diagnosis, and date of onset of night blindness and constriction of visual fields. The outcome of Arden's data analysis was impressive. Out of 75 diabetic patients with RP, there was a total absence of any signs of diabetic retinopathy such as microaneurysms, exudates or retinal haemorrhages, despite the presence of other diabetic complications in more than half the cohort. Arden interpreted his findings in terms of the retinal oxygen environment. As

retinal hypoxia is thought to be a major underlying cause of diabetic retinopathy (Lowitt et al., 1993; Harris et al., 1996; Hotta et al., 1997; Linsenmeier et al., 1998; Drasdo et al., 2002), Arden suggests that RP-induced retinal hyperoxia counters diabetes-induced hypoxia, thereby preventing the development of diabetic retinopathy.

1.5.2.4 Cone starvation

A novel mechanism of cone cell death in RP has recently been proposed based on observations by Punzo and colleagues (2009). The authors studied four different animal models of RP with defects in rod-specific genes; the P23H mouse, the rhodopsin knockout mouse, the PDE subunit-γ knockout mouse and the PDE subunit-β mutant mouse. An analysis of gene expression levels during the course of photoreceptor degeneration showed that the onset of cone death was accompanied by changes in genes involved with cellular metabolism. In addition, dying cones showed signs of autophagy, a form of cellular self-digestion. Collectively, these results suggest that cones in the RP retina suffer from a shortage of nutrients and prolonged starvation.

In addition, gene expression analyses by Punzo and colleagues showed that cone degeneration coincided with defects in the insulin/mTOR metabolic pathway, prompting the researchers to manipulate insulin levels in the mice. The outcome of these manipulations was prolonged cone survival in insulin-treated mice, and decreased cone survival in insulin-deficient mice. These results further support cell starvation as a possible cause of cone death in RP.

At present, the mechanisms that might lead to cone starvation in the degenerative retina remain speculative. The authors of this initial study suggest that substantial rod loss may disrupt interactions between cone cells and the RPE, leading to reduced flow of nutrients to cones. Given the strength and distinct nature of this initial work, it is likely that several studies in the near future will explore the concept of cone starvation in detail.

1.5.3 Light and Retinal Degenerations

It was first suggested over 100 years ago that light exposure might modify the course of disease in patients with retinal degeneration (Johnson, 1901 cited in; Berson, 1971). Since then, investigations into the effect of ambient light levels on the degenerative retina have occupied a considerable portion of the retinal degeneration field and today, light modulation remains one of only few potential therapies for RP patients.

In the last 20 years, the effects of light exposure on animal models of RP have been comprehensively assessed using a range of animals (mouse, rat, dog), with various underlying genetic defects (mutations, deletions, insertions, knockouts) and affected genes (rhodopsin, arrestin, peripherin, Mertk). These findings are summarised in Table 1.1 and while there are exceptions, the overwhelming pattern that has emerged from this body of work is that disease progression is accelerated by light and slowed by darkness.

1.5.3.1 Photopic and mesopic ambient light

While bright (photopic) light is well known to damage the normal retina, degenerative retinas are sensitive to even modest (mesopic) levels of illumination, which have no measurable effect on non-degenerative tissue (Walsh et al., 2004). The damaging effects of light on the degenerative retina include acceleration of photoreceptor apoptosis (Wang et al., 1997; Vaughan et al., 2003; Walsh et al., 2004; Jozwick et al., 2006), shortening and disorganisation of rod outer segments (Vaughan et al., 2003; Cideciyan et al., 2005; Jozwick et al., 2006), thinning of the outer nuclear layer (Vaughan et al., 2003; Walsh et al., 2004; Jozwick et al., 2006), upregulation of FGF-2 and GFAP expression (Walsh et al., 2004), reduction of ERG amplitudes (Kaitz and Auerbach, 1979a; Walsh et al., 2004; Jozwick et al., 2006), reduction in optokinetic head-tracking responses (Thomas et al., 2007), and loss of rhodopsin and retinal DNA content (Wang et al., 1997; Organisciak et al., 1999; Bicknell et al., 2002). The action spectrum of this light-induced damage follows the absorption curve of rhodopsin (Kaitz and Auerbach, 1979b).

Table 1.1 Effects of light exposure on animal models of retinal degeneration (adapted from Paskowitz et al. 2006).

Gene Product	Genetic Defect	Species	Accelerated by Light?	Protected by Dark Rearing?	Human Counterpart
Rhodopsin	T4A mutation	Dog	✓ (Cideciyan et al. 2005)		Autosomal dominant RP
	V20G mutation	Mouse	✓ (Wang et al. 1997)	✓ (Naash et al. 1996)	Autosomal dominant RP
	P23H mutation	Mouse	✓ (Wang et al. 1997)	✓ (Naash et al. 1996)	Autosomal dominant RP
	P27L (VPP) mutation	Mouse	✓ (Wang et al. 1997)	✓ (Naash et al. 1996)	Autosomal dominant RP
	P23H mutation	Rat	✓ (Organisciak et al. 2003; Bicknell et al. 2002; Vaughan et al. 2003; Walsh et al. 2004; Jozwick et al. 2006)	✓ (Organisciak et al. 2003)	Autosomal dominant RP
	S334ter mutation	Rat	× (Organisciak et al. 2003) ✓ (Vaughan et al. 2003; Thomas et al. 2007)	× (Organisciak et al. 2003; Green et al. 2000)	Autosomal dominant RP
	L296G	Mouse		× (Li et al. 1995)	Autosomal dominant RP
Arrestin	Knockout	Mouse	✓ (Chen J et al. 1999; Hao et al. 2002)	✓ (Chen J et al. 1999)	Autosomal recessive RP
Rhodopsin kinase	Knockout	Mouse	✓ (Hao et al. 2002 ; Chen CK et al. 1999)	✓ (Chen CK et al. 1999)	Oguchi disease
Rds/peripherin	Insertion	Mouse	✓ (Sanyal and Hawkins 1986)	× (Sanyal and Hawkins 1986)	Several forms of retinal dystrophy
Mertk	Deletion	Rat	✓ (Kaitz and Auerbach 1979a; Organisciak et al. 1999)	✓ (Kaitz and Auerbach 1979a; LaVail and Battelle 1975; Dowling and Sidman 1962)	Autosomal recessive RP
Crumbs homologue 1	Knockout	Mouse	✓ (van de Pavert et al. 2004)		Autosomal recessive RP
ATP/GTP binding protein 1	Purkinje cell degeneration mutation	Mouse	✓ (LaVail et al. 1999)		Unknown

Further investigations have revealed that the exacerbation of retinal degenerations by light depends on the brightness of light (Walsh et al., 2004; Cideciyan et al., 2005), time of day of light exposure, prior lighting environment, and levels of transgene expression (Organisciak et al., 2003). Of promise, is the recent finding that rod photoreceptors in the P23H-3 rhodopsin-mutant retina have the capacity to partially recover from light-induced damage, seen as regrowth of outer segments and restoration of ERG amplitudes (Jozwick et al., 2006; Valter et al., 2008).

1.5.3.2 Scotopic ambient light

Rearing animals in darkness or in dim (scotopic) light has been shown to slow but not completely prevent the progression of retinal disease. Some of the protective effects of dim rearing include prolonged photoreceptor survival (CK Chen et al., 1999; Organisciak et al., 2003; Fan et al., 2005), preservation of retinal histology (CK Chen et al., 1999), increased photocurrent (Fan et al., 2005), maintenance of ERG amplitudes (Naash et al., 1996), and preservation of photoreceptor outer segment length (Naash et al., 1996). In contrast to the degenerative retina, the normal retina appears to be unaffected, both structurally and functionally, by dim rearing (Naash et al., 1993).

Collectively, the modifying effects of light on retinal degeneration in animal models imply a potential therapeutic benefit of light deprivation. Light restriction as a therapy for human RP patients has been trialled with mixed success and is discussed in detail in Section 1.5.4.5.1.

1.5.4 Therapeutic Approaches

There is currently no effective treatment for RP. The availability of animal models of the disease has led to the development of a range of potential therapeutic approaches including gene therapy, dietary supplementation, pharmacological neuroprotection, transplantation, and the manipulation of environmental conditions.

1.5.4.1 Gene therapy

Gene-mediated strategies have been successful in slowing down photoreceptor degeneration in several different animal models of RP: the rd mouse (Bennett et al., 1996; Jomary et al., 1997; Kumar-Singh and Farber, 1998; Takahashi et al., 1999), the rds mouse (Ali et al., 2000), the RCS rat (Vollrath et al., 2001) and the ~~RPE-/-~~ RPE65$^{-/-}$ dog (Acland et al., 2001). In all these cases, wildtype versions of mutated genes have been introduced into cells to correct a loss of function. In an alternative method, gene silencing techniques to correct a toxic gain of function have been applied to the P23H transgenic rat model of RP (LaVail et al., 1998; LaVail et al., 2000), and have resulted in a significant delay of photoreceptor degeneration.

The immense genetic diversity of RP limits the practicality of gene therapies that target specific causal mutations. To counter this, gene therapy directed at the apoptotic cascade, the common pathway of photoreceptor death in RP, has been trialled. In rodent models, retinal degeneration has been delayed by introducing anti-apoptotic genes (Bennett et al., 1996; Chen et al., 1996; Nir et al., 2000) or by inhibiting pro-apoptotic genes (Liu et al., 1999). Regardless of the targeted gene, the use of genetic therapies for the treatment of retinal diseases remains limited to cases in which retinal circuits are largely unchanged by the degenerative process.

Gene-mediated therapies have not yet been trialled in human patients with retinal degenerations. However, the use of similar techniques to treat human diseases such as severe combined immunodeficiency syndrome has resulted in serious, and in some cases fatal, side effects (Check, 2003; Hacein-Bey-Abina et al., 2003; Raper et al., 2003). Additional developments in delivery techniques and systems are clearly required before gene therapy can be considered a viable therapy option.

1.5.4.2 Dietary supplementation

Vitamin A supplementation of 15 000 IU/day is currently advised for patients with RP. This recommendation came about after Berson and colleagues showed, through a randomised,

controlled, double-masked clinical trial, that high daily doses of vitamin A palmitate slows the rate of photoreceptor degeneration in RP patients by approximately 2% per year (Berson et al., 1993). Vitamin A, a precursor to the visual pigment retinal, is essential for phototransduction and the structural integrity of photoreceptors. The therapeutic benefit of vitamin A in retinal degeneration is not well understood, although studies in transgenic mouse models suggest that vitamin A acts by stabilising mutant opsins through increased availability of the chromophore (Li et al., 1998).

Dietary supplement of docosahexanoic acid (DHA), an omega-3 fatty acid and structural component of photoreceptor outer segments, has had mixed success as a therapy for RP. In a randomised, controlled, double-masked clinical trial of 221 RP patients receiving vitamin A treatment, Berson et al. (2004a) initially reported that 1200 mg/d of DHA supplementation over a four year period did not, on average, slow the course of disease. After further evaluation of the data, including a subgroup analysis, it was reported that addition of 1200 mg/d DHA to RP patients beginning vitamin A therapy slowed the course of disease for two years. Among patients on vitamin A for at least two years, a diet rich in omega-3 fatty acids slowed the decline in visual field sensitivity (Berson et al., 2004b). Hoffman and colleagues found that DHA supplementation had no effect on the rate of cone functional loss, as measured by the electroretinogram, in male patients with X-linked RP (Hoffman et al., 2004).

More recently, leutin, a potential antioxidant shown to improve visual function in age-related macular degeneration (Richer et al., 2004), has been trialled in RP patients. A double-masked, randomised, placebo-controlled clinical trial showed that supplementation with leutin (10 mg/d for 12 weeks followed by 30 mg/d for 12 weeks) improved visual fields and may improve visual acuity slightly in adult RP patients (Bahrami et al., 2006).

1.5.4.3 Pharmacological neuroprotection

The introduction of trophic factors to the degenerating retina, by a variety of delivery techniques, has been comprehensively explored as a potential therapy. The first approach involved subretinal injection of the neutrotrophic factor FGF-2 in the RCS rat model of RP. This resulted in extensive rescue of photoreceptors for up to two months post-injection (Faktorovich et al., 1990). Since then, many trophic factors have been shown to protect photoreceptors from degeneration when introduced either by intravitreous injection or by gene transfer systems such as adeno-associated virus vectors that encode secretable factors. Photoreceptor-protective trophic factors include FGF-2 (Akimoto et al., 1999; Uteza et al., 1999; Ali et al., 2000; Lau et al., 2000), CNTF (Cayouette and Gravel, 1997; Cayouette et al., 1998; LaVail et al., 1998; Chong et al., 1999), PEDF (Cayouette et al., 1998), Axokine (LaVail et al., 1998), BDNF (LaVail et al., 1998; Okoye et al., 2003) and GDNF (LaVail et al., 1998; Frasson et al., 1999). The positive effects that these substances have on degenerative retinas include prolonged photoreceptor survival, increased amplitudes of ERG responses, increased rhodopsin content and increased length of photoreceptor outer segments.

However, while still inducing morphological rescue of photoreceptors, in some cases FGF-2 and CNTF have been shown to suppress the functional (ERG) response of the retina (Gargini et al., 1999; Bok et al., 2002; Schlichtenbrede et al., 2003; Valter et al., 2003), and FGF-2 may also trigger pathological neovascularisation (Perry et al., 1995). The mechanisms behind these undesirable side effects must be understood before human clinical trials can begin.

1.5.4.4 Transplantation

Retinal neuronal transplantation aims to replace degenerate photoreceptor cells with grafted healthy retinal tissue. Transplanted tissue may range from whole retina to specific retinal layers or specific types of retinal cells. Subretinal transplants of dissociated embryonic or

early post-natal retinal sheets have been performed in the rd/rd mouse and S334ter rat models of retinal degeneration. Outcomes of these experiments have been promising, with the authors reporting survival of transplanted tissue up to six week post-surgery (Kwan et al., 1999), integration of transplanted tissue with remaining host retina in a way sufficient to mediate a light-dark preference (Kwan et al., 1999), rescue of cone cells in the host retina (Leveillard et al., 2004), evidence of synaptic connections between transplant and host (Seiler et al., 2008), and positive visual responses in the region of the superior colliculus that correspond topographically to the transplant (Sagdullaev et al., 2003; Arai et al., 2004; Thomas et al., 2004).

The extrapolation of these successes to humans remains to be demonstrated. The major issues still facing the field include the development of safe surgical procedures, elimination of host immune rejection, and formation of adequate synaptic integration of transplanted tissue such that an improvement in functional vision can be achieved.

1.5.4.5 Environmental control

The manipulation of environmental conditions such as ambient light and oxygen is an inexpensive and non-invasive therapy option for retinal degeneration.

1.5.4.5.1 Light The therapeutic benefit of light restriction in patients with retinal disease was first suggested over a century ago (Johnson, 1901; Berson, 1971). Since then, dark rearing has been shown to slow the progression of photoreceptor degeneration in a range of animal models (Section 1.5.3.2). However, light deprivation in human patients has shown mixed results.

Berson (1971) conducted a three month trial using monocular sunglasses worn by three children with RP. Later, a longer study was performed using opaque scleral contact lenses to occlude one eye for 6-8 hours a day for five years in two young adult RP patients (Berson, 1980). In both studies, no protective effect of light restriction was seen. Another report describes a RP patient who, as a result of a traumatic injury, developed a thick

occluding membrane over one pupil that correlated to protection of a 1.2 log unit filter (Miyake et al., 1990). No sign of slowed degeneration was detected in the occluded eye by ERG or fundus examination. Another trial of light restriction was performed by Merin and Pe'er in 1981 who followed RP patients wearing dark contact lenses, which blocked the transmission of 60-90% of light, on one eye for 1-3 years (cited in Stone et al., 1999). In ten out of fourteen patients, the rate of visual field loss was slower in the light-restricted eye.

Clinical evidence suggestive of a protective role of light deprivation has been described by Heckenlively and colleagues (1991). A 28-year old RP patient with an eight year history of bright light exposure (as a ski instructor and lifeguard) had more advanced disease than his 52-year old mother, despite the fact that both individuals carried the same genetic mutation.

Although no benefit of light restriction has been convincingly demonstrated in human RP patients, the limited support from clinical trials and observations call for further work. Ultimately, the success of light restriction as a therapy may depend on the genotype of the affected individual. In the trials of the 1970s and 1980s, the underlying genetic defect was not defined for any of the patients. It is now known that RP exhibits immense genetic heterogeneity and, as suggested by animal studies, some mutations may be more responsive to light modulation than others (reviewed in Paskowitz et al., 2006).

1.5.4.5.2 Oxygen Manipulation of the retinal oxygen environment by hyperbaric oxygen (HBO) therapy has been trialled in human RP patients with positive results. The first RP patient treated with HBO showed improved lateral vision after five days of oxygen therapy for four weeks, with no adverse neurological effects detected (Skogstad et al., 1994). Vingolo and colleagues conducted a more comprehensive study of 24 RP patients with autosomal dominant, autosomal recessive and X-linked forms of the disease, who received oxygen therapy over a three year period (Vingolo et al., 1998). HBO-treated patients showed significant improvement in ERG responses, but it was not known if this corresponded to any improvement in visual acuity. A follow-up study by the same group assessed 44 RP patients

in a comparative, longitudinal, case-controlled, randomised clinical trial. Over a ten year period, the visual acuity, visual fields and ERG responses of HBO-treated patients remained stabilised and significantly larger compared to non-HBO-treated patients (Vingolo et al., 2008).

1.5.4.6 Future directions

Gene therapy, the only potential 'cure' for RP, shows promising results in animal models but it will take considerable advancements in delivery techniques to make this a safe option for human patients. In addition, the diverse genetic heterogeneity of RP requires equally diverse modes of gene therapies. Mutation-independent therapies such as dietary supplementation, pharmacological neuroprotection, light management and oxygen therapy, provide versatile treatment options that are potentially applicable to all RP patients regardless of the underlying genetic defect. These forms of therapy, while not curing the disease, offer a means of slowing the degenerative process. Finally, tissue transplantation offers long-term treatment, however, the establishment of functional synaptic connections between transplant and host tissue, to maintain high-order visual processing, is a significant issue that must be overcome in this field. Ultimately, the development and refinement of any therapy for RP requires ongoing analysis of the cellular and molecular mechanisms underlying photoreceptor damage, death and dysfunction, in particular the pathway from gene mutation to photoreceptor apoptosis.

1.6 SUMMARY

The mammalian photoreceptor is a highly specialised, highly active cell with an exceptional task; the initiation of visual perception. The site of much of the photoreceptors' specialisations is the distinctive outer segment, a dynamic structure that is biochemically equipped for the detection and transduction of light. The morphological and functional specialisations of the photoreceptor cell, and the enormous energy expenditure that they

demand, has forced extreme adaptations within the retina such as inversion of the retinal tissue and evolution of the choroidal circulation. As photoreceptors reside and function in a high-photon, high-oxygen environment, they are inherently sensitive to environmental damage. They are also sensitive to genetic mutations, as evidenced by the large group of clinically significant retinal degenerations known as RP. The diverse genetic backgrounds that underlie RP converge to a common phenotype; the gradual loss of photoreceptors leading to blindness. The pathways from genetic defect to photoreceptor cell death remain unclear but the retina's exposure to light appears to modulate the rate of photoreceptor degeneration. There is a clear cone-rod dependence component to RP, and much of the current research in the field is aimed at understanding the basis of the tight relationship between rod survival and cone survival. Treatment options for RP patients remain limited at present and are largely aimed at deferring or slowing the degenerative process rather than stopping it altogether.

1.7 PRESENT RESEARCH

The present thesis describes three investigations of cone photoreceptors in an animal model of RP (Chapters 3-5). Each of these investigations is presented as an original research article that has been published in the journal, *Investigative Ophthalmology & Visual Science (IOVS)*. Focus is given to cones because (1) the death of cones during the course of RP remains largely unexplained since most underlying mutations are in rod-specific genes, and (2) the loss of cone vision is the overriding cause of blindness in RP and is most devastating to the affected individual. Understanding the status of cones in the RP retina, including mechanisms of their survival, damage and death, is therefore of utmost importance. Focus is also given to the interaction between light and cone cells due to the established modulating effect of light on the progression of retinal degeneration.

Chapter 3 describes the life history of cones, including their numbers, morphology and function, across the lifetime of the P23H-3 rhodopsin-mutant rat, the animal model used throughout subsequent studies. Presumably because of the low number of cones in the rodent retina, such descriptive data on cone cells in either normal or degenerative retina are largely lacking. The findings of Chapter 3 provide a vital baseline for the two following studies, which explore the modulating effect of light on cones in the P23H-3 rat retina. Previous work on the response of the degenerative retina to variations in ambient illumination is extensive (Section 1.5.3), but has largely been restricted to rod photoreceptors. Chapter 4 investigates the effects of ambient light levels on the structure and function of cone photoreceptors; firstly, the response of cones to an increase in light levels, and secondly, their response to light restriction. The central finding of Chapter 4 is that cones in the P23H-3 retina have the capacity to self-repair after being damaged by exposure to raised levels of illumination. Chapter 5 investigates several features of this light-induced cone damage, such as the time course of structural and functional damage, the involvement of different subgroups of cones and the relationship between cone damage and rod damage. The findings from the current studies raise issues of the mechanism of cone-rod dependence and therapeutic opportunity, which are considered.

CHAPTER 2

Materials and Methods

2.1 INTRODUCTION

In the subsequent three Chapters, protocols specific to each study are outlined in a Methods section. Where Methods are described in brief in the subsequent Chapters, detailed descriptions are provided below.

2.2 ANIMALS

All procedures were in accordance with the ARVO Statement for the Use of Animals in Ophthalmic and Vision Research and with the requirements of The Australian National University Animal Experimentation Ethics Committee. Observations were made in animals aged from postnatal day (P) 10 to 540, and both males and females were used equally throughout the studies.

2.2.1 Rat Strains

2.2.1.1 Sprague-Dawley

Albino Sprague-Dawley (SD) rats were born and reared in the Animal Facility at the Research School of Biological Sciences, The Australian National University, Canberra. The original breeding pairs were sourced from the Animal Resources Centre, Western Australia.

2.2.1.2 P23H Transgenic

P23H Line 3 (P23H-3) homozygote rats were born and reared in the Animal Facility at the Research School of Biological Sciences, The Australian National University, Canberra. The

original breeding pairs were sourced from the Beckman Eye Institute, California. The animals used in the current experiments were heterozygotes, the offspring of mating P23H-3 homozygotes with SD albinos, and express a mouse P23H mutant opsin transgene in addition to two endogenous opsin genes.

2.2.2 Housing Conditions

Animals were housed in standard litter boxes in a room with an ambient temperature of 21°C. All animals were monitored daily and were provided with an enriched environment in which food and water was available *ad libitum*.

2.2.3 Light Management

Animals were born and raised in dim cyclic ambient illumination (12 hours light/12 hours dark) with the light phase set at 5 lux (scotopic conditions). For some experiments, the light phase of the cycle was increased to 300 lux (photopic conditions). The source of photopic illumination was cold-white fluorescent tubes, placed directly above the litter boxes. To minimise shading of the retina, animals were housed individually in custom-designed Perspex litter boxes during photopic light exposure, with food placed on the base of the litter box.

2.3 TISSUE COLLECTION AND PROCESSING

Animals were euthanised by an overdose of sodium pentobarbital (>60 mg/kg, Valabarb, Jurox) containing 2% lignocaine hydrochloride (Troy Laboratories), administered by intraperitoneal injection. Eyes were marked at the superior aspect of the limbus with an insoluble marker pen for orientation, before being enucleated and immersion-fixed in 4% paraformaldehyde in 0.1 M phosphate buffered saline (PBS) at pH 7.4. Enucleated eyes were processed for cryosectioning, wholemounting or electron microscopy as outlined in the Methods section of each Chapter.

2.4 IMMUNOHISTOCHEMISTRY

Tissue was labeled for rhodopsin, long-medium wavelength-sensitive (LM) opsin, and short wavelength-sensitive (S) opsin using fluorescence immunohistochemistry. Details of the primary and secondary antibodies used for immunolabeling are shown in Tables 2.1 and 2.2.

2.4.1 Labeling of Cryosections

Retinal cryosections were thawed at room temperature for 5 min. To prevent leakage of reagents, a liquid-repellent barrier was applied around the sections. Sections were washed in 70% ethanol for 5 min to aid adhesion of sections to slides, followed by a 5 min wash in deionised water (dH_2O) and two 10 min washes in 0.1 M PBS. To reduce non-specific binding of secondary labels, sections were incubated with 10% normal horse serum in 0.1 M PBS for 1 hour. After a 15 min wash in 0.1 M PBS sections were incubated overnight at 4°C with primary antibodies diluted with 0.1 M PBS and containing 1% normal horse serum. The following day, sections were washed for 15 min in 0.1 M PBS before overnight incubation at 4°C with fluorescently labeled secondary antibodies. After washing in 0.1 M PBS for 15 min sections were incubated for 2 min with the DNA-specific dye bisbenzamide (1:10000) before being coverslipped with a glycerol/gelatin medium. To control for non-specific labeling, some retinal sections were prepared as negative controls, i.e. they were taken through all the above steps, except that the primary antibody was omitted. Unless stated otherwise, all steps were carried out at room temperature and washes were performed in 50 ml Coplin jars on an orbital shaker.

2.4.2 Labeling of Wholemounts

Retinal wholemounts were washed for 20 min in 0.1 M PBS before being dehydrated by 20 min washes in 25%, 50%, 75% and 90% ethanol. Samples were left in 100% overnight at 4°C before rehydration in 90%, 75%, 50% and 25% ethanol (20 min wash in each). To increase tissue permeability, samples were washed in 0.01% Triton in 0.1 M PBS (2 x 5 min)

Table 2.1 Primary antibodies used for immunohistochemical labeling of retinal cryosections and wholemounts.

Specificity	Source	Host Species	Working Dilution
Long/medium wavelength-sensitive opsin	Chemicon, California	Rabbit	1:1000
Short wavelength-sensitive opsin	Chemicon, California	Rabbit	1:1000
Rhodopsin (clone Rho 1D4)	Chemicon, California	Mouse	1:200

Table 2.2 Secondary antibodies used for immunohistochemical labeling of retinal cryosections and wholemounts.

Specificity	Source	Host Species	Working Dilution
Anti-rabbit Alexa Fluor 488	Invitrogen-Molecular Probes, Oregon	Goat	1:1000
Anti-mouse Alexa Fluor 594	Invitrogen-Molecular Probes, Oregon	Rabbit	1:1000

before overnight incubation at 4°C with primary antibody. The following day, samples were washed in 0.1 M PBS (3 x 20 min) before overnight incubation at 4°C with secondary antibody. After 2 x 20 min washes in 0.1 M PBS, wholemounts were mounted on glass slides and coverslipped with a glycerol-gelatin medium. Tissue was oriented so that photoreceptor outer segments were facing up. Unless stated otherwise, all steps were carried out at room temperature and washes were performed in 3 ml polypropylene well plates on an Orbital Shaker.

2.5 TUNEL LABELING

Retinal cryosections were stained using the TdT-mediated dUTP-biotin nick end labelling (TUNEL) technique to identify fragmented DNA characteristic of apoptosis. Retinal cryosections were thawed at room temperature for 5 min. To prevent leakage of reagents, a liquid-repellent barrier was applied around the sections. Sections were washed in 70% ethanol for 15 min to aid adhesion of sections to slides, followed by two 5 min washes in dH_2O and a 10 min wash in 1 x TdT buffer (3 mM Trizma base, 14 mM sodium cacodylate, 0.1 mM cobalt chloride). Sections were incubated for 60 min at 37°C with a reaction solution containing terminal deoxytransferase (TdT) (final concentration 0.03 units/µl, Roche) and biotinylated dUTP (final concentration 4 µM, Roche) in 10 x TdT buffer and dH2O. The reaction was terminated by a 15 min wash in 2 x SSC (0.3 M sodium chloride, 30 mM sodium citrate). To reduce non-specific binding of the streptavidin-conjugated fluorophore, sections were incubated in 10% normal goat serum in 0.1 M PBS for 10 min, followed by 30 min incubation at 37°C with Cy3-labelled streptavidin (Amersham Pharmacia, UK) diluted 1:1000 in 0.1 M PBS. After washing in 0.1 M PBS (2 x 5 min) sections were counterstained for 2 min with the DNA-specific dye bisbenzamide (1:10 000 dilution) before washing in 0.1 M PBS (2 x 5 min) and subsequently coverslipped with a glycerol/gelatin medium. Unless

stated otherwise, all steps were carried out at room temperature and washes were performed in 50 ml Coplin jars.

2.6 CONFOCAL FLUORESCENT MICROSCOPY

Preparations were viewed on an Axio Imager.M1 upright microscope equipped with a LSM5 PASCAL laser-scanning confocal module (Carl Zeiss MicroImaging, Thornwood, NY). The confocal unit was fitted with argon (458, 488, and 514 nm excitation) and He/Ne (543 nm excitation) lasers. Digital images were acquired using the Zeiss LSM 5 PASCAL system and software. The dyes Alexa Fluor 488, Alexa Fluor 594 and bisbenzamide were excited, respectively, with the 488 nm line of the argon laser, the 543 nm line of the He-Ne laser and a 405 nm diode laser.

2.7 QUANTIFICATION OF LABELING

2.7.1 Cryosections

Measurements of rod and cone outer segment length, and retinal thickness, were made on digital images of immunolabeled and bisbenzamide-stained cryosections. Images were captured using an AxioCam MRc digital camera (Carl Zeiss) mounted on an Axio Imager.M1 microscope (Carl Zeiss) and measurements were taken using AxioVision 4.6 software. Detailed descriptions of the procedure for taking these measurements are included in the Methods section of each Chapter.

2.7.2 Wholemounts

Measurements of LM-cone outer segment length and density were made on digital images of immunolabeled retinal wholemounts. Images were captured using an AxioCam MRm digital camera (Carl Zeiss) mounted on an Axioplan 2 microscope (Carl Zeiss) and measurements were taken using AxioVision 4.3 software. A detailed description of the procedure for taking these measurements is included in the Methods section of Chapter 2.

2.8 ELECTRORETINOGRAPHY

The full field flash-evoked electroretinogram (ERG) was used to assess rod and cone function in the rat retina.

2.8.1 Ganzfeld Unit

ERG recordings were obtained using a 200 mm diameter Ganzfeld with illumination provided by internal arrays of white LEDs (FS-250, Photometric Solutions International). Two separate banks of LEDs within the Ganzfeld module were utilised: a "high intensity pulse" bank with high intensity LEDs to provide high luminance pulses; and a "low intensity pulse" bank with a single, smaller wattage LED to provide very low luminance pulses. The Ganzfeld system was controlled using LEDControl Software (FS-250, Photometric Solutions International). ERG traces were recorded and displayed using the PowerLab 4/200 system (ADInstruments) and Scope V3.8 software (ADInstruments).

2.8.2 Animal Preparation

Animals were dark-adapted overnight (minimum of 15 hours) and prepared for recording under dim red illumination. Anaesthesia was initiated and maintained by intraperitoneal injection of ketamine (60 mg/kg; Troy Laboratories) and xylazine (10 mg/kg; Troy Laboratories). All recordings were taken from the right eye which was anaesthetised with 1 drop of proxymetacaine hydrochloride (Ophthetic 5 mg/ml; Allergan). The pupil was dilated with 1 drop of tropicamide (Mydriacyl 0.5%; Alcon Laboratories) and a single loop of thread was secured around the eye ball to prevent eyelid activity from interfering with recordings. Animals were positioned on a plastic stage and were dark adapted for 10 min inside the Ganzfeld unit to optimise retinal responsiveness. Body temperature was maintained at 37°C with a homoeothermic blanket unit (Harvard Apparatus Limited) controlled by feedback from a rectal temperature probe.

2.8.3 Electrodes

The response of the retina was recorded with a 4 mm platinum wire loop electrode contacting the cornea, while a Ag/AgCl pellet placed in the cheek served as the reference electrode. A subdermal needle electrode inserted at the base of the tail acted as the ground. Corneal hydration of both eyes was maintained with synthetic tears (Viscotears 2 mg/ml; Novartis), which also aided in maintaining electrical contact with the corneal electrode.

2.8.4 Recording Protocols

Following previous reports (Nixon et al. 2001), responses to a single pulse stimulus were considered to be 'mixed' with contributions from rods and cones. Responses to a pulse preceded, by 395 msec, by a conditioning flash were considered those of cones. By subtracting the cone response from the 'mixed' response, the rod response was isolated. Responses were recorded to a series of pulse intensities, varied over 6.0 log units. The luminance, duration and number of repetitions of each pulse are outlined in Table 2.3 (mixed responses) and Table 2.4 (cone responses). The number of repetitions and interval between pulses were selected to ensure maximal rod and cone responses. The brightest pulse stimulus was sufficient to elicit saturated responses.

2.8.5 Waveform Analysis

Three measurements of ERG amplitude were used for analysis: rod a-wave, rod b-wave and cone b-wave. Details of how these measurements were taken are outlined in the Methods section and first Figure of Chapter 4.

Table 2.3 Pulse settings used to record mixed (rod and cone) ERG responses.

Log Flash Attenuation	Luminance (cds/m^2)	Duration (ms)	Repetitions	Interval (s)
0	79.1	2	2	60
0	38.8	1	4	40
0.7	7.74	1	4	30
1.0	3.80	1	4	30
1.7	0.77	1	8	20
2.0	0.399	1	16	5
2.7	0.077	1	16	5
3.7	0.0077	1	16	5
4.0	0.0034	1	16	5
6.0	0.000044	1	16	5

Table 2.4 Pulse settings used to record cone ERG responses. All pulses were preceded, by 395 ms, by a rod-saturating conditioning flash of ~~19.5~~ 12.0 cds/m^2.

Log Flash Attenuation	Luminance (cds/m^2)	Duration (ms)	Repetitions	Interval (s)
0	79.1	1	16	1
0.3	19.5	1	16	1
0.7	7.74	1	16	1
1.0	3.80	1	16	1
1.7	0.77	1	16	1
2.0	0.399	1	16	1
2.3	0.194	1	16	1
2.7	0.077	1	16	1
3.7	0.0077	1	16	1
6.0	0.000044	1	16	1

CHAPTER 3

Life History of Cones

Life History of Cones in the Rhodopsin-Mutant P23H-3 Rat: Evidence of Long Term Survival

Vicki Chrysostomou,[1,2] *Jonathan Stone*,[1,2,3] *and Krisztina Valter*[1,2]

PURPOSE. To follow the status of cones over the life of the P23H-3 transgenic rat, while the rod population is depleted. **METHODS.** We studied P23H-3 heterozygote and Sprague-Dawley (SD) control rats raised in dim, cyclic light from postnatal day (P) 10 to P540. Retinas were examined for cone density, cone outer segment (OS) length, cone axon and soma morphology, and the amplitude of rod and cone components of the electroretinogram (ERG). **RESULTS.** In the P23H-3 retina cone density followed a developmental pattern, increasing from P10 until P20, declining during early adult life (to P150), then steadying at levels found in the SD retina until P540. Cone OSs elongated to P30, and then slowly shortened during late adulthood; at P350 and P540, cone OSs were significantly shorter than in the background SD strain. Cone axons shortened slowly throughout adult life as the outer nuclear layer thinned. The rod a-wave declined steadily in the P23H-3 retina from P10, falling below amplitudes seen in the SD strain from early life. By contrast, the cone b-wave maintained amplitude at SD levels, until P380. **CONCLUSIONS.** Despite the ongoing loss of rod function and numbers, cone numbers in the P23H-3 retina were maintained at levels found in the SD rat to the oldest age examined, and cone function and OS morphology were maintained for approximately 1 year, indicating a long period of cone independence. The long period of cone survival creates an opportunity to induce self-repair, if the stress causing their dysfunction can be reduced.

From the [1]Research School of Biological Sciences, and [2]ARC Centre of Excellence in Vision Science, The Australian National University, Canberra, Australia; and the [3]Save Sight Institute and Discipline of Physiology, University of Sydney, Sydney, Australia.

Supported by grants from Retina Australia, the National Health and Medical Research Council of Australia, and the Australian Research Council.

Submitted for publication October 14, 2008; revised November 23 and 27, 2008; accepted December 5, 2008.

Disclosure: V. Chrysostomou, None; J. Stone, None; K. Valter, None

Corresponding author: Vicki Chrysostomou, Research School of Biological Sciences, The Australian National University, GPO Box 475, Canberra, ACT 2601, Australia; vicki.chrysostomou@anu.edu.au.

Investigative Ophthalmology & Visual Science. First published on Dec 30, 2008 as doi: doi:10.1167/iovs.08-3003

The loss of cone vision is a progressive, debilitating and currently untreatable feature of many retinal dystrophies. In many forms of human retinal dystrophy, cones degenerate despite the causal mutation being in a protein expressed specifically in rods. This dependence of cones on rod survival is devastating for the sufferer; understanding and limiting this dependence has been identified as a priority of the development of treatment.

The transgene in the P23H-3 transgenic rat was engineered to mimic a mutation of rhodopsin which causes autosomal dominant retinitis pigmentosa (RP) in humans, and causes a similar, well-documented degeneration in the rat. In the P23H-3 rat, rods degenerate at a rate dependent on ambient illumination, and late loss of cone function has also been described.[1-4]

Cones make up approximately 1% of the total photoreceptor population in the albino rat retina.[5, 6] Electroretinography, behavioural and spectrophotometric studies have identified two classes of cones in rat retina, identified by their photopigment. In one class, the photopigment has a peak absorption at 509 nm (LM-sensitive), and a second has a peak absorption at 359 nm (UV-sensitive).[7-10] Immunolabelling of the two rat cone classes has shown that approximately 90% of the cone population contain the LM-sensitive pigment and 10% express the UV-sensitive pigment.[6, 11, 12]

To understand and test therapeutic interventions aimed at cones in the rat retina, a careful and detailed description of their life history is necessary. To date, the study of cones in the P23H-3 retina has been largely restricted to assessment by the photopic electroretinogram (ERG), and to the first 200 days of life.[3, 13] Because cone pathology in human disease may begin relatively late, it is important to understand the status of cones in the aging and aged retina.

The current study assesses the life history of cones in the heterozygous P23H-3 rat retina, from before eye opening until late mature adulthood (18 months), in animals raised in scotopic ambient light. We paired electrophysiological measures of cone function with a morphological analysis of cone density, distribution and outer segment structure. We report that cone function is maintained, despite progressive loss of rod function and numbers, through the first year of life, and that cone numbers are maintained at normal levels to the oldest age

examined. The results suggest that cones maintain their integrity for long periods, independent of rods, and that the late loss of function observed is due to outer segment shortening rather than loss of cone numbers. Possible mechanisms of this independence and eventual damage are discussed, and it is noted that the persistence of cone numbers allows the possibility of cone repair, as reported previously.[1]

METHODS

Animals

All procedures were in accordance with the ARVO Statement for the Use of Animals in Ophthalmic and Vision Research, and with the requirements of The Australian National University Animal Experimentation Ethics Committee. Observations were made in P23H transgenic rats (Line 3, Beckman Laboratories, University of California, San Francisco) and Sprague-Dawley (SD) controls aged from postnatal day (P) 10 to P540. The P23H animals used were heterozygotes, the offspring of mating P23H-3 homozygotes with SD albinos, and express a mouse P23H mutant opsin transgene in addition to the two endogenous opsin genes.[14-16] Both male and female animals of each strain were used equally throughout the study. All animals were born and raised in dim cyclic light (12 h 5 lux, 12 h dark), and housed in a room with an ambient temperature of 21°C where food and water were available *ad libitum*.

Tissue Collection

Animals were euthanized with an overdose of sodium pentobarbital (>60 mg/kg, intraperitoneal). Eyes were marked at the superior aspect of the limbus for orientation, enucleated and immersion-fixed in 4% paraformaldehyde in 0.1 M phosphate-buffered saline (PBS) at pH 7.4 for 3 h. One eye from each animal was processed for cryosectioning, while the fellow eye was processed for wholemounting. For cryosectioning, eyes were rinsed twice in 0.1 M PBS and left in a 15% sucrose solution overnight to provide cryoprotection. Eyes were embedded in Tissue-Tek OCT Compound (Sakura Finetek, Tokyo, Japan), and snap frozen in

liquid nitrogen before being cryosectioned at 12 μm (Leica CM1850 Cryostat). Sections were mounted on gelatin and poly-L-lysine-coated slides and dried overnight at 50°C before being stored at -20°C. For retinal wholemounts, the retina was dissected from the eyecup, flattened by making radial incisions, gently sandwiched between two glass slides and immersed in 4% paraformaldehyde at 4°C for up to 2 weeks before immunolabeling.

Immunohistochemistry of Retinal Wholemounts

To assess the status of cones during the life of the P23H-3 rat, retinal wholemounts were immunolabelled for the long-medium wavelength-sensitive (LM) cone outer segment (OS) opsin, the dominant cone opsin in the rat retina. Flattened retinas were dehydrated and rehydrated in ethanol before being blocked with normal goat serum and incubated overnight with rabbit polyclonal antibodies to LM opsin (1:1000, Chemicon, Temecula, CA). After washing with 0.01% Triton-PBS, retinas were incubated for 24 h with an antibody to rabbit IgG conjugated to Alexa Fluor 488 (1:1000, Molecular probes, Eugene, OR) and subsequently mounted and coverslipped on glass slides. To control for non-specific labeling, some retinal wholemounts were prepared as negative controls, i.e. they were taken through all the above steps, except that the primary antibody was omitted.

LM opsin-labeled cone OSs were assessed for both density and length. Samples were visualized by fluorescence microscopy (10 x objective, Zeiss Axioplan 2) and images of the OS layer were captured with a digital camera (Zeiss AxioCam MRc). Using the Panorama feature of Axiovision suite software, we systematically reconstructed the whole retinal surface by splicing 100-200 separate digital images into a montage. Using the digital montage, LM opsin-labeled OSs were counted over areas of 0.01 mm^2 at 0.5 mm intervals across the entire retinal surface (approximately 100-250 fields per retina). At each counting field, the average length of cone OSs was also recorded. Counts of OSs per 0.01 mm^2 were averaged across the entire retina to give an overall cone density for each sample. To assess regional variations in OS density and length the

retinal surface area was divided into superior and inferior regions, into nasal and temporal regions, and into central and peripheral regions (all relative to the optic nerve head).

Immunohistochemistry of Retinal Sections

Cryosections were labeled with rabbit polyclonal antibodies to LM opsin (1:1000, Chemicon, Temecula, CA). Sections were washed for 15 minutes in 75% ethanol, followed by a 5 minute wash in distilled water and two 5 minute washes in 0.1M PBS. Sections were blocked with 10% normal goat serum for 1 h before being incubated for 24 h at 4°C with primary antibody. After washing in 0.1M PBS, sections were treated with an antibody to rabbit IgG conjugated with Alexa Fluor 488 (1:1000, Molecular Probes, Eugene, OR) for 24 h at 4°C before incubation for 2 min with the DNA-specific dye bisbenzamide (1:10 000). To control for non-specific labeling, some sections were prepared as negative controls, i.e. they were taken through all the above steps, except that the primary antibody was omitted.

Retinal Thickness Measurements

To assess retinal thickness, cryosections were labelled with the DNA-specific dye bisbenzamide. Sections were thawed at room temperature before washing in 70% ethanol for 15 min, followed by a 5 min wash in distilled H_2O and two 5 min washes in 0.1 M PBS. The sections were then incubated for 2 min with bisbenzamide (1:10 000), washed in 0.1 M PBS, and coverslipped with a glycerol/gelatin medium. Retinal thickness measurements were made on digital images of stained cryosections. At each measurement location, the thickness of the outer nuclear layer (ONL) as well as the thickness of the retina, from inner to outer limiting membrane (ILM-OLM), was recorded. The ratio of ONL to ILM-OLM was used for analysis to account for obliquely-cut sections. In at least two sections per animal, we took four measurements, approximately 100 μm apart, from both the superior and inferior mid-peripheral areas of the retina (a total of at least 16 measurements per animal). Results from 5 animals at each time point were averaged and analysed by the statistical method described below.

Electroretinography

The function of photoreceptors was assessed by the flash-evoked electroretinogram (ERG). Animals were dark-adapted overnight and prepared for recording in dim red illumination as described previously.[4] Following previous reports,[17] responses to a standard test flash (44.5 cds/m^2) were considered to be 'mixed' with contributions from rods and cones. Responses to the test flash preceded, by 395 msec, by a conditioning flash (12 cds/m^2) were considered those of cones. By subtracting the cone response from the 'mixed' response, the rod response was isolated. Using this method, three measurements of amplitude were used for analysis: rod a-wave, rod b-wave and cone b-wave. The standard flash stimulus was of sufficient intensity to elicit saturated a-wave and b-wave responses.

Statistical Analyses

Data were analyzed using a two-tailed Student's t-test with $P<0.05$ considered to represent a statistically significant difference. All data are presented as the mean ± 1 SEM.

RESULTS

Quantitative Analysis of Cones

The relatively low number of cones in the rat retina meant that individual OSs could be clearly distinguished in LM opsin-labeled wholemounts (Fig. 1). This form of preparation enabled us to assess the number, distribution and OS length of LM cones across the entire retinal surface at 11 ages during the life of the P23H-3 rat (Figs. 1A-L), from before eye opening (P10) until the late stages of the rodent's lifespan (P500).

Cone Density. Cone density in the P23H-3 retina was calculated by counting the number of LM-labeled OSs across the surface of the flat-mounted retinas shown in Figure 1. The density of LM cones increased by 26% between P10 and P16, reaching a peak of 4481/mm^2 (Fig. 2A and Table 1), a time during which the eyes of the rat open and terminal photoreceptor differentiation is occurring. Over the next ten days of retinal development (P20-

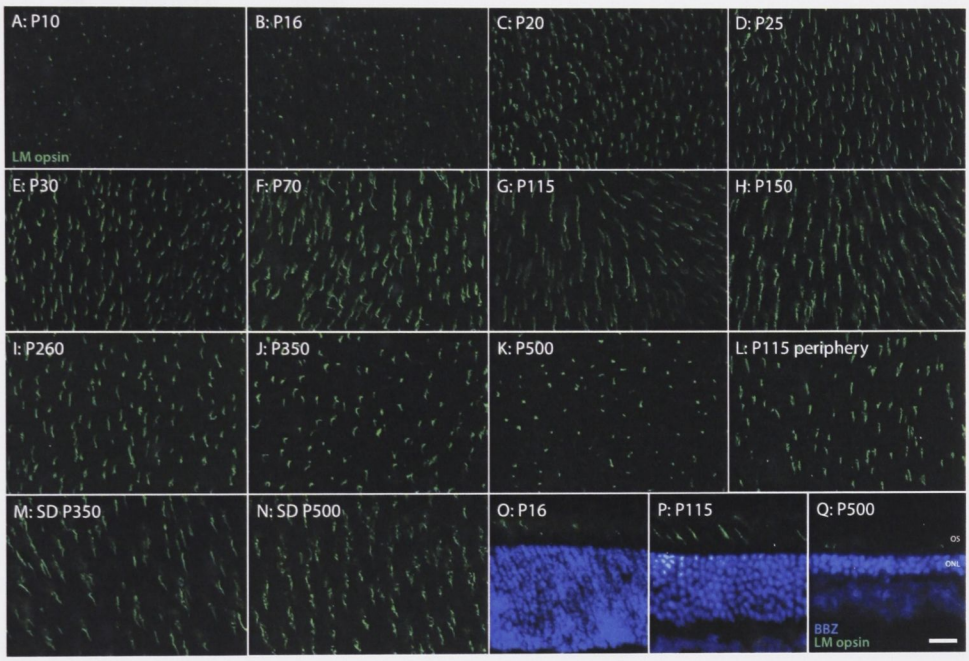

FIGURE 1. Immunohistochemical labeling of LM cone photoreceptors in P23H-3 and SD retinas. In wholemount preparations (**A-N**) individual cone OSs (*green*) could clearly be distinguished, allowing the quantification of both cone density and OS length. (**A-K**) Representative images from the superior central P23H-3 retina at successive ages spanning the lifetime of the rodent; from before eye opening at P10 to late adulthood at P500. (**L**) Anterior edge of the young adult P23H-3 retina. (**M-N**) Age-matched SD controls for the two oldest ages studied (P360 and P500). (**O-Q**) LM opsin-labeled retinal sections, used to confirm the OS length seen in wholemount preparations. Scale bar, 20 μm.

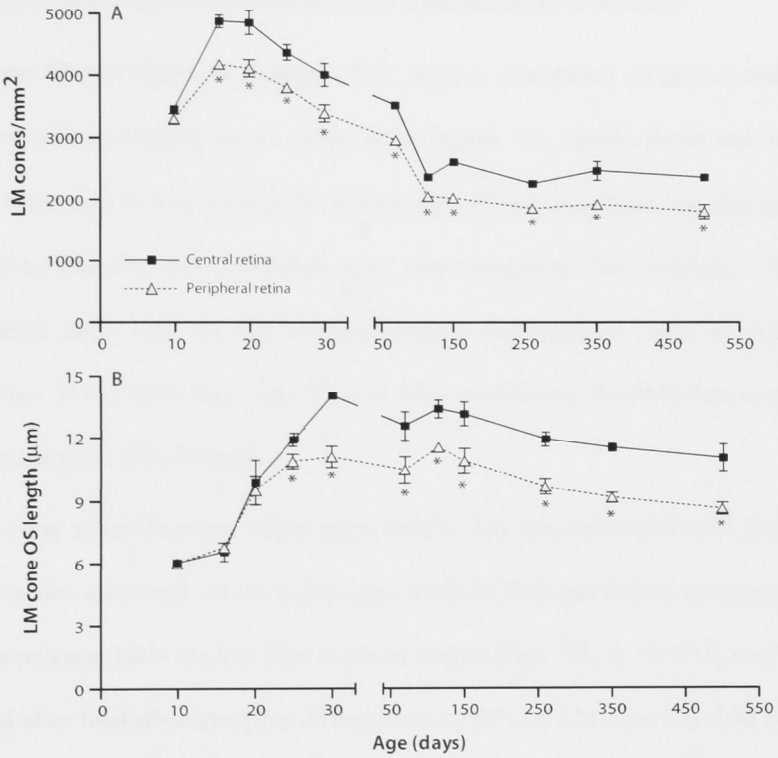

FIGURE 2. Cone density and OS length in the P23H-3 retina across ages 10 to 500 days. The average density of LM cones (**A**) and their OS length (**B**) was determined by assessing immunolabeled OSs across the surface of retinal wholemounts. The retinal surface was divided equally in two, into central and peripheral areas, to assess regional variations. For each age studied, retinas from 3 different animals were assessed and data are presented as the mean ± SEM. Asterisks indicate data points that are significantly different ($P<0.05$) by a Student's t-test.

P30) when the photoreceptor population in the normal retina undergoes a period of developmental culling, P23H-3 cone numbers dropped by 20%. The P23H-3 dystrophy begins during this period when the onset of cell death in the ONL matches that of the non-degenerative retina but is several orders of magnitude higher.[13] Between P30 and P115, as the rat reached adulthood, the population of LM cones declined steadily, dropping by 40% before appearing to stabilize. At all ages studied over the next 13 months, from P115 to P500, cone density in the P23H-3 retina remained steady at approximately 2000/mm^2.

Cone Outer Segment Length. The oblique orientation of immunolabeled OSs on flat-mounted retinas enabled us to assess their length. To ensure there was no mechanical damage or distortion to OSs during the preparation of wholemounts, we also immunolabeled retinal cryosections for three selected ages and compared the histology. The length of immunolabeled cone OSs on flat-mounted retinas and sections were in good agreement (compare Figs. 1O-Q with Figs. 1B, 1G and 1K), confirming that wholemounts allowed the reliable quantification of OS length.

At every retinal location where cone density was quantified (100-250 fields per retina), the OSs were also measured. At the earliest age studied (P10) and before eye opening, the entire LM cone population had OSs less than 8 μm in length (Figs. 2B, 3). At P16, two days after eye opening and after final photoreceptor differentiation, 10% of LM cone OSs had elongated to 8-15 μm. By P30, 90% of all LM cones had OSs greater than 15 μm in length. From P30 until adulthood (P150), the OSs of the cone population remained stable at an average length of 16 μm. Beyond 150 days of age, cone OSs steadily shortened until, by P500, 40% of all LM cone OSs were less than 8 μm in length and only 5% remained longer than 15 μm.

Topography of Cone Density and Outer Segment Length. Cone density and OS length were not uniform across the P23H-3 retina. There was no significant difference in the density or OS length of LM cones between the superior and inferior, or temporal and nasal, regions of retina (data not shown). However, cone density was significantly ($P<0.05$), and on average 20%, higher in the central retina at all ages from P16-P500 compared to the peripheral

TABLE 1. Cone Density Across Ages in the P23H-3 Rat.

Age (days)	LM cones/mm^2
10	3322 ± 3.50
16	4481 ± 103
20	4409 ± 156
25	4003 ± 68.5
30	3571 ± 185
70	3117 ± 15.1
115	2196 ± 69.3
150	2273 ± 31.7
260	1989 ± 16.7
350	2111 ± 127
500	1992 ± 75.5
SD P350	2178 ± 81.8
SD P500	2163 ± 102

$n = 3$ at each age.
Tabulated values give mean ± SEM.

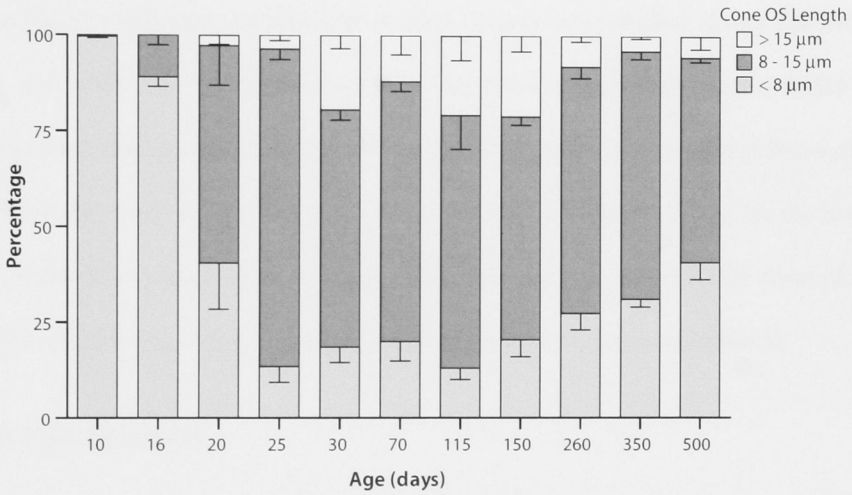

FIGURE 3. Variations in the length of LM cone OSs in the P23H-3 retina across age. The histograms show the proportion of the cone population at each age with OSs that are <8 µm, 8-15 µm and >15 µm in length. Data are presented as the mean ± SEM of 3 animals.

retina (Fig. 2A). As well as being at a higher density, cones in the central retina had significantly ($P<0.05$) longer OSs than those in the retinal periphery at every age above P20 (Fig. 2B).

Soma and Axon Morphology of Cones

We used the tendency of LM opsin to accumulate in the membrane of stressed cones[18-20] to demonstrate the morphology of the somas and axons of cones in the P23H-3 retina (Fig. 4, left), and in the aged SD retina (Fig. 4, right). Because the somas of LM cones are located at the outer limiting membrane, the process between the soma and the OS corresponds to the inner segment, while the process between the soma and the outer plexiform layer is the cell's axon (diagram in Fig. 4). Although not all cones in these retinas were labelled in this full-length way, those that did label may be representative. Cone soma morphology in the P23H-3 retina appeared constant during adulthood, but the length of the axon was steadily reduced after P30. This shortened the cone cell in a striking way, but may be an adaptive change (to the thinning of the ONL), rather than a degenerative change. In the SD retina by contrast, this form of labelling was rare before P500 (Fig. 4 right), and the length of the cone cell was maintained.

Cone and Rod Function

The dark-adapted ERG was recorded in P23H-3 animals across ages 16 to 500 days and compared to age-matched SD controls (Figs. 5, 6). Descriptions are available[3, 21, 22] of ERG responses in the developing and adult P23H rat retina, but a systematic investigation extending to the later stages of the animals' life spans has not previously been reported.

Rod-Mediated Responses. In the non-degenerative SD retina, rod ERG responses were robust and well developed at P16, only days after eye opening. The amplitudes of the SD rod a-wave and rod b-wave remained virtually constant until 230 days of age, after which both amplitudes began to deteriorate at a similar rate, dropping by 20-30% between P230 and P540 (Figs. 6A, 6B and Table 2).

In the degenerative P23H-3 retina, like the SD, rod ERG responses were apparent and well-developed at P16. After this point, the amplitude of the rod a-wave and b-wave steadily

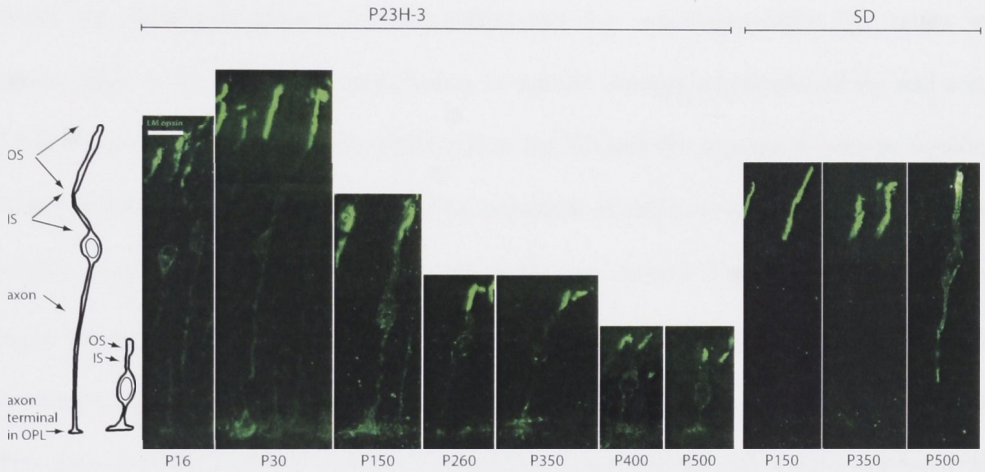

FIGURE 4. Immunofluorescent labeling of LM opsin in the P23H-3 retina (*left*) from the juvenile (P16) to late adulthood (P500), and in the SD retina (*right*) during adulthood (P150-500). The images have been arranged so that the outer plexiform layer (OPL) is aligned between images; the length of the image then approximates the overall length of the cone cells. LM opsin is strongly expressed in OSs in both strains, and at all ages. In some P23H-3 cones at all ages and some SD cones at P500, LM opsin was detected throughout the cell membrane, allowing visualization of the process between the soma and the OS (the inner segment, IS) and of the process between the soma and the OPL (the axon). The diagrams at left show our interpretation of the labeling observed, for one of the cells labeled in the P23H-3 P16 material and for one of the cells labeled in the P23H-3 P500 material. In the P23H-3 retina, cones shorten strikingly with age, adapting to the thinning of the ONL, as rods die. No comparable thinning of the ONL was apparent in age-matched SD retinas. Scale bar, 10 μm.

deteriorated with age (Figs. 6A, 6B and Table 2). The a-wave amplitude underwent a more severe decline than the b-wave, dropping by 45% between P16 and P120, and a further 60% between P180 and P540. This compared to drops of 20% and 50% in the amplitude of the rod b-wave over comparable periods. The overall drop in amplitude over 540 days of life in the P23H-3 rat was 80% for the rod a-wave and 55% for the post-receptoral b-wave. Preservation of the rod b-wave after deterioration of the a-wave has been described previously in the P23H-3 retina,[3] and is thought to be due to remodelling in rod bipolar cell pathways.[23]

After P16, early in retinal development, differences in rod-mediated ERG responses between the rhodopsin-mutant P23H-3 retina and the non-degenerative SD retina were apparent (Figs. 5, 6A, 6B). At 20 and 24 days of age the average amplitudes of the rod a-wave and rod b-waves were smaller in the P23H-3 than the SD and this separation became significant ($P<0.05$) at P30, as reported previously.[3] The amplitude of rod responses remained significantly ($P<0.01$) lower in the P23H than in the SD at all ages studied. The difference in amplitude between the two strains of rat widened with age, and the effect was more pronounced in the a-wave than for the b-wave. The a-wave amplitude in the P23H-3 retina was 72% of the SD value at P30, 56% at P180, and 28% at P540. Comparable values for the rod b-wave amplitude were 74%, 62% and 51%.

Cone-Mediated Responses. It has previously been shown that the photopic b-wave in P23H-3 animals is normal until 200 days of age.[3] Present data confirm this finding and extend it, showing that cone-driven ERG responses in P23H-3 animals closely match those of SD controls up to 380 days of age (Figs. 5A-C, 6C and Table 2). Only at the oldest age studied (P540) could we see a significant ($P<0.01$) separation in post-receptoral cone responses between the non-degenerative and degenerative retinas (Figs. 5D, 6C). Between P380 and P540, the b-wave amplitude remained unchanged in the SD retina but dropped by 45% in the degenerative P23H-3 retina.

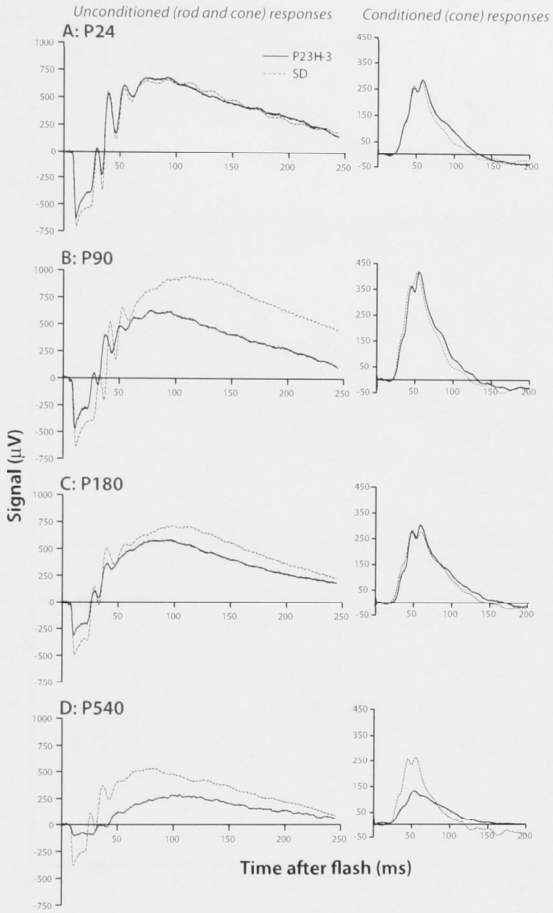

FIGURE 5. Sample waveforms of rod and cone ERG responses recorded from P23H-3 transgenic and age-matched SD control rats. The unconditioned responses (*left*) were recorded to a single flash stimulus of 44.5 cds/m^2 and include contributions from both rods and cones. The conditioned responses (*right*) were recorded to a flash (44.5 cds/m^2) given 395 ms after a rod-saturating conditioning flash, so that the responses represent cone activity.

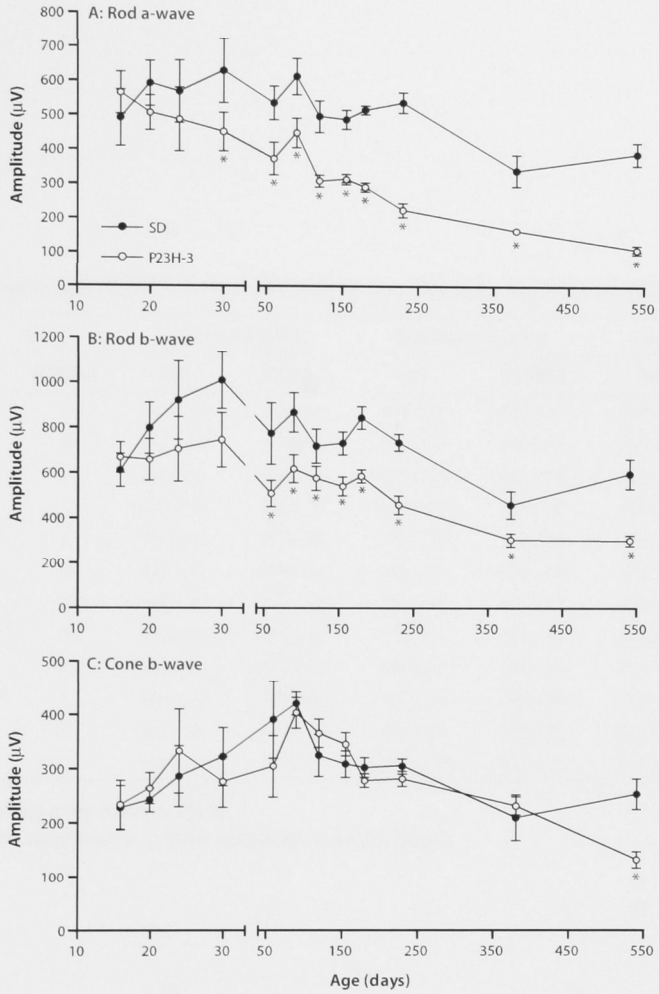

FIGURE 6. Comparison of rod and cone ERG responses between P23H-3 and SD retinas across ages 16 to 540 days. In response to a stimulus flash of 44.5 cds/m^2, three measures of amplitude were taken: (**A**) rod a-wave, (**B**) rod b-wave and (**C**) cone b-wave. Rod-mediated responses were significantly lower in the P23H-3 retina than the SD retina at all ages above P30, while there was no separation of cone function between the two strains up to P380. Data are presented as the mean ± SEM of 5-12 animals (see Table 2). Asterisks indicate data points that are significantly different from age-matched SD controls ($P<0.05$) by a Student's t-test.

TABLE 2. Comparison of ERG Responses Across Age Between the SD and P23H-3 Rat.

Age (days)	*n*		Rod a-wave (μV)*		Rod b-wave (μV)*		Cone b-wave (μV)*	
	SD	P23H-3	SD	P23H-3	SD	P23H-3	SD	P23H-3
16	4	7	492 ± 82	565 ± 61	611 ± 73	669 ± 67	228 ± 40	234 ± 45
20	5	6	593 ± 65	507 ± 51	798 ± 113	659 ± 91	243 ± 22	265 ± 28
25	5	5	569 ± 91	488 ± 92	921 ± 174	706 ± 142	287 ± 56	333 ± 77
30	5	6	630 ± 94	452 ± 56	1010 ± 126	747 ± 120	323 ± 53	277 ± 47
60	9	6	537 ± 48	375 ± 48	775 ± 135	510 ± 58	391 ± 71	305 ± 56
90	5	6	614 ± 53	450 ± 42	869 ± 87	620 ± 61	421 ± 21	404 ± 28
120	8	10	498 ± 46	310 ± 17	721 ± 75	578 ± 53	325 ± 39	366 ± 23
155	11	5	490 ± 28	315 ± 15	733 ± 50	542 ± 42	309 ± 24	346 ± 21
180	5	6	518 ± 12	292 ± 13	845 ± 50	588 ± 28	303 ± 18	279 ± 12
230	5	5	540 ± 30	225 ± 20	737 ± 36	460 ± 40	311 ± 14	282 ± 14
380	5	12	342 ± 45	166 ± 10	461 ± 60	305 ± 29	210 ± 42	232 ± 16
540	5	6	392 ± 33	111 ± 13	599 ± 65	303 ± 22	254 ± 28	132 ± 15

Tabulated values give mean ± SEM.
*Amplitude of response to a flash stimulus of 44.5 cds/m^2.

Retinal Thickness

To track total (rod and cone) photoreceptor loss over the time course of this study, measures of ONL thickness were made in the P23H-3 retina and compared to age-matched SD controls (Fig. 7). In both the degenerative and non-degenerative retina there was a 20% thinning of the ONL as the retina matured between P16 and P90, presumably reflecting developmental culling of the photoreceptor population. In the SD retina, no further ONL thinning was detected up to 540 days of age, while in the P23H-3 retina, cell loss in the ONL continued steadily and by 230 days of age the layer had thinned to 68% of the SD value. These findings are consistent with previous studies[3, 24] and the thinning of the P23H-3 retina can be explained by excess photoreceptor loss during development and a continuous low level of cell death during adulthood.[13] We extended the analysis of the ONL to the aged P23H-3 retina; the ONL remained approximately half the thickness of control retinas, but did not reduce measurably in thickness after P230.

Cones in the Mature Adult Retina

The status of cones in the aged P23H-3 retina, at a time when both rod and cone ERG responses are severely depressed, was compared to aged SD retina. There was no significant difference in the average density of LM cones between the P23H-3 retina and the SD retina at P350 or P500 (Fig. 8A, Table 1). However, while their numbers were comparable, cones in the aged P23H-3 retina had substantially shorter OSs than those in the SD aged retina (Figs. 1M-N, Fig. 8B).

DISCUSSION

Summary: Maintenance of Cone Numbers, Late Failure of Cone Function

From late retinal development to early adulthood (P16-P120), the excess rod loss that characterizes the P23H-3 rat retina begins, peaks and declines to low but still abnormal adult levels.[13] Clinically, this period corresponds to the initial development of symptoms of impaired

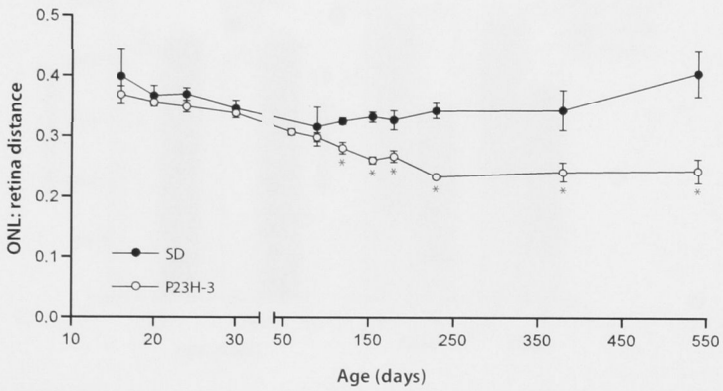

FIGURE 7. Measurements of ONL thickness in the P23H-3 and SD rat retina across ages 16 to 540 days. The P23H-3 retina thinned dramatically between 90 and 230 days of age, and then remained stable until P540. Over the same time (P90-P540), the thickness of the ONL in the SD rat was unchanged. Data are presented as the mean ± SEM of 5 animals. Asterisks indicate data points that are significantly different from age-matched SD controls ($P<0.05$) by a Student's t-test.

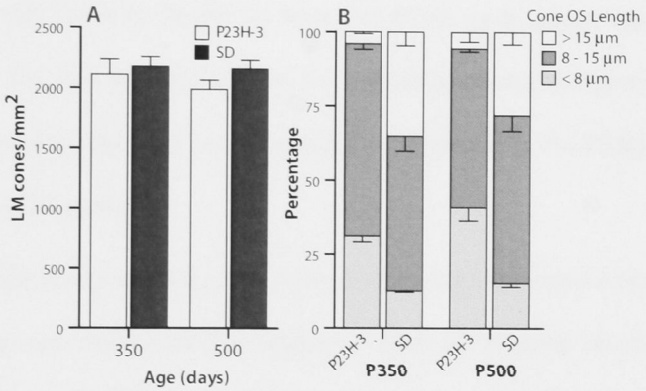

FIGURE 8. Comparison of cone density and OS length between aged P23H-3 and aged SD retinas. The mean density of LM cones (A) and the length of their OSs (B) in P23H-3 and SD retinas at 350 and 500 days of age was quantified using immunolabeled wholemounts. Data are presented as the mean ± SEM of 3 animals.

rod function, such as night blindness.[25] The current results show a 23% thinning of the ONL, and 45% and 20% reductions in the amplitude of the rod a-wave and b-wave during this period, supporting the histological and functional findings of rod loss previously reported.[3]

Novel data presented here show a 50% drop in cone density in the P23H-3 retina between 16 and 120 days of age. This fall in density may not result, however, from the death of cones. The growth in the area of retina continues to as late as P70,[26] while cone generation ends before birth[27] and, further, the amplitude of the cone b-wave increases during this period. This increase may be partly or wholly due to the substantial lengthening (by 80%) of cone OSs throughout early adulthood. The amplitude of the cone b-wave in the P23H-3 retina is maintained at levels found in the SD rat from P16-P120, again suggesting that cone function is not affected by the loss of rod numbers and signalling during this period. There is thus no evidence in these data that cone loss in this period is greater in the P23H-3 strain, than in the non-degenerative SD strain.

As the laboratory rat rarely lives beyond two years, the period from 120 to 540 days (18 months) of age covers mature and late adulthood. Data are available on photoreceptor status in the P23H-3 strain up to 200 days age.[3, 13] Present data show that the loss of rod ERG responses in the P23H-3 retina, both the a-wave and the postsynaptic b-wave, continues to P540. Cone function, by contrast, is maintained at levels seen in the SD until P365, falling below SD levels only at the oldest age examined (P540). This late period of cone failure in the P23H-3 rat retina may correspond to mature adulthood in humans with the same rhodopsin mutation, when the cone visual field constricts, and can fail completely.[25]

Previous work has shown that visual performance in rat models of retinal dystrophy cannot always be predicted from ERG amplitudes or ONL quantification.[28] The present evidence that cones maintain their signalling level and OSs longer than rods, and then survive as cells even when their signalling falls and OSs shorten, provides a basis for the persistence of cone-based behaviour. We are currently testing behavioural vision as a function of age in the P23H-3 rat using the optomotor head-turning response.

The steady decline of rod function and the late decline of cone function in the P23H-3 retina cannot be accounted for in terms of cell death. The thickness of the ONL does not decrease measurably after P200 and the density of cones also does not fall measurably during this period. For cones, the loss of b-wave amplitude can be explained, at least in part, by a substantial (20%) shortening of cone OSs. Thus it appears that both rods and cones are surviving at these late stages, but are damaged morphologically and functionally. In human patients with rhodopsin-mutant RP, cone function remains normal until more than 75% of rod OSs are lost, and cone dysfunction declines 3-4 times more slowly than rods.[29] The present finding that cone function in the P23H-3 rat persists undiminished for a year after the loss of rod function can be detected, indicates that this strain is a good model of cone degeneration in comparable human retinal dystrophies.

The accumulation of LM opsin in the inner segment, soma, processes and synaptic terminals, seen in a minority of cone cells in the P23H-3 retina at all ages from P16 to P500, and in aged SD retinas, allowed the overall morphology of cones to be followed. This 'redistribution' of opsins has been described in rods in the rd mouse,[30] rds mouse,[31, 32] P23H rat,[33] RCS rat,[34] an experimental model of retinal detachment,[35] a light damage model,[36] and the developing rat retina,[37] and for cones in human retinas with enhanced S cone syndrome,[19] X-linked cone degeneration,[20] and an autosomal dominant cone dystrophy.[18]

It has been postulated that redistribution of opsins results from either misplacement of newly synthesized opsin molecules or back diffusion of old opsin molecules from damaged OSs.[30, 34] In primates, cone opsins are present throughout the entire cell body when they are first expressed in the fetal period, and become restricted to the OS later in development.[38] In the present context, these observations show that cones adapt to the thinning of the ONL (as rods die) by reducing the length of their processes. The shortening of OSs can be considered a degenerative change, because it is associated with a reduction in ERG amplitude, but the overall shortening to cone cell length may be adaptive.

The Limits to Cone Survival

The survival of cones in retinas degenerating because of rod-specific mutations may depend on the rate and extent of rod dysfunction. The P23H-3 heterozygous rat used in the current study displays a relatively slow rate of rod degeneration, and cone function is not affected until P540. In the P23H-1 and homozygous P23H-3 strains, rod degeneration is more rapid, and cone dysfunction in these animals is evident much earlier, at P56[3] and P21[21, 22] respectively. In the *rd/rd* mouse, which carries a mutation in the gene for cGMP phosphodiesterase β-subunit, rod degeneration is particularly rapid. Cone degeneration is marked (25%) by 7 weeks of age, when 99.7% of rods have degenerated.[39] We are currently testing whether cone dysfunction can be induced by increasing rod degeneration rates in the P23H-3 heterozygote. The present results suggest that the cone ERG can fall 50% in amplitude, without a measurable loss of cone cells. If this is true in humans with comparable dystrophies, the repair of cones, induced by reducing the stress which is damaging, may restore cone function.

The Mechanism of Late Cone Damage

The question arises as to what causes cone dysfunction in the P23H-3 retina, given that cone numbers remain constant. As noted above, the shortening of cone OSs is an obvious cause of the functional decline, but the trigger for this shortening remains unclear. It has been suggested that dying rods release substances that are damaging to cones,[40] that alternatively cones are dependent on a rod-derived trophic factor,[41-43] and that cones are injured by oxidative damage due to decreased oxygen consumption by rods.[44, 45] In aged human RP retinas with various rhodopsin mutations, including the P23H, shortening of cone OSs is accompanied by downregulated expression of specialized cytoplasmic proteins such as calbindin, cone arrestin and cytochrome oxidase.[46, 47] Such protein expression changes may contribute to cone dysfunction in the late stages of RP. Further, it has been suggested that a general decrease in renewal of structural proteins may directly result in cone OS shortening.[47] Upregulation of

stress-induced factors known to suppress the ERG, such as FGF-2[48, 49] and CNTF[50, 51] are also likely to contribute to reductions in rod and cone responses in the aged P23H-3 retina.

Clinical Implications

The present results provide a baseline for assessing the impact of rod loss on cone integrity. Separately we report on the long-term impact of different levels of ambient illumination on the stability and performance of the adult P23H-3 retina,[52] and are currently testing the damaging effects of rapid rod loss on cones in the P23H-3 retina. Here we note that, when ambient conditions are held steady and low, cones are stable in function for a long period during which rods fail. Two avenues for optimizing the status of the adult retina can be identified. First, adult status is improved (more photoreceptors surviving and functional) if ambient conditions are optimized throughout life. Second, because many cones survive but suffer OS damage and shortening, the opportunity to create conditions for their self-repair[1] remains.

REFERENCES

1. Chrysostomou V, Stone J, Stowe S, Barnett NL, Valter K. The status of cones in the rhodopsin mutant P23H-3 retina: light-regulated damage and repair in parallel with rods. *Invest Ophthalmol Vis Sci* 2008;49:1116-1125.

2. Jozwick C, Valter K, Stone J. Reversal of functional loss in the P23H-3 rat retina by management of ambient light. *Exp Eye Res* 2006;83:1074-1080.

3. Machida S, Kondo M, Jamison JA, et al. P23H rhodopsin transgenic rat: correlation of retinal function with histopathology. *Invest Ophthalmol Vis Sci* 2000;41:3200-3209.

4. Walsh N, van Driel D, Lee D, Stone J. Multiple vulnerability of photoreceptors to mesopic ambient light in the P23H transgenic rat. *Brain Res* 2004;1013:194-203.

5. La Vail MM. Survival of some photoreceptor cells in albino rats following long-term exposure to continuous light. *Invest Ophthalmol* 1976;15:64-70.

6. Szél Á, Röhlich P. Two cone types of rat retina detected by anti-visual pigment antibodies. *Exp Eye Res* 1992;55:47-52.

7. Deegan JF, 2nd, Jacobs GH. On the identity of the cone types of the rat retina. *Exp Eye Res* 1993;56:375-377.

8. Neitz J, Jacobs GH. Reexamination of spectral mechanisms in the rat (Rattus norvegicus). *J Comp Psychol* 1986;100:21-29.

9. Radlwimmer FB, Yokoyama S. Genetic analyses of the green visual pigments of rabbit (Oryctolagus cuniculus) and rat (Rattus norvegicus). *Gene* 1998;218:103-109.

10. Yokoyama S, Radlwimmer FB, Kawamura S. Regeneration of ultraviolet pigments of vertebrates. *FEBS Lett* 1998;423:155-158.

11. Jacobs GH, Fenwick JA, Williams GA. Cone-based vision of rats for ultraviolet and visible lights. *J Exp Biol* 2001;204:2439-2446.

12. Szél A, Röhlich P, Van Veen T. Short-wave Sensitive Cones in the Rodent Retinas. *Exp Eye Res* 1993;57:503-505.

13. Yu D-Y, Cringle S, Valter K, Walsh N, Lee D, Stone J. Photoreceptor death, trophic factor expression, retinal oxygen status, and photoreceptor function in the P23H rat. *Invest Ophthalmol Vis Sci* 2004;45:2013-2019.

14. Goto Y, Peachey NS, Ripps H, Naash MI. Functional abnormalities in transgenic mice expressing a mutant rhodopsin gene. *Invest Ophthalmol Vis Sci* 1995;36:62-71.

15. Green ES, Menz MD, LaVail MM, Flannery JG. Characterization of rhodopsin mis-sorting and constitutive activation in a transgenic rat model of retinitis pigmentosa. *Invest Ophthalmol Vis Sci* 2000;41:1546-1553.

16. Steinberg RH, Flannery JG, Naash MI, et al. Transgenic rat models of inherited retinal degeneration caused by mutant opsin genes [ARVO Abstract]. *Invest Ophthal Vis Sci* 1996;37:S698. Abstract 3190.

17. Nixon PJ, Bui BV, Armitage JA, A.J. V. The contribution of cone responses to rat electroretinograms. *Clin Exp Ophthalmol* 2001;29:193-196.

18. Bonilha VL, Hollyfield JG, Grover S, Fishman GA. Abnormal distribution of red/green cone opsins in a patient with an autosomal dominant cone dystrophy. *Ophthalmic Genet* 2005;26:69-76.

19. Milam AH, Rose L, Cideciyan AV, et al. The nuclear receptor NR2E3 plays a role in human retinal photoreceptor differentiation and degeneration. *Proc Natl Acad Sci U S A* 2002;99:473-478.

20. To KW, Adamian M, Jakobiec FA, Berson EL. Histopathologic and immunohistochemical study of an autopsy eye with X-linked cone degeneration. *Arch Ophthalmol* 1998;116:100-103.

21. Pinilla I, Lund RD, Sauve Y. Enhanced cone dysfunction in rats homozygous for the P23H rhodopsin mutation. *Neuroscience Letters* 2005;382:16-21.

22. Cuenca N, Pinilla I, Sauve Y, Lu B, Wang S, Lund RD. Regressive and reactive changes in the connectivity patterns of rod and cone pathways of P23H transgenic rat retina. *Neuroscience* 2004;127:301-317.

23. Aleman TS, LaVail MM, Montemayor R, et al. Augmented rod bipolar cell function in partial receptor loss: an ERG study in P23H rhodopsin transgenic and aging normal rats. *Vision Res* 2001;41:2779-2797.

24. LaVail MM, Yasumura D, Matthes MT, et al. Ribozyme rescue of photoreceptor cells in P23H transgenic rats: long-term survival and late-stage therapy. *Proc Natl Acad Sci USA* 2000;97:11488-11493.

25. Berson EL, Rosner B, Sandberg MA, Dryja TP. Ocular findings in patients with autosomal dominant retinitis pigmentosa and a rhodopsin gene defect (Pro-23-His). *Arch Ophthalmol* 1991;109:92-101.

26. McCall M, Robinson S, Dreher B. Differential retinal growth appears to be the primary factor producing the ganglion cell density gradient in the rat. *Neurosci Lett* 1987;78-84.

27. Rapaport DH, Wong LL, Wood ED, Yasumura D, LaVail MM. Timing and topography of cell genesis in the rat retina. *J Comp Neurol* 2004;474:304-324.

28. McGill TJ, LaVail MM, Douglas RM, et al. Discrepant Anatomical, Electrophysiolgical, and Behavioral Profiles of Retinal Degeneration in Rat Models of Retinal Degenerative Disease. *Invest Ophthalmol Vis Sci* 2007;48:3448-.

29. Cideciyan AV, Hood DC, Huang Y, et al. Disease sequence from mutant rhodopsin allele to rod and cone photoreceptor degeneration in man. *Proc Natl Acad Sci USA* 1998;95:7103-7108.

30. Nir I, Agarwal N, Sagie G, Papermaster DS. Opsin distribution and synthesis in degenerating photoreceptors of rd mutant mice. *Experimental Eye Research* 1989;49:403-421.

31. Nir I, Papermaster DS. Immunocytochemical localization of opsin in the inner segment and ciliary plasma membrane of photoreceptors in retinas of rds mutant mice. *Invest Ophthalmol Vis Sci* 1986;27:836-840.

32. Usukura J, Bok D. Changes in the localization and content of opsin during retinal development in the rds mutant mouse: immunocytochemistry and immunoassay. *Exp Eye Res* 1987;45:501-515.

33. Roof DJ, Adamian M, Hayes A. Rhodopsin accumulation at abnormal sites in retinas of mice with a human P23H rhodopsin transgene. *Invest Ophthalmol Vis Sci* 1994;35:4049-4062.

34. Nir I, Papermaster DS. Immunocytochemical localization of opsin in degenerating photoreceptors of RCS rats and rd and rds mice. *Prog Clin Biol Res* 1989;314:251-264.

35. Lewis GP, Erickson PA, Anderson DH, Fisher SK. Opsin distribution and protein incorporation in photoreceptors after experimental retinal detachment. *Exp Eye Res* 1991;53:629-640.

36. Edward DP, Lim K, Sawaguchi S, Tso MO. An immunohistochemical study of opsin in photoreceptor cells following light-induced retinal degeneration in the rat. *Graefes Arch Clin Exp Ophthalmol* 1993;231:289-294.

37. Nir I, Cohen D, Papermaster DS. Immunocytochemical localization of opsin in the cell membrane of developing rat retinal photoreceptors. *J Cell Biol* 1984;98:1788-1795.

38. Xiao M, Hendrickson A. Spatial and temporal expression of short, long/medium, or both opsins in human fetal cones. *J Comp Neurol* 2000;425:545-559.

39. Mohand-Said S, Hicks D, Dreyfus H, Sahel JA. Selective transplantation of rods delays cone loss in a retinitis pigmentosa model. *Arch Ophthalmol* 2000;118:807-811.

40. Ripps H. Cell death in retinitis pigmentosa: gap junctions and the `Bystander' Effect. *Exp Eye Res* 2002;74:327-336.

41. Hicks D, Sahel J. The implications of rod-dependent cone survival for basic and clinical research. *Invest Ophthalmol Vis Sci* 1999;40:3071-3074.

42. Leveillard T, Mohand-Said S, Lorentz O, et al. Identification and characterization of rod-derived cone viability factor. *Nat Genet* 2004;36:755-759.

43. Mohand-Said S, Deudon-Combe A, Hicks D, et al. Normal retina releases a diffusible factor stimulating cone survival in the retinal degeneration mouse. *Proc Natl Acad Sci USA* 1998;95:8357-8362.

44. Shen J, Yang X, Dong A, et al. Oxidative damage is a potential cause of cone cell death in retinitis pigmentosa. *J Cell Physiol* 2005;203:457-464.

45. Stone J, Maslim J, Valter-Kocsi K, et al. Mechanisms of photoreceptor death and survival in mammalian retina. *Prog Ret Eye Res* 1999;18:689-735.

46. Zhang H, Cuenca N, Ivanova T, et al. Identification and Light-Dependent Translocation of a Cone-Specific Antigen, Cone Arrestin, Recognized by Monoclonal Antibody 7G6. *Invest Ophthalmol Vis Sci* 2003;44:2858-2867.

47. John SK, Smith JE, Aguirre GD, Milam AH. Loss of cone molecular markers in rhodopsin-mutant human retinas with retinitis pigmentosa. *Mol Vis* 2000;6:204-215.

48. Gargini C, Belfiore MS, Bisti S, Cervetto L, Valter K, Stone J. The impact of basic fibroblast growth factor on photoreceptor function and morphology. *Invest Ophthalmol Vis Sci* 1999;40:2088-2099.

49. Gargini C, Bisti S, Demontis GC, Valter K, Stone J, Cervetto L. Electroretinogram changes associated with retinal upregulation of trophic factors: observations following optic nerve section. *Neuroscience* 2004;126:775-783.

50. Bok D, Yasumura D, Matthes MT, et al. Effects of adeno-associated virus-vectored ciliary neurotrophic factor on retinal structure and function in mice with a P216L rds/peripherin mutation. *Exp Eye Res* 2002;74:719-735.

51. Schlichtenbrede FC, MacNeil A, Bainbridge JW, et al. Intraocular gene delivery of ciliary neurotrophic factor results in significant loss of retinal function in normal mice and in the Prph2Rd2/Rd2 model of retinal degeneration. *Gene Ther* 2003;10:523-527.

52. Valter K, Kirk DK, Stone J. The potential of ambient light restriction to restore function to the degenerating P23H-3 rat retina. *Adv Exp Med Biol* 2008;613:193-199.

CHAPTER 4

Cone Recovery

Cones in the Rhodopsin Mutant P23H-3 Retina: Light-Regulated Damage and Repair in Parallel with Rods

Vicki Chrysostomou,[1] *Jonathan Stone,*[1] *Sally Stowe,*[1] *Nigel L. Barnett,*[2] *and Krisztina Valter*[1]

PURPOSE. This study tests whether cones in the rhodopsin-mutant transgenic P23H-3 retina are damaged by ambient light, and whether subsequent light restriction allows repair of damaged cones. **METHODS.** P23H-3 rats were raised in scotopic cyclic (12 h at 5 lux, 12 h dark) ambient light. At postnatal day 90-130, some were transferred to photopic conditions (12 h 300 lux, 12 h dark) for 1 week, and then returned to scotopic conditions for up to 5 weeks. Photoreceptor function was assessed by the dark-adapted flash-evoked electroretinogram, using a two-flash paradigm to isolate the cone response. Outer segment structure was demonstrated by immunohistochemistry for cone and rod opsins, and by electron microscopy. **RESULTS.** Exposure for 1 week to photopic ambient light reduced the cone b-wave, the rod b-wave and the rod a-wave by 40-60%, and caused shortening and disorganization of cone and rod outer segments. Restoration of scotopic conditions for 2-5 weeks allowed partial recovery of the cone b-wave as well as the rod a- and b-waves, and regrowth of outer segments. **CONCLUSIONS.** Modest increases in ambient light cause rapid and significantly reversible loss of cone and rod function in the P23H-3 retina. The reduction and recovery of cone function are associated with shortening and regrowth of outer segments. Because the P23H mutation affects a protein expressed specifically in rods, this study emphasizes the close dependence of cones on rod function. It also demonstrates the capacity of cones, as well as rods, to repair their structure and regain function.

From the [1]CNS Stability and Degeneration Group and the ARC Centre of Excellence in Vision Science, Research School of Biological Sciences, The Australian National University, Canberra, Australia; and the [2]Vision, Touch, and Hearing Research Centre, School of Biomedical Sciences, University of Queensland, Brisbane Australia.

Supported by grants from Retina Australia, the National Health and Medical Research Council of Australia, and the Australian Research Council.

Submitted for publication September 5, 2007; revised October 5 and 10, 2007; accepted December 26, 2007.

Disclosure: V. Chrysostomou, None; J. Stone, None; S. Stowe, None; N. L. Barnett, None; K. Valter, None

Corresponding author: Jonathan Stone, Research School of Biological Sciences, The Australian National University, GPO Box 475, Canberra, ACT 2601, Australia; stone@rsbs.anu.edu.au.

Investigative Ophthalmology & Visual Science, March 2008, Vol. 49, No. 3; 49:1116-1125.

Cone vision is affected in virtually all forms of retinal degeneration, even though many of the mutations known to cause photoreceptor degeneration affect proteins expressed specifically in rods. The loss of cone vision is therefore considered secondary to damage to rods. For the individuals affected, however, the loss of cone vision is particularly debilitating, and its amelioration is of prime concern.

Two mechanisms have been proposed which might lead from rod damage to cone damage. One is that rods produce a factor essential for cone survival,[1-3] and that rod loss reduces the expression of this factor below the levels required for cone integrity. In 1999 we[4] suggested a more general mechanism, involving oxidative damage. We proposed that depletion of the photoreceptor population (rod or cone) by any cause would reduce consumption of oxygen flowing from the choroidal circulation. Because this flow of oxygen is unregulated, photoreceptor depletion will cause a chronic rise in oxygen tension in outer retina,[5, 6] and this rise in oxygen tension is toxic to surviving photoreceptors (cones as well as rods). The vulnerability of photoreceptors to hyperoxia has also been confirmed,[7-9] and evidence has been reported that rod loss results in oxidative damage to cones.[10] We further proposed that this chronic hyperoxia will cause sub-lethal damage to surviving photoreceptors, and that that damage may be reversible, allowing the restoration of photoreceptor function.

The idea that limiting the exposure of the retina to light might slow retinal degeneration goes back over 100 years[11] (cited in Ref. 12). In animal models, including the Royal College of Surgeons (RCS) rat,[12, 13] the P23H-3 transgenic mouse[14, 15] and rat,[16] and in the rhodopsin-mutant dog,[17] light restriction (typically dark-rearing) has been shown to slow, or light exposure to accelerate, retinal degeneration. In humans suffering retinal degeneration, however, attempts to slow degenerations by light restriction have reported mixed success, Berson[18] reporting no effect, while Pe'er and Meron[4] reported slowing of visual field loss in 10 of 14 patients. Several recent reports have called for the trial of light restriction in human retinal degenerations, based on evidence that retinas undergoing many forms of degeneration are abnormally sensitive to damage by light,[17, 19] and that restriction slows mutation-induced degenerations (reviewed in Ref.

[20]) and can reverse damage to rod structure and function caused by physiological variations in ambient light.[21] In this study we confirm that rods in the P23H-3 retina are hypersensitive to physiological increases in ambient light,[19] when compared to a similarly pigmented control Sprague-Dawley strain, and can recover structure and function when ambient light levels are reduced.[21] We test whether cones are damaged by the same light exposure, and can recover structure and function when light levels are reduced. The results give insight into the dependence of cones on rod function, and demonstrate the capacity of cones to recover structure and resume function after damage.

METHODS

Animals

All procedures were in accord with the ARVO Statement for the Use of Animals in Ophthalmic and Vision Research, and with the requirements of The Australian National University Animal Experimentation Ethics Committee. Observations were made in transgenic rats containing the P23H mutation on the rhodopsin gene (Line 3, from Beckman Laboratories, University of California, San Francisco). P23H-3 homozygous animals were established as a breeding colony. The animals used in the present experiments were heterozygotes, the offspring of mating P23H-3 homozygotes with Sprague-Dawley (SD) albinos.

Experimental Design

P23H-3 animals were raised in cyclic ambient light (12 h light, 12 h dark) with the light phase at 5 lux (scotopic conditions), to postnatal day 90-130. Animals were moved to photopic ambient conditions (12 h 300 lux, 12 h dark) for 1 week (1w), and then returned to scotopic conditions for up to 5 weeks (5w). The status of photoreceptors was assessed (as below) before the exposure to photopic conditions, at the end of the 1w exposure, and 2w and 5w after exposure. The electroretinogram (ERG) was recorded serially from seven animals at each of the above four time points. Tissue was collected from an additional five animals at each time point. Tissue from scotopic-reared SD rats was processed for comparison.

Tissue Collection and Processing

Animals were euthanized with an overdose of sodium pentobarbital (>60 mg/kg, intraperitoneal). Eyes were marked with an insoluble projection pen at the superior aspect of the limbus for orientation, enucleated and immersion-fixed in 4% paraformaldehyde in 0.1 M phosphate-buffered saline (PBS) at pH 7.4 for 3 h. The left eye of each animal was processed for cryosectioning and the right eye was processed for wholemounts or electron microscopy. For cryosectioning, eyes were rinsed twice in 0.1 M PBS and left in a 15% sucrose solution overnight to provide cryoprotection. Eyes were embedded in Tissue-Tek OCT Compound (Sakura Finetek, Tokyo, Japan), and snap frozen in liquid nitrogen before taking 12 μm cryosections at -20 °C (Leica CM1850 Cryostat). Sections were mounted on gelatin and poly-L-lysine-coated slides and dried overnight at 50°C before being stored at -20°C. For retinal wholemounts, the retina was dissected from the eyecup, flattened by making radial incisions, gently sandwiched between two glass slides and immersed in 4% paraformaldehyde at 4°C for up to 2w before labeling.

Outer Segment Status

Immunohistochemistry of Sections. Cryosections were labeled with rabbit polyclonal antibodies to L/M opsin (1:1000, Chemicon, Temecula, CA) and mouse monoclonal antibodies to rod opsin (1:100, Rho4D2, a gift from Dr. Robert Molday, Vancouver, Canada). Sections were washed in 70% ethanol for 15 min, followed by a 5 min wash in distilled H2O and two 5 min washes in 0.1 M PBS. Sections were then blocked with 10% normal goat serum in 0.1 M PBS for 1 h before being incubated for 24 h at 4°C with a mixture of the above primary antibodies. After two 10 min washes in 0.1 M PBS, sections were treated with an antibody to rabbit IgG conjugated with Alexa Fluor 488 and with an antibody to mouse IgG conjugated to Alexa Fluor 594 (1:1000, Molecular probes, Eugene, OR) for 24 h at 4°C. After washing twice in 0.1 M PBS, sections were incubated for 2 min with the DNA-specific dye bisbenzamide (1:10 000) in 0.1 M PBS before being coverslipped with a glycerol/gelatin medium.

Measurements of cone outer segment (OS) length were made on digital images of cryosections immunolabeled with L/M opsin. Sections were scanned from the superior to inferior edge of the retina and, at regularly spaced intervals, the length of L/M opsin-stained OSs was measured (a total of at least 24 measurements per retina). Results from 5 animals at each time point were averaged and analyzed by the statistical method described below.

Immunohistochemistry of Wholemounts. Retinas were dehydrated in ascending ethanols, incubated in 100% ethanol for 24 h at 4°C and then rehydrated. The tissue was rinsed twice in 0.01% Triton-PBS and blocked in normal goat serum for 2 h before incubation with rabbit polyclonal antibodies to L/M opsin (1:1000, Chemicon, Temecula, CA) for 24 h. After washing in 0.01% Triton-PBS, retinas were incubated for 24 h with an antibody to rabbit IgG conjugated to Alexa Fluor 488 (1:1000, Molecular probes, Eugene, OR) and subsequently mounted and coverslipped on glass slides with the photoreceptor OSs facing up. To measure L/M cone density we photographed the OS layer using a 10x objective, systematically reconstructing the whole surface; this required ~ 200 separate digital images, spliced into a full montage. Cone OS density was then measured over areas of 0.01 mm^2, spaced at 0.5 mm intervals across the whole surface.

Electron Microscopy. After removal, eyes were immersed in cold fixative (2.5% glutaraldehyde plus 3.5 % formaldehyde in 0.1 M sodium cacodylate buffer, pH 7.4. with 5 mM EGTA and 2 mM MgCl2), and the lens removed rapidly. Within 10-15 min, eyes were microwaved on ice using 6 x 10s bursts at 10s intervals, at 80 mW, in a Pelco histological Biowave microwave oven. After 2-4 h further fixation at 4°C, the anterior portions of the eyes were removed and selected retinal pieces dissected out. After washing in cacodylate buffer and postfixation in 1% osmium tetroxide in the same buffer, the tissue was dehydrated through ethanol and acetone and embedded in Epon-Araldite. Sections were cut at 50-80 nm (Leica Ultracut E), stained with uranyl acetate alone or followed by Reynold's lead citrate, and viewed at 75 kV in a Hitachi H7100 transmission electron microscope (TEM). Half-micron thick sections from the same blocks were stained with toluidine blue for light microscopy.

Retinal Thickness Measurements

Measurements were made on digital images of cryosections stained with bisbenzamide. At each measurement location, the thickness of the outer nuclear layer (ONL) as well as the thickness of the retina, from inner to outer limiting membrane (ILM-OLM), was recorded. The ratio of ONL to ILM-OLM was used for analysis to account for obliquely-cut sections. In at least two sections per animal, we took four measurements, approximately 100 μm apart, from both the superior and inferior mid-peripheral areas of the retina (a total of at least 16 measurements per animal). Results from 5 animals at each time point were averaged and analysed by the statistical method described below.

Electroretinography

The function of photoreceptors was assessed from the flash-evoked ERG, as described previously.[19] Animals were dark-adapted overnight, and prepared in dim red illumination. We used a two flash paradigm to isolate the cone and (by subtraction) the rod responses of the ERG. To establish consistent recording conditions, we recorded responses to a range of test flash intensities (4.45×10^{-4} to 4.45×10^{2} cd.s.m^{-2}). For the quantitative comparisons in Figures 3-4, we recorded responses to a standard test flash (44.5 cd.s.m^{-2}); and then repeated the recordings with the test flash preceded, by 395 msec, by a conditioning flash (12 cd.s.m^{-2}). Following previous reports,[22] the unconditioned response can be considered to be 'mixed', with contributions from rods and cones. The conditioned responses are those of cones and, by subtracting the latter from the former, the rod response can be isolated.

We used three measurements of ERG amplitude, as shown in Figure 1. First, because there was no measurable a-wave in the cone response, confirming,[22] we measured the a-wave in the mixed response and recorded it as the rod a-wave (downward arrow). Second, we measured the amplitude of the b-wave in the cone response (right double-headed arrow). Third, we measured the b-wave in the mixed response, subtracted the cone response to obtain an isolated rod response, and measured the b-wave in that waveform (left double-headed arrow).

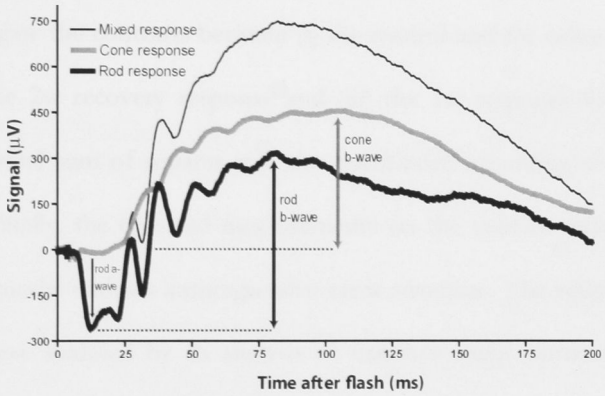

FIGURE 1. Representative ERG responses, from an adult P23H-3 rat. One is the response of the dark-adapted retina to a single flash (44.5 cd.s.m^{-2}), and contains both rod and cone components ('mixed response'). One response is to the same flash, preceded at 395 msec by a rod-saturating flash (12 cd.s.m^{-2}) and shows the cone component ('cone response'). The third trace ('rod response') was obtained by subtracting the latter from the former. *Down arrow:* the rod a-wave was measured. *Double-headed arrows:* the cone and rod b-waves were measured. Because an a-wave could not be elicited in the cone response, the a-wave has the same amplitude in the mixed and rod responses.

Only responses recorded when body temperature was in the range 36.8 –37.6°C were included. Seven animals raised in scotopic (5 lux) ambient light were studied. In each, the ERG was recorded before and after a 1w exposure to photopic (300 lux cyclic) ambient light, and then 2w and 5w after the animal was returned to scotopic conditions.

Statistical Analyses

To account for inter-animal variability in ERG responses, the ERG data were analysed as a randomized complete block design using the seven animals as blocks and the interaction between animals and the four treatments as residual. The analysis of variance was then sub-modeled to investigate the contrasts between (i) the control and the other treatments (ii) the 1w response versus the 2w recovery response and (iii) the 1w response versus the 5w recovery response. The residual sum of squares was also partitioned according to interactions with the above contrasts. Finally, the repeated measurements on the animals were investigated using a generalized linear model with an autoregressive error structure. The retinal thickness and cone OS length data were analysed by an analysis of variance using contrasts to compare (i) the control versus the 1w photopic values (ii) the 1w versus the 2w recovery values and (iii) the 1w versus the 5w recovery values. For all analyses, $P<0.05$ was considered to represent a statistically significant difference.

RESULTS

Effects of Ambient Light on the Function of the P23H-3 Retina

Ambient Light-Induced Loss and Recovery of the Cone and Rod b-Waves. The amplitude of the cone b-wave fell after a 1w exposure to 300 lux cyclic light (Figs. 2A-B), then recovered significantly over the next 2-5w (Figs. 2C-D). As shown in Figure 3A for seven different animals, each recorded serially, the amplitude of the cone b-wave varied considerably between animals. In every animal, however, 1w exposure to photopic ambient light reduced the b-wave by approximately 50%, and reduction of illumination to scotopic levels for 2-5w led to a recovery of amplitude. When values were averaged over the seven animals studied at each time

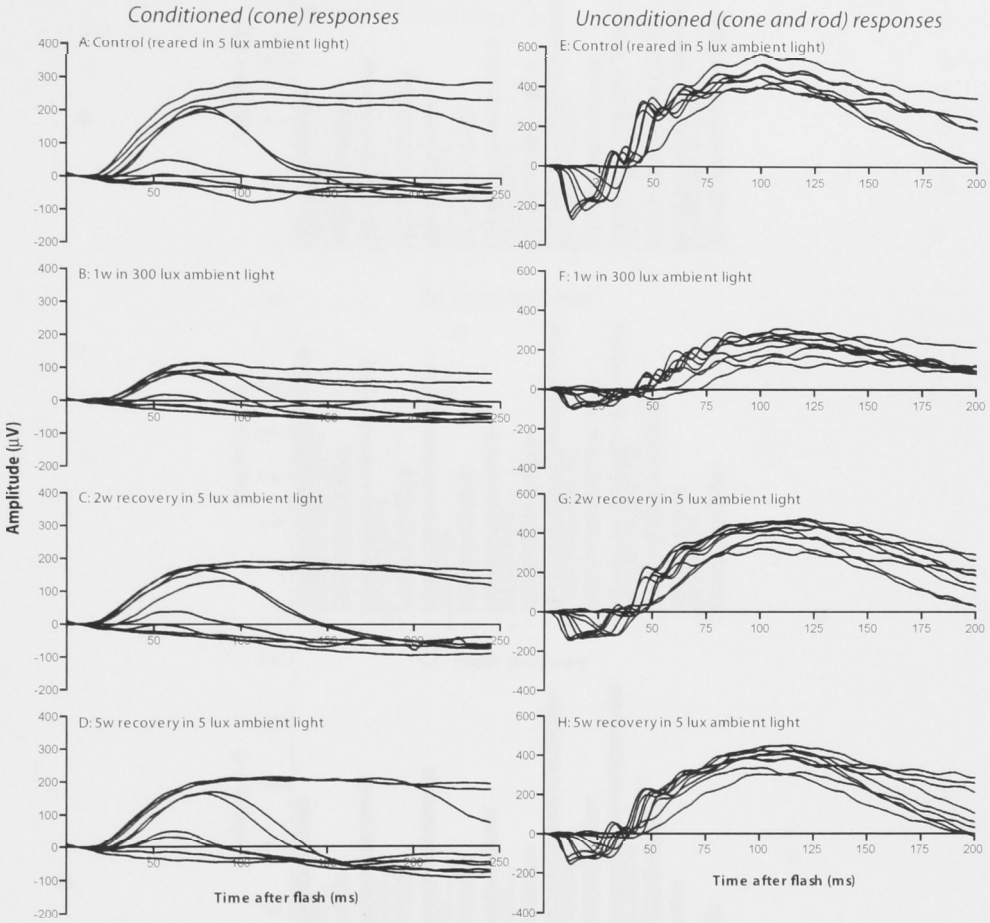

FIGURE 2. Sample intensity series. In each case the retina was dark adapted and the responses were elicited to flashes with intensities from 4.45 x 10^{-4} to 4.45 x 10^{2} cd.s.m^{-2}. All traces are from the same animal, recorded serially. (**A-D**) These responses were recorded to a flash given 395 msec after a conditioning flash. The conditioning flash saturates the rods at the time of the second flash, so that the responses obtained represent cone activity. (**E-H**) These responses were recorded without a preconditioning flash, and include contributions from both rods and cones. The amplitudes of both cone and rod responses were reduced by 1w photopic light exposure and then recovered substantially after 2-5w recovery in scotopic conditions.

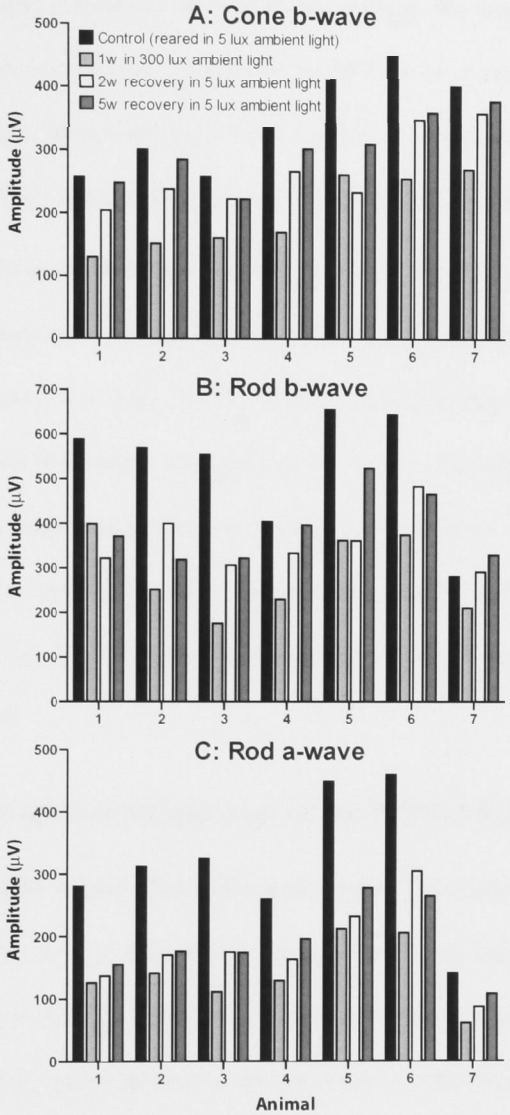

FIGURE 3. Amplitudes of the ERG cone b-wave (**A**), rod b-wave (**B**) and rod a-wave (**C**) for seven P23H-3 animals. The stimulus used for all measures was a flash of intensity 44.5 cd.s.m^{-2}. For each animal, four values are shown: the amplitudes recorded before (control) and immediately after the 1w exposure to photopic ambient light; and the amplitudes recorded 2w and 5w after the animal was returned to scotopic conditions. The absolute values of the signal vary, but in each case photopic light exposure reduced amplitude, and the amplitude recovered in scotopic conditions.

point (Fig. 4A), the fall and recovery were both statistically significant (Table 1). When the data for each animal were normalized to the control value, photopic ambient light reduced the cone b-wave, on average, to 57% of the control value. From this, it recovered to 87% of the control value after 5w in scotopic conditions. By the same analysis, the amplitude of rod b-wave was reduced by 1w exposure to photopic conditions to 56% of its control value, and recovered in scotopic conditions (Figs. 3B and 4B) to 78% of control, in a pattern very similar to the cone b-wave. The fall and recovery in amplitude of the rod b-wave was statistically significant (Table 1).

Ambient Light-Induced Loss and Recovery of the Rod a-Wave. The amplitude of the rod a-wave fell sharply after 1w exposure to 300 lux cyclic light (Figs. 2E-F), then recovered significantly over the next 2-5 w (Figs. 2G-H). When quantified (Figs. 3C and 4C), it was evident that the amplitude of the rod a-wave was reduced by the 1w photopic ambient light to 45% of control value, and then recovered to 63% of control. The reduction of the a-wave at the end of 1w exposure to photopic ambient light and the recovery after 2w and 5w in scotopic conditions were significant (Table 1). The reduction and recovery of the a-wave confirm earlier reports from this laboratory.[19, 21]

Effects of Ambient Light on Morphology of the P23H-3 Retina

Relative Stability of the Outer Nuclear Layer. The marked reductions of cone and rod responses caused by the 1w exposure to photopic ambient light (above) were associated with a limited thinning of the ONL (Fig. 5; Table 2), confirming Jozwick and colleagues.[21] The slow thinning of the ONL continued during the recovery of cone and rod function, over the 5w period examined. In the present data the reduction in thickness reached statistical significance in the vulnerable superior region of retina after 2w and 5w recovery. Thinning of the inferior retina was significant only at the 5w recovery time point. In a minority of animals, the ONL thinned appreciably during the 2-5w recovery period, over a small area of superior mid-peripheral retina. In these animals, the recovery of the ERG occurred despite this localized area of photoreceptor death.

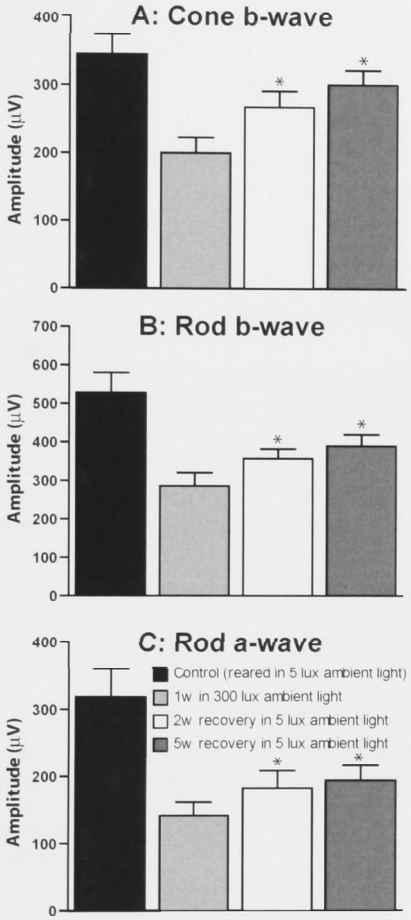

FIGURE 4. Average amplitudes of the cone b-wave (**A**), rod b-wave (**B**) and rod a-wave (**C**). The stimulus used for all measures was a flash of intensity 44.5 cd.s.m^{-2}, as for Figure 3. The histograms show means and standard errors for the seven animals studied. The asterisks on the 2w and 5w recovery values indicate that they are significantly larger than the 1w 300 lux value (Table 1).

TABLE 1. Reduction and recovery of the ERG in the P23H-3 rat in response to variations of ambient light.

	n	ERG amplitude (μV)*	P†
Cone b-wave			
Control vs 1w photopic	7 vs 7	351 ± 32 vs 201 ± 23	<0.001
1w photopic vs 2w recovery	7 vs 7	201 ± 23 vs 268 ± 24	<0.001
1w photopic vs 5w recovery	7 vs 7	201 ± 23 vs 303 ± 22	<0.001
Rod b-wave			
Control vs 1w photopic	7 vs 7	529 ± 52 vs 287 ± 34	<0.001
1w photopic vs 2w recovery	7 vs 7	287 ± 34 vs 357 ± 25	0.028
1w photopic vs 5w recovery	7 vs 7	287 ± 34 vs 390 ± 30	0.017
Rod a-wave			
Control vs 1w photopic	7 vs 7	327 ± 36 vs 147 ± 17	<0.001
1w photopic vs 2w recovery	7 vs 7	147 ± 17 vs 191 ± 22	<0.001
1w photopic vs 5w recovery	7 vs 7	147 ± 17 vs 200 ± 19	0.003

*Non-normalized; mean ± SEM.
†By analysis of variance.

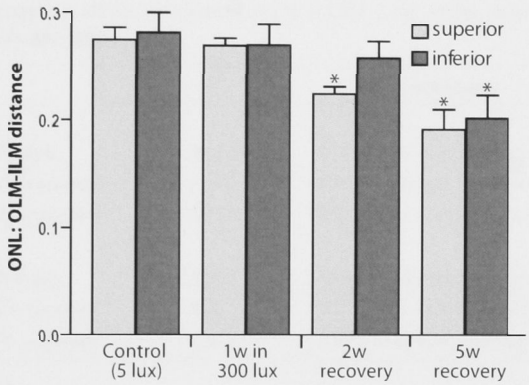

FIGURE 5. During the 6w course of the experiment the ONL thinned slightly, presumably reflecting the underlying death of photoreceptors in the P23H-3 strain. Thinning of the ONL was most pronounced in the superior retina. The histograms show means and standard errors (n=5) and asterisks indicate values significantly different from the control (Table 2).

TABLE 2. Changes in retinal thickness in the P23H-3 rat retina in response to variations of ambient light.

	n	ONL thickness	P†
Superior retina			
Control vs 1w photopic	5 vs 5	0.27 ± 0.01 vs 0.27 ± 0.01	0.789
1w photopic vs 2w recovery	5 vs 5	0.27 ± 0.01 vs 0.22 ± 0.01	0.032
1w photopic vs 5w recovery	5 vs 5	0.27 ± 0.01 vs 0.19 ± 0.02	<0.001
Inferior retina			
Control vs 1w photopic	5 vs 5	0.28 ± 0.02 vs 0.27 ± 0.02	0.705
1w photopic vs 2w recovery	5 vs 5	0.27 ± 0.02 vs 0.26 ± 0.02	0.751
1w photopic vs 5w recovery	5 vs 5	0.27 ± 0.02 vs 0.20 ± 0.02	0.030

*Mean ± SEM.
†By analysis of variance.

Lability of Cone and Rod Outer Segments. Both cone and rod OSs, identified by opsin immunohistochemical labeling, were markedly reduced in length by 1w exposure to photopic ambient illumination (Figs. 6A, 6B). During the 5w recovery in scotopic conditions, both cone and rod OSs lengthened substantially (Figs. 6C, 6D). Quantitatively, exposure to photopic light for 1w resulted in a 61% reduction of cone OS length. After 5w recovery in scotopic conditions, cone OS length regrew to 89% of the control value (Fig. 7). Both the reduction and recovery of cone OS length was significant (Table 3).

The relatively low density of cone OSs, approximately 2,000/mm^2 in the mid-periphery, meant that the distribution of individual cones could be clearly seen in L/M opsin-labeled wholemount preparations. The lability of cone OS length in response to changes in ambient light levels was clear in these preparations (Figs. 6E-L). After 1w in photopic conditions (Figs. 6F, 6J) the OSs were still present but much shorter. After 2w and 5w recovery in scotopic conditions (Figs. 6G, 6K, 6H, 6L), cone OSs had regained length. Their density remained close to 2,000/mm^2 throughout.

In half-micron thick sections of blocks taken from central retina and prepared for electron microscopy, cone and rod OSs are difficult to distinguish, but their overall shortening and regrowth were confirmed (Fig. 8).

Topography of the Shortening and Regrowth of Cone Outer Segments. The effects of light exposure and restriction on OS structure were not uniform across the retina. Two non-uniformities were observed. First, in control retinas, OSs of cones were shorter and more damaged at the anterior edge of the retina than in the mid-periphery (compare Fig. 6M with Figs. 6E, 6I). This confirms a previous report[23] of chronic photoreceptor damage at the anterior edge of the retina. OSs at the edge were not further damaged by the 1w exposure to photopic ambient light and, correspondingly, did not repair themselves in the subsequent 2-5w in scotopic conditions (Figs. 6N-P). Second, the shortening effect of 1w in 300 lux was consistently more severe in superior than inferior retina (compare Figs. 6F and 6J). It is

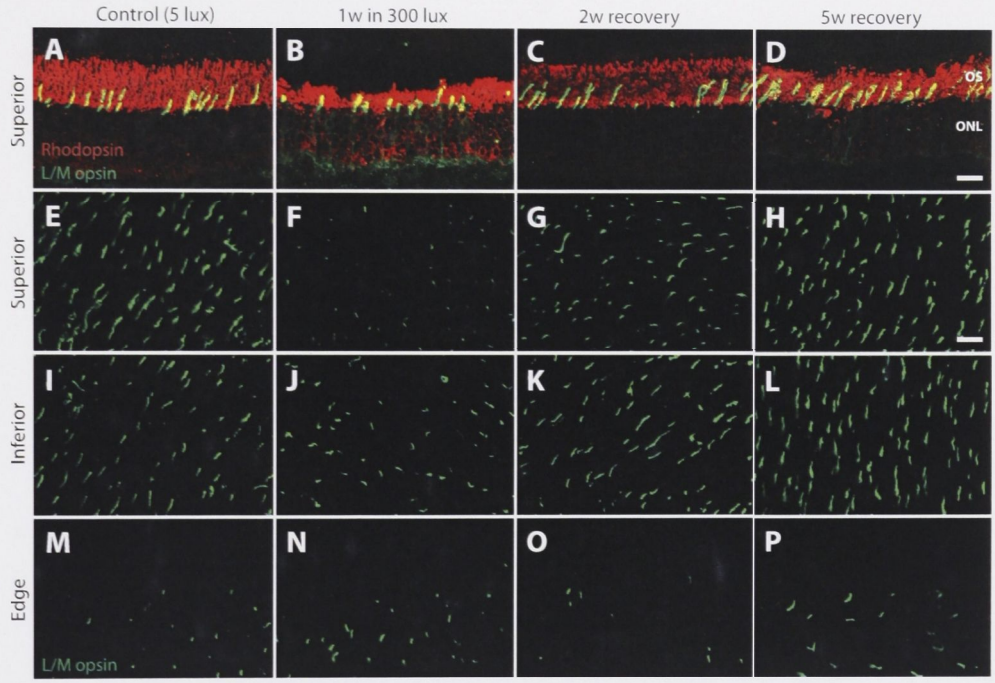

FIGURE 6. Immunohistochemical labeling of photoreceptor OSs using antibodies for cone L/M opsin (*green*) and rhodopsin (*red*). (**A-D**) In retinal sections, the OSs of cones and rods was markedly reduced in length by 1w exposure to photopic ambient illumination and regrew significantly over the recovery period. (**E-P**) The shortening and regrowth of cone OSs was also seen in wholemount preparations, where shortening was more severe in superior (**E-H**) than inferior (**I-L**) mid-peripheral regions of retina. Cone OSs at the anterior edge (**M-P**) of the retina were shorter than in the mid-periphery and did not shorten further in response to photopic light exposure. Scale bars, 50 μm.

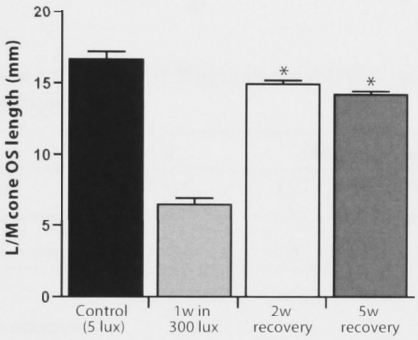

FIGURE 7. Quantitative analysis of immunolabeled L/M opsin cone OSs. Exposure to photopic ambient light for 1w substantially reduced the length of cone OSs. After 2-5w recovery in scotopic conditions, cone OSs regrew significantly and their length approached that of controls. The histograms show means and standard errors (n=5) and asterisks indicate values that are significantly larger than the 1w 300 lux value (Table 1).

TABLE 3. Changes in L/M cone OS length in the P23H-3 rat retina in response to variations of ambient light.

	n	OS length (μm)*	P†
Control vs 1w photopic	5 vs 5	16.7 ± 0.54 vs 6.53 ± 0.43	<0.001
1w photopic vs 2w recovery	5 vs 5	6.53 ± 0.43 vs 14.97 ± 0.27	<0.001
1w photopic vs 5w recovery	5 vs 5	6.53 ± 0.43 vs 14.25 ± 0.22	<0.001

*Mean ± SEM.
†By analysis of variance.

suggested in Discussion that these non-uniformities are determined by the prior stress experience of the retina during rearing.

Recovery of Cone and Rod Ultrastructure. Of the several structural criteria by which rods and cones have been distinguished in the electron microscope (reviewed in Refs. 24-26), the OS disc ultrastructure was the most useful in this study. In the P23H-3 rat retina, cone and rod OSs were similar in diameter, and both extended to the retinal pigmented epithelium (RPE) without tapering. Cone OSs were not obviously associated, as they are in the Nile rat,[27] with a cone matrix or specialized regions of the RPE. Both rods and cones lacked regular well-defined incisures. However, at the level of the disc membranes, the distinction was possible. Rod OSs could be identified by membranous discs forming internal cisternae enclosed by a separate plasma membrane (Fig. 9A), while discs of cone OSs were continuous with the plasma membrane for much of their length, so that the cone OS edge appeared corrugated, without a separate border of unfolded plasma membrane (Fig. 10A). This morphological distinction is not absolute, as discussed previously.[24-26] Over short stretches the plasma membrane in rods may be lost, and the outer membranes of several adjacent cone discs may fuse. Positive identification of cones was therefore restricted to instances where the appearance of the OS border was consistent, coupled where possible with an undulation or rippling of disc membranes, described as characteristic of cones,[28-30] and with particularly conspicuous concentrations of mitochondria in the ellipsoid region of the inner segment.[26] Cones were less clearly defined in control P23H-3 retinas (Figs. 10B, 10C) than in the SD retina (Figs. 10A, 10G).

After 1w exposure to 300 lux ambient light, the array of OSs was disorganized. Rods and cones could not be distinguished, as their internal disc structure was severely distorted. Many OSs had extensive regions of swollen, delaminated and vesiculated discs (Fig. 9B). Other OSs appeared condensed, and some could be identified as OSs only by their attachment to the cilium (Fig. 9C). We noted areas where numerous disconnected lengths of OSs several microns long abutted the apical surface of the RPE, suggesting that the quantity of discarded membrane was such that the RPE had incorporated it only incompletely. There was no clear evidence in

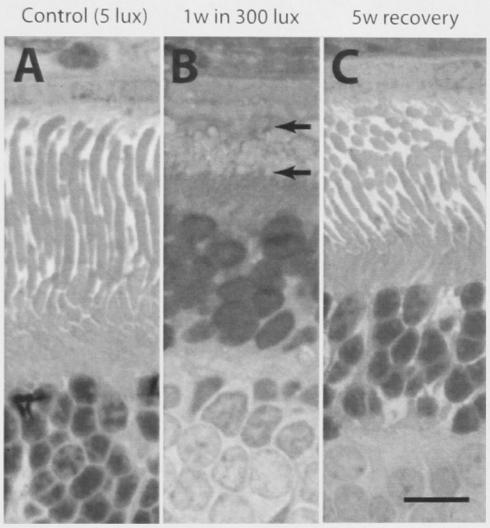

FIGURE 8. Representative light micrographs of epoxy sections of P23H-3 retinas showing regrowth of OSs. (**A**) Retina from a control animal raised under scotopic illumination. (**B**) After 1w exposure to photopic light, photoreceptor OSs (between *arrows*) appeared short and disorganized. (**C**) After 5w recovery in scotopic conditions, the length and regularity of OSs approached those of controls. Scale bar, 10 μm.

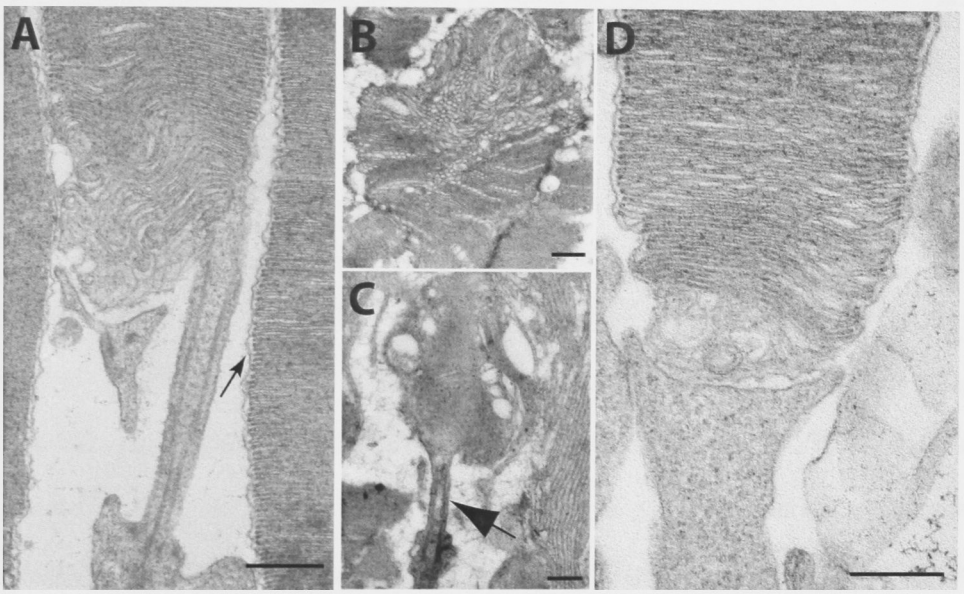

FIGURE 9. Electron micrographs of P23H-3 rod OSs. (**A**) Ciliary connection from inner segment to OS. Note the wavy distortion of the nascent disc membranes at the base of the OS. The mature disc structure is apparent at right in a neighboring rod, showing the plasma membrane external to the edges of the discs. (**B-C**) Exposure to 300 lux cyclic ambient light for 1w had a devastating effect on the organization of most OSs. All were shortened, and in some (**B**) disc stacking was severely distorted and vesiculated, while in others (**C**) the OS could be recognized only by its attachment to a ciliary process (*arrow*). (**D**) After 5w recovery in 5 lux ambient conditions, almost all OSs present were well organized. Ciliary region, section plane orthogonal to that of (**A**). Scale bars, 0.5 μm.

the 1w exposure material that cone OSs remained less affected than rod OSs. Considering the degree of disruption of rod OSs, cone OSs should have been easily detectable, had they remained undamaged.

After 2w recovery, and even more after 5w recovery (Figs. 8C, 8D), well-organized OSs were again apparent, and their fine structure was generally indistinguishable from control scotopic-reared retinae (compare Figs. 9A and 9D). Cone OSs (Figs. 10D-F) were again recognizable. Many OSs were elongated and highly parallel in arrangement. At both recovery times we detected patches of retina in which there was no regrowth of OSs; the ONL was thin, and the RPE was close to the outer limiting membrane. In most of the retina however, there was evidence of significant regrowth of OSs.

DISCUSSION

Rapid Damage of Cones by Ambient Light in a Rod-Specific Mutant Strain

The present results show that the visual responsiveness of cones in the P23H-3 retina is rapidly and significantly reduced by a modest increase in ambient illumination, in parallel with a reduction in rod function. Within a week of exposure to photopic (300 lux) cyclic ambient conditions, both cone and rod responses were reduced to approximately half their amplitude. Morphologically, this reduction cannot be explained by photoreceptor loss, as the ONL typically remained almost constant in thickness and the density of L/M cones remained constant, but can be explained by a marked shortening of OSs (Figs. 3, 4, 5). This loss occurred much more rapidly than the normal age-correlated loss of cone function in scotopic rearing, which is delayed significantly after the loss of rods.[31] We are currently comparing the rates of cone and rod deterioration during the 1w exposure to photopic conditions, to see if a temporal sequence can be established.

Induction of Cone Recovery by Light Restriction

When, after the 1w exposure to photopic conditions, ambient light was returned to scotopic levels (light restriction), OSs of cones and rods lengthened, and the corresponding ERG

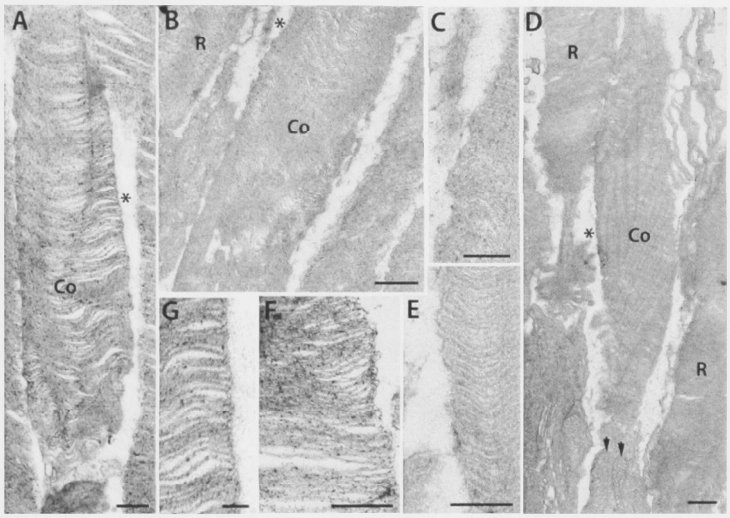

FIGURE 10. Electron micrographs of cone OSs. Cones (labeled Co in **A**, **B**, **D**) are identified by the lack of an outer membrane surrounding the disc stack, and by varying degrees of "waviness" of the disc membranes when compared to rod OSs (R). (*) Regions clearly lacking a surrounding membrane, and are shown in detail in (**C**), (**E**), and (**G**). (**A**, **G**) Young adult SD rat raised in 5 lux illumination. (**B**, **C**) Control P23H-3 rat raised in 5 lux illumination. (**D**, **E**) Cone from P23H-3 rat after 2w recovery. Identification is confirmed by the concentration of mitochondria (*arrows*) in the inner segment (compare rods in Fig. 9). (**F**) Cone border in a P23H-3 rat after 5w recovery. Scales: (**A**, **B**, **D**, **F**) 500 nm; (**C**, **E**, **G**) 200 nm.

components recovered amplitude. The magnitude of the damage and recovery was similar in rods and cones (Fig. 4), at the time-points examined. Closer testing will be needed to test whether the damage and recovery of rods can be shown to precede that of cones. Cone function (the cone b-wave) recovered over 5w to 85% of control values, and we are currently testing the level of recovery achieved after longer periods of reduced ambient light. This is the first description of cone recovery induced by light restriction.

Link between Rod Damage and Cone Damage

Because the P23H-3 transgene is a rhodopsin mutation, it is a reasonable initial assumption that the breakdown of photoreceptor structure and function induced by photopic ambient light begins with rods. Correspondingly, under scotopic rearing conditions the cone component of the ERG maintains amplitude for many weeks after the rod component declines.[31] In the present experiments, by contrast, both cone and rod function declined rapidly (within 1w), and it seems possible that rods and cones are damaged by the same stress. We have suggested previously[21] that the mechanism of light-induced damage is oxidative stress. In a comparable model of cone damage after the degeneration of rods, evidence of oxidative stress to the surviving cones has been identified,[10] and antioxidants have been shown to slow both rod and cone death in rodent models of photoreceptor degeneration.[32, 33] A viable hypothesis therefore is that light induces a reduction of rod function and metabolism, causing a rise in oxygen tension in outer retina,[6] and that this rise causes oxidative stress to both rods and cones.[10] This is the oxygen toxicity hypothesis, previously proposed.[4]

Non-Uniform Effect of Light on Cones across the Retina

The insensitivity of photoreceptors at the anterior edge of the retina to ambient light conditions (Fig. 6) probably results from the chronically stressed status of the retinal edge. Photoreceptors and Müller cells at the retinal edge express high levels of stress inducible factors (FGF-2, CNTF, GFAP).[23] Rod and cone OSs are shortened and distorted and opsin accumulates to abnormally high levels in their somas. In long-lived retinas such as the human, the retinal edge is eroded by

a slow but progressive cystoid degeneration[34, 35] with pigmentary infiltration of the residual retina, comparable to the pigmentation seen in retinitis pigmentosa[23]. We have argued that these changes are induced by chronic hyperoxic stress beginning early in life. Because their OSs are short and damaged and their expression of the metabolic enzyme cytochrome oxidase is down-regulated and because factors such as FGF-2 are known to suppress responsiveness to light,[36] the photoreceptors at the edge of the retina may be only poorly functional. Because they are conditioned to stress, however, they are relatively resistant to light damage[37] and to increased ambient light (above). In the terms of previous studies,[38, 39] the edge of the retina is 'preconditioned' by hyperoxic stress, making it resistant to the stress caused by increased ambient light.

The superior – inferior difference in the vulnerability of photoreceptors to photopic ambient light, confirming Semple-Rowland and Dawson,[40] may also be determined by pre-conditioning of the retina. The difference adds to previous evidence that, in rodents, the superior retina is more vulnerable to light damage.[37] The reason for this difference probably lies in the location of the source of ambient light in the ceiling of the holding rooms used. By the time the exposure to photopic light began, the inferior retina had had more exposure to light and, even though the light was dim (5 lux), was pre-conditioned.

Clinical Relevance

The vulnerability of cones to the degeneration of rods became clear clinically when rod-cone dystrophies, in which loss of cone vision follows loss of rod vision, were shown to result from mutations in genes expressed specifically in rods (especially rhodopsin).[1] Loss of cone structure and function follows the loss of rod function, both spatially and temporally,[1, 41] even though cones do not express the product of the mutant gene. The present study shows the same vulnerability in an animal model, and demonstrates that cones recover function as rods recover function. The evidence of recovery of cone function with light restriction reinforces recent calls for the trial of light restriction as therapy in selected human cases.[4, 20]

Several studies [21, 40, 42] have shown the OSs of rods in the non-degenerative albino SD strain shorten and show signs of membrane damage when ambient light is raised, and regrow the OSs with less damaged membranes when ambient light was restricted. This shortening and lengthening of rods in response to ambient light gave rise to the concept of photostasis,[43, 44] which describes the response of rods in the rat retina to variations in ambient light. The responses of rods and cones in the P23H-3 retina to variations in ambient light can be viewed as an exaggerated form of photostasis, in which both the shortening of and the damage to OSs are more marked than in the wild-type retina. The clinically important point is that the capacity of photoreceptors to regrow and repair their OSs when ambient light is reduced is present in the wild-type photoreceptors, and should be available in many forms of mutation-induced photoreceptor degeneration.

ACKNOWLEDGMENTS

The authors are grateful to Dr. Emlyn R. Williams, of the Statistical Consulting Unit, The Australian National University, for advice and help with the analysis of data.

REFERENCES

1. Hicks D, Sahel J. The implications of rod-dependent cone survival for basic and clinical research. *Invest Ophthalmol Vis Sci* 1999;40:3071-3074.

2. Mohand-Said S, Deudon-Combe A, Hicks D, et al. Normal retina releases a diffusible factor stimulating cone survival in the retinal degeneration mouse. *Proc Nat Acad Sci USA* 1998;95:8357-8362.

3. Chalmel F, Leveillard T, Jaillard C, et al. Rod-derived Cone Viability Factor-2 is a novel bifunctional-thioredoxin-like protein with therapeutic potential. *BMC Mol Biol* 2007;8:74 Epub.

4. Stone J, Maslim J, Valter-Kocsi K, et al. Mechanisms of photoreceptor death and survival in mammalian retina. *Prog Ret Eye Res* 1999;18:689-735.

5. Yu DY, Cringle SJ, Su EN, Yu PK. Intraretinal oxygen levels before and after photoreceptor loss in the RCS Rat. *Invest Ophthalmol Vis Sci*, 2000;41:3999-4006.

6. Yu D, Cringle S, Valter K, Walsh N, Lee D, Stone J. Photoreceptor Death, Trophic Factor Expression, Retinal Oxygen Status, and Photoreceptor Function in the P23H Rat. *Invest Ophthalmol Vis Sci* 2004;45.

7. Walsh N, Bravo-Nuevo A, Geller S, Stone J. Resistance of photoreceptors in the C57BL/6-c2J, C57BL/6J, and BALBB/cj mouse strains to oxygen stress: Evidence of an oxygen phenotype. *Curr Eye Res* 2004;29:441-448.

8. Wellard D, Lee D, Valter K, Stone J. Photoreceptors in the rat retina are specifically vulnerable to both hypoxia and hyperoxia. *Vis Neurosci* 2005;22:501-507.

9. Yamada H, Yamada E, Ando A, et al. Fibroblast growth factor-2 decreases hyperoxia-induced photoreceptor cell death in mice. *Am J Pathol* 2001;159:1113-1120.

10. Shen J, Yang X, Dong A, et al. Oxidative damage is a potential cause of cone cell death in retinitis pigmentosa. *J Cell Physiol* 2005;203:457-464.

11. Johnson G. Contributions to the comparative anatomy of the mammalian eye chiefly based on ophthalmoscopic examination. *Phil Trans Roy Soc London* 1901; 194.

12. Dowling J, Sidman R. Inherited retinal dystrophy in the rat. *J Cell Biol* 1962;14:73-109.

13. Kaitz M. Protection of the dystrophic retina from susceptibility to light stress. *Invest Ophthalmol* 1976;15:153-156.

14. Naash M, Peachey N, Yi Li Z, et al. Light-induced acceleration of photoreceptor degeneration in transgenic mice expressing mutant rhodopsin. *Invest Ophthalmol Vis Sci* 1996;37:775-782.

15. Wang M, Lam T, Tso M, Naash M. Expression of a mutant opsin gene increases the susceptibility of the retina to light damage. *Vis Neurosci* 1997;14:55-62.

16. Bicknell IR, Darrow R, Barsalou L, Fliesler SJ, Organisciak DT. Alterations in retinal rod outer segment fatty acids and light-damage susceptibility in P23H rats. *Mol Vis* 2002;8:333-340.

17. Cideciyan AV, Jacobson SG, Aleman TS, et al. In vivo dynamics of retinal injury and repair in the rhodopsin mutant dog model of human retinitis pigmentosa. *Proc Natl Acad Sci U S A* 2005;102:5233-5238.

18. Berson E. Light deprivation for early retinitis pigmentosa. *Arch Ophthalmol* 1971;85:521-529.

19. Walsh N, Van Driel D, Lee D, Stone J. Multiple vulnerability of photoreceptors to mesopic ambient light in the P23H transgenic rat. *Brain Res* 2004;1013:197-203.

20. Paskowitz DM, LaVail MM, Duncan JL. Light and inherited retinal degeneration. *Br J Ophthalmol* 2006;90:1060-1066.

21. Jozwick C, Valter K, Stone J. Reversal of functional loss in the P23H-3 rat retina by management of ambient light. *Exp Eye Res* 2006;83:1074-1080.

22. Nixon PJ, Bui BV, Armitage JA, A.J. V. The contribution of cone responses to rat electroretinograms. *Clin Exp Ophthalmol* 2001;29:193-196.

23. Stone J, Mervin K, Walsh N, Valter K, Provis J, Penfold P. Photoreceptor stability and degeneration in mammalian retina: lessons from the edge. In: Penfold P, Provis J (eds), *Macular Degeneration: Science and Medicine in Practice*: Springer Verlag; 2005:149-165.

24. Fisher S, Anderson D, Erickso P, Guérin C, GP L, Linberg K. Light and Electron Microscopy of Vertebrate Photoreceptors. In: Hargrave P (ed), *Methods in Neurosciences*. San Diego: Academic Press; 1993:3-36.

25. Anderson DH, Fisher SK, Steinberg RH. Mammalian cones: disc shedding, phagocytosis, and renewal. *Invest Ophthalmol Vis Sci* 1978;17:117-133.

26. Carter-Dawson L, LaVail M. Rods and cones in the mouse retina. I. Structural analysis using light and electron microscopy. *J Comp Neurol* 1979;188:245-262.

27. Bobu C, Craft CM, Masson-Pevet M, Hicks D. Photoreceptor organization and rhythmic phagocytosis in the nile rat Arvicanthis ansorgei: a novel diurnal rodent model for the study of cone pathophysiology. *Invest Ophthalmol Vis Sci* 2006;47:3109-3118.

28. Cohen AI. Some Observations on the Fine Structure of the Retinal Receptors of the American Gray Squirrel. *Invest Ophthalmol* 1964;3:198-216.

29. West RW, Dowling JE. Anatomical evidence for cone and rod-like receptors in the gray squirrel, ground squirrel, and prairie dog retinas. *J Comp Neurol* 1975;159:439-460.

30. Anderson DH, Fisher SK. Disc shedding in rodlike and conelike photoreceptors of tree squirrels. *Science* 1975;187:953-955.

31. Machida S, Kondo M, Jamison JA, et al. P23H rhodopsin transgenic rat: correlation of retinal function with histopathology. *Invest Ophthalmol Vis Sci* 2000;41:3200-3209.

32. Komeima K, Rogers BS, Lu L, Campochiaro PA. Antioxidants reduce cone cell death in a model of retinitis pigmentosa. *Proc Natl Acad Sci U S A* 2006;103:11300-11305.

33. Komeima K, Rogers BS, Campochiaro PA. Antioxidants slow photoreceptor cell death in mouse models of retinitis pigmentosa. *J Cell Physiol* 2007.

34. Vrabec F. Neurohistology of cystoid degeneration of the peripheral human retina. *Am J Ophthal* 1967;64:90-99.

35. Bell FC, Stenstrom WJ. *Atlas of the Peripheral Retina*. Philadelphia: W.B. Saunders Company; 1983.

36. Gargini C, Belfiore MS, Bisti S, Cervetto L, Valter K, Stone J. The impact of basic fibroblast growth factor on photoreceptor function and morphology. *Invest Ophthalmol Vis Sci* 1999;40:2088-2099.

37. Bowers F, Valter K, Chan S, Walsh N, Maslim J, Stone J. Effects of Oxygen and bFGF on the Vulnerability of Photoreceptors to Light Damage. *Invest Ophthalmol Vis Sci*, 2001;42:804-815.

38. Li Y, Roth S, Laser M, Ma JX, Crosson CE. Retinal preconditioning and the induction of heat-shock protein 27. *Invest Ophthalmol Vis Sci* 2003;44:1299-1304.

39. Liu C, Peng M, Laties AM, Wen R. Preconditioning with bright light evokes a protective response against light damage in the rat retina. *J Neurosci* 1998;18:1337-1344.

40. Semple-Rowland S, Dawson W. Cyclic light intensity threshold for retinal damage in albino rats raised under 6 Lx. *Exp Eye Res* 1987;44:643-661.

41. Cideciyan AV, Hood DC, Huang Y, et al. Disease sequence from mutant rhodopsin allele to rod and cone photoreceptor degeneration in man. *Proc Nat Acad Sci USA* 1998;95:7103-7108.

42. Penn J, Anderson R. Effects of light history on the rat retina. *Prog Ret Res* 1991;11:75-98.

43. Penn JS. Early studies of the photostasis phenomenon. *Photostasis and Related Phenomenon.* New York: Plenum Press; 1998:1-16.

44. Williams TP. Light history and photostastis. *Photostasis and Related Phenomena.* New York: Plenum Press; 1998:17-32.

CHAPTER 5

Rapid Cone Damage

Acceleration of Rod Damage Causes Rapid Cone Damage: Evidence from the Rat

Vicki Chrysostomou,[1,2] *Krisztina Valter*,[1,2] *and Jonathan Stone*[1,2,3]

PURPOSE. To assess the effect of accelerated rod damage on the integrity of cones in the rat retina. **METHODS.** Rhodopsin-mutant P23H-3 and Sprague-Dawley (SD) rats were raised in scotopic ambient conditions (12h dark, 12h 5 lux) and then exposed to photopic conditions (12 h dark, 12 h 300 lux). Rods and cones were assessed for cell death, outer segment (OS) morphology, and electroretinogram (ERG) responses. **RESULTS.** Cones in the P23H- retina were affected rapidly by photopic exposure. Exposure for 2d caused 50% reductions in LM- and S-cone OS length and cone ERG responses, associated with and preceded by reductions in rod OS length and ERG responses. Although 2d exposure increased the rate of rod death, outer nuclear layer thinning was minimal and no evidence of cone death was detected. In the SD retina, the same photopic exposure had no measurable effects on death rates, OS length or ERG responses in either rods or cones. Longer (7d) photopic exposure reduced cone and rod OS length and ERG responses in SD, as well as P23H-3 retinas, but less severely than in the P23H-3 strain. **CONCLUSIONS.** Cones are damaged rapidly in the P23H-3 retina when rod damage is accelerated by raised ambient illumination. This close dependence of cone integrity on rod integrity contrasts with the life-long persistence of cone function in the scotopic reared P23H-3 rat. In humans suffering comparable photoreceptor dystrophies, the maintenance of steady, low ambient light may, by minimizing acute rod damage, optimize the function of surviving cones.

From the [1]Research School of Biological Sciences, and [2]ARC Centre of Excellence in Vision Science, The Australian National University, Canberra, Australia; and the [3]Save Sight Institute and Discipline of Physiology, University of Sydney, Sydney, Australia.

Supported by grants from Retina Australia, the National Health and Medical Research Council of Australia, and the Australian Research Council.

Submitted for publication October 14, 2008; revised December 15, 2008 and January 13, 2009; accepted January 14, 2009.

Disclosure: V. Chrysostomou, None; K. Valter, None; J. Stone, None

Corresponding author: Vicki Chrysostomou, Research School of Biological Sciences, The Australian National University, GPO Box 475, Canberra, ACT 2601, Australia; vicki.chrysostomou@anu.edu.au.

Investigative Ophthalmology & Visual Science. First published on Jan 31, 2009 as doi: doi:10.1167/iovs.08-3004

The vulnerability of cone photoreceptors when rods degenerate is a clinically important feature of retinal disease. Mutations in proteins specifically expressed in rods, for example rhodopsin, cause the degeneration of rods primarily, and of cones secondarily.[1] The loss of cone vision is devastating for the patient, giving urgency to understanding the mechanisms that make cones vulnerable.

To date, three mechanisms of cone-rod dependence have been proposed. Evidence has been reported that rods secrete a factor essential for cone survival.[2-4] Alternatively, we have noted that tissue oxygen levels in outer retina rise chronically in the photoreceptor-depleted retina,[5-7] that oxygen is specifically toxic to photoreceptors,[8-10] and that the toxicity involves oxidative damage.[11] We proposed therefore that rod depletion causes oxidative damage to cones, (the oxygen toxicity hypothesis).[12] More recently, Ripps has proposed that a toxin generated by dying rods reaches cones by gap junctions, and induces their damage and death.[13] None of these mechanisms is exclusive, and more than one may contribute to the vulnerability of cones to rod damage.

Previous work in the P23H transgenic rat suggests that the rate of rod degeneration may influence the onset of cone dysfunction. The genetic defect in the P23H strain, a point mutation in the rhodopsin gene, causes an autosomal dominant photoreceptor dystrophy characterized by a rod-cone sequence of degeneration; however, the onset of cone dysfunction varies between genetic subtypes. P23H line 1 (P23H-1) animals and P23H homozygotes have a higher level of transgene expression and display faster rod degenerations than P23H line 3 (P23H-3) animals and heterozygotes. Cone ERG responses in P23H-1 heterozygotes are normal at P28 but are significantly depressed by P56; [14] in P23H-3 heterozygotes they are normal until P360 and are depressed by P540. [15] In the young adult P23H-1 animal, cone ERG responses are 12% of control values in the homozygote[16] but remain at 50% of control values in the heterozygote.[14] In all these cases, severe rod loss precedes the onset of cone ERG changes.

In this study we investigate the effect of rod damage on cone integrity in the P23H-3 heterozygous strain. In the adult P23H-3 retina, rod loss is continuous but slow and cones are

highly stable.[14, 15] Here we have accelerated the rate of rod damage in the P23H-3 strain, by a modest increase in ambient illumination.[17-19] Evidence is presented that cones are damaged rapidly when rods are damaged rapidly, even in the absence of substantial rod loss. The temporal effects of photopic exposure on cone and rod morphology and function are also described.

METHODS

Animal Strains

All procedures were in accordance with the ARVO Statement for the Use of Animals in Ophthalmic and Vision Research, and with the requirements of The Australian National University Animal Experimentation Ethics Committee. Observations were made in two strains of rat, the P23H-3 transgenic (Beckman Laboratories, University of California, San Francisco) and Sprague-Dawley (SD) albino, aged from postnatal day (P) 90 to 150. The P23H-3 animals were heterozygotes, the offspring of mating P23H-3 homozygotes with SD rats.

Ambient Light Protocols

All animals were raised from birth in cyclic light (12 h dark, 12 h white light), with the brightness of the light phase set at 5 lux (scotopic conditions). At adulthood, some rats were moved to photopic ambient conditions (12 h dark, 12 h 300 lux) for up to 7 days (d). P23H-3 animals were exposed to photopic cyclic light for 1, 2 or 7d while SD animals were exposed for 2, 4 or 7d.

Tissue Collection and Processing

Animals were euthanized with an overdose of sodium pentobarbital (>60 mg/kg, intraperitoneal). Eyes were marked at the superior aspect of the limbus for orientation, enucleated and immersion-fixed in 4% paraformaldehyde in 0.1 M phosphate-buffered saline (PBS) at pH 7.4 for 3 h. One eye from each animal was processed for cryosectioning, while the fellow eye was processed for wholemounting. For cryosectioning, eyes were rinsed twice in 0.1

M PBS and left in a 15% sucrose solution overnight to provide cryoprotection. Eyes were embedded in Tissue-Tek OCT Compound (Sakura Finetek, Tokyo, Japan) and snap frozen in liquid nitrogen before being cryosectioned at 12 μm (Leica CM1850 Cryostat). Sections were mounted on gelatin and poly-L-lysine-coated slides and dried overnight at 50°C before being stored at -20°C. For retinal wholemounts, the retina was dissected from the eyecup, flattened by making radial incisions, gently sandwiched between two glass slides and immersed in 4% paraformaldehyde at 4°C for up to 2 weeks before immunolabeling.

TUNEL Labeling and Quantification

Retinal cryosections were labeled using the TUNEL technique to identify the fragmentation of DNA characteristic of apoptotic cells, using a previously published protocol.[20] TUNEL-labeled sections were scanned from superior to inferior edge in 1 mm steps and the number of TUNEL+ profiles in the ONL was recorded. The frequency of TUNEL+ profiles/mm of ONL was averaged from at least two sections per animal, and a minimum of 5 animals were analyzed at each time point. To assess the regional distribution of dying cells, the retinal was divided into superior and inferior hemispheres (relative to the optic nerve head).

Immunohistochemistry

Cryosections. Rod and cone outer segment (OS) morphology was assessed by immunohistochemistry. Retinal cryosections were labeled for rhodopsin, long-medium wavelength-sensitive (LM) opsin, and short wavelength-sensitive (S) opsin, using methods described previously.[19] Briefly, cryosections were incubated overnight at 4°C with an antibody to rhodopsin (mouse monoclonal Rho1D4, 1:1000, Chemicon, Temecula, CA) and LM opsin (rabbit polyclonal, 1:1000, Chemicon, Temecula, CA) or S opsin (rabbit polyclonal, 1:1000, Chemicon, Temecula, CA). The next day, sections were treated with goat anti-mouse Alexa Fluor 594 and goat anti-rabbit Alexa Fluor 488 antibodies (1:1000, Molecular probes, Eugene, OR) for 24 h at 4°C. Sections were incubated for 2 min with the DNA-specific dye bisbenzamide (1:10000) before being coverslipped with a glycerol/gelatin medium.

Wholemounts. Retinal wholemounts were immunolabelled for LM opsin, as described previously.[19] Briefly, flattened retinas were blocked with normal goat serum before overnight incubation with a rabbit polyclonal antibody to LM opsin (1:1000, Chemicon, Temecula, CA). After washing with 0.01% Triton-PBS, retinas were incubated for 24 h with an antibody to rabbit IgG conjugated to Alexa Fluor 488 (1:1000, Molecular probes, Eugene, OR) and subsequently mounted and coverslipped on glass slides, with the outer surface up.

LM opsin-labeled cone OSs were assessed for both density and length. Labeled wholemounts were visualized by fluorescence microscopy and images of the OS layer were captured with a digital camera (Zeiss AxioCam MRc). Using the digital images, LM opsin-labeled OSs were counted over areas of 0.01 mm^2 at 0.5 mm intervals across the entire retinal surface (approximately 100-250 fields per retina). At each counting field, the average length of cone OSs was also recorded. Counts of OSs per 0.01 mm^2 were averaged across the entire retina to give an overall cone density for each sample.

Quantification of Retinal Thickness and Outer Segment Length

Retinal thickness measurements were made on digital images of bisbenzamide-stained cryosections. Sections were scanned from superior to inferior edge and the retinal thickness was determined every 500 μm (a total of eight measurements per retina). At each measurement location, the thickness of the outer nuclear layer (ONL) as well as the thickness of the retina, from inner to outer limiting membrane (ILM-OLM), was recorded. The ratio of the thickness of the ONL to the thickness of the retina (measured from the ILM to the OLM) was used for analysis, to account for obliquely-cut sections.

Measurements of rod and cone OS length were made on digital images of immunolabeled cryosections. Retinal sections were scanned from superior to inferior edge and, at regularly spaced intervals, the length of rhodopsin, LM opsin-labeled and S opsin-labeled OSs were measured (a total of at least 24 measurements per retina). For measurements of OS length and retinal thickness, results from 5 animals at each time point were averaged and analyzed by the statistical method described below.

Electroretinography

The function of photoreceptors was assessed by the flash-evoked electroretinogram (ERG). Animals were dark-adapted overnight and prepared for recording in dim red illumination as described previously.[17] Following previous reports,[21] responses to a standard test flash (44.5 cds/m^2) were considered to be 'mixed' with contributions from rods and cones. Responses to the test flash preceded, by 395 msec, by a conditioning flash (12 cds/m^2) were considered those of cones. By subtracting the cone response from the 'mixed' response, the rod response was isolated. Using this method, three measurements of amplitude were used for analysis: rod a-wave, rod b-wave and cone b-wave, as described previously (see Figure 1 in [19]).

Statistical Analyses

Paired data from P23H-3 and SD animals were compared using a two-tailed Student's t-test. Comparisons within each rat strain were made by an analysis of variance using a Tukey post-test to compare group means. All data are presented as the mean ±1 SEM.

RESULTS

Impact of Increased Ambient Light on Rods

The P23H transgene makes rods vulnerable to damage when ambient light is increased. When the level of ambient light is increased from scotopic to mesopic[17] or photopic[18, 19] levels, the death of rods is accelerated, rod ERG responses are reduced, and the OSs of the survivors are damaged and shortened. These effects were confirmed in the current data. Figure 1A shows that increasing the intensity of the 'day' component of cyclic ambient light from 5 to 300 lux for 2d increased the TUNEL-labeling of P23H-3 photoreceptors by 40-fold. A more limited increase was observed in the SD rat, in response to the same increase (Fig. 1B). Further, the acceleration was more rapid in the P23H-3 strain, the frequency of TUNEL+ profiles reaching its observed maximum at 2d, as against 4-7d in the SD strain. The spatial distribution of the TUNEL+ photoreceptors was not uniform. As reported previously,[22, 23] photoreceptors near the edge of

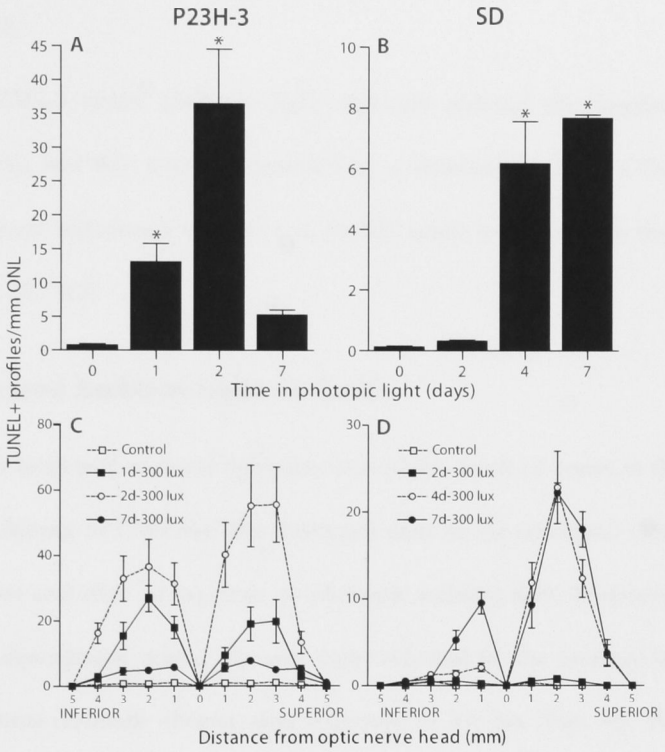

FIGURE 1. Frequency of TUNEL-labeled photoreceptor cells in the P23H-3 and SD rat retina during 7d exposure to cyclic photopic light. Fragmentation of photoreceptor DNA occurred earlier and was several orders of magnitude greater in the P23H-3 retina (**A**) than in the SD retina (**B**). TUNEL+ photoreceptors were most frequent in the superior mid-peripheral region of retina in both the P23H-3 (**C**) and SD (**D**) strain. Data are presented as the mean ±1 SEM for groups of 6 animals at each time point. Asterisks indicate data points that are significantly different from 0d control values, using an analysis of variance ($P<0.05$).

the retina were relatively unaffected, and there was a strong concentration of TUNEL+ cells in the superior mid-periphery in both strains (Figs. 1C, 1D).

The cell death induced by photopic light exposure did not cause a change in the thickness of the retina in either the P23H-3 or SD retina. ONL thickness was greater in the SD retina (confirming previous reports [6, 24]) by a small margin (the ONL/retina ratio was 0.32 vs 0. 28), but a significant thinning of the layer during 7d exposure to 300 lux was not apparent in either strain (Fig. 2).

In the P23H-3 strain, photopic light exposure reduced the amplitude of rod ERG responses (Fig. 3A), and this was accompanied by a shortening of rod OSs (*red* in Fig. 3B). Slower and less severe reductions were seen in the SD strain in response to the same increase in illumination (Figs. 3C, 3D).

Impact of Increased Ambient Light on Cones

We tested whether increased ambient light also caused the death of cones in the P23H-3 retina, by examining the density of LM cone (the dominant cone in the rat retina) OSs in whole mount preparations, before and after 7d exposure to photopic ambient light. Measurements were made in the superior midperipheral retina, the area most affected by the increase in ambient light.[19] While cone OSs were distinctly shorter after exposure to 300 lux (Figs 4B, 4D), the density of OSs was not measurably reduced (Fig. 4A). In addition, we labeled sections from eyes exposed for 2d for both cell death and cone OSs, following Geller et al.,[8] and examined several sections for evidence of TUNEL+ cones, without finding any.

In both P23H-3 and SD strains, the increase in ambient light from scotopic (5 lux) to photopic (300 lux) levels had a major impact on the function of cones and the length of their OSs. In the P23H-3, the b-wave of the cone ERG response declined (Fig. 3A), and correspondingly, the length of LM- and S-cone OSs (green and blue in Fig. 3B) reduced. A similar trend, but slower and less severe, was apparent in the SD strain (Figs. 3C, 3D).

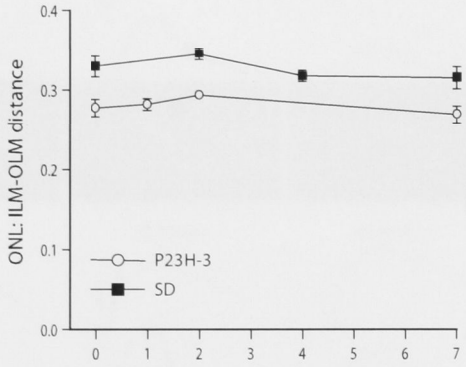

FIGURE 2. Measurements of retinal thickness in the P23H-3 and SD rat retina after a rise in ambient illumination. The thickness of the ONL was greater in the SD retina, but there was no thinning of the layer in either strain during 7d exposure to photopic light.

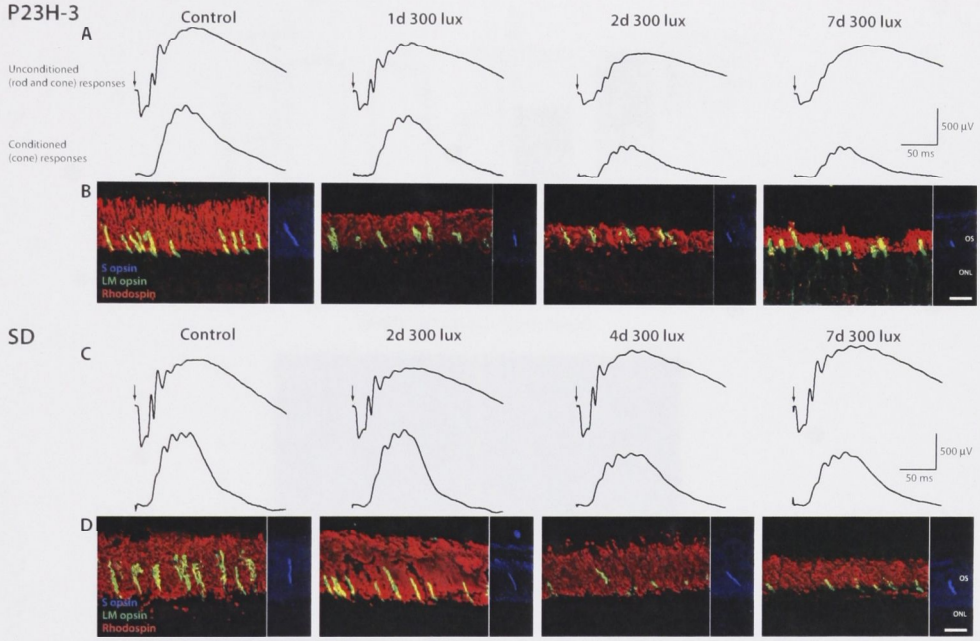

FIGURE 3. Sample waveforms of rod and cone ERG responses matched with immunohistochemical labeling of rod (*red*), LM-cone (*green*) and S-cone (*blue*) OSs. In P23H-3 (**A**, **B**) and SD (**C**, **D**) retinas, 7d exposure to photopic light reduced the amplitude of rod and cone ERG responses, and was accompanied by a shortening of photoreceptor OSs. This effect was more rapid and severe in the P23H-3. The ERG waveforms in (**A**) and (**C**) were elicited to a flash stimulus of 44.5 cds/m^2. The time of the flash stimulus is indicated by the vertical *arrow*. Scale bars, 20 µm.

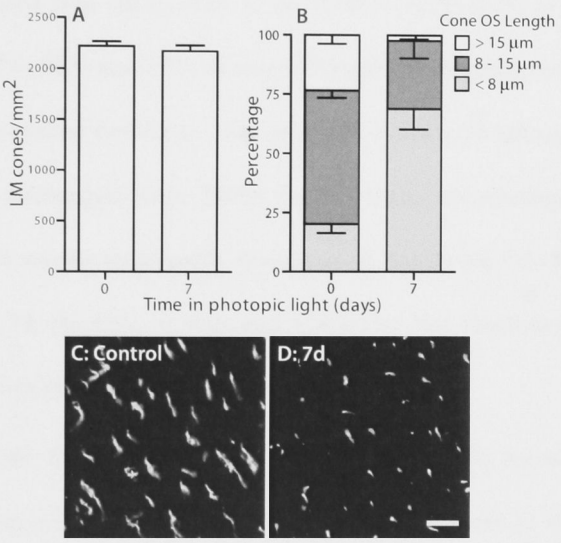

FIGURE 4. Analysis of cone survival in the P23H-3 retina after photopic light exposure. The average density of cones (**A**) and the length of their OSs (**B**) were quantified from flat-mounted retinas immunolabeled for LM opsin. (**C**, **D**) Representative images from the superior mid-periphery of LM opsin-labeled retinal flat-mounts. Flat-mounts from 3 animals were assessed and data are presented as means ±1 SEM. Scale bar, 20 µm.

Quantitative Analysis: Time Course of ERG and Outer Segment Length Changes

In the P23H-3 retina, the increase of ambient light to photopic levels caused rod and cone components of the ERG to fall in amplitude to less than 50% of control values within 2d (Fig. 5A). The loss was progressive over this time. In the SD retina, rod and cone ERG components maintained amplitude at 2d but fell to 60-70% of control values at 4d (Fig. 5B).

Correspondingly, the increase in ambient illumination caused a progressive shortening of rod (Fig. 6A) and cone (Fig. 6B,C) OSs. In the P23H-3 retina, OSs of rods, LM-cones and S-cones shortened to 77%, 55% and 57% of control lengths respectively within 2d. By 7d, rod and LM-cone OSs had shortened further to 54% and 34% of control values, while the length of S-cones OSs remained unchanged from 2d. In the SD retina, shortening of both rod and cone OSs was delayed; there was no measurable change at 2d, but by 4d, OSs had shortened to ~70% of control values. By 7d, the OSs of rods and LM-cones had shortened further to 45-55% of control values, while S-cone OS values remained unchanged.

It was significant that, after 2d exposure to photopic light, the amplitude of the cone b-wave and cone OS lengths were both maintained at control levels in the SD retina, but were reduced to 50% of initial values in the P23H-3 retina (Figs. 5D, 6B,C). This point is stressed because it is evidence that cones are not directly damaged by 2d exposure to photopic conditions. The loss of cone b-wave response and cone OS length at this time of exposure is specific to the P23H-3 strain, in which rods are damaged with abnormal speed and severity.

We saw limited evidence that the changes induced by the increase in ambient illumination occurred first in rods, as anticipated by previous observations that cones are more resistant to light damage.[25, 26] Specifically, by the 1d time point (Fig. 5), the cone b-wave had lost 18% of its amplitude, the rod a-wave had lost 37% and the rod b-wave 27% of amplitude. Perhaps the most striking feature of these data is how closely the changes to cones matched the

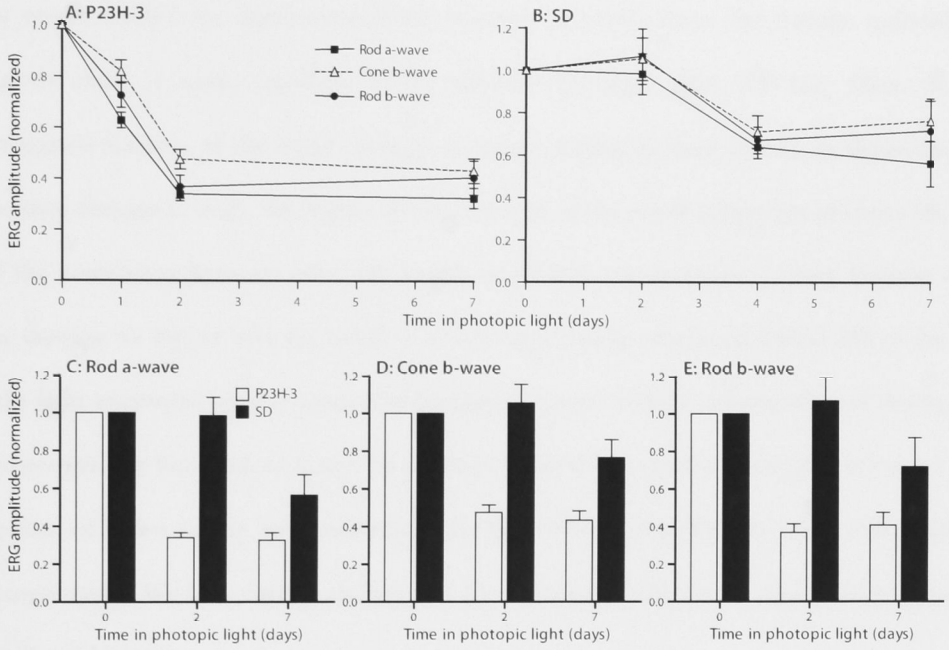

FIGURE 5. Time course of loss of rod and cone ERG amplitudes in P23H-3 and SD retinas in response to photopic light exposure. (**A**) In the P23H-3 retina, rod and cone ERG components were rapidly reduced in amplitude by an increase in photopic light levels. (**B**) In the SD retina, rod and cone ERG responses were also reduced by photopic light exposure but the reductions were delayed and less severe. Direct comparison of rod a-wave (**C**), cone b-wave (**D**) and rod b-wave (**E**) amplitudes between the P23H-3 and SD rat retina during 7d photopic light exposure. The stimulus used for all ERG measures was a flash of 44.5 cds/m^2 intensity. Data is presented as the mean ±1 SEM for 8 animals.

changes to rods, despite the fact that the transgene which creates this vulnerability of the P23H-3 retina is for a protein expressed specifically in rods.

DISCUSSION

Summary: Accelerated Rod Damage Causes Rapid Cone Damage, with Minimal Rod Death

In a recent study[19] we demonstrated the recovery of cones from the damage induced by a relatively short (1 week) exposure of the retina to photopic light (300 lux). Here, we have investigated features of the initial damage to cones, tracing its time course, its dependence on preceding damage to rods, the degree of involvement of the major subgroups of cones (S-, LM-) and the correlation between cone OS length and ERG responsiveness. Three features of the cone damage we report here are novel: it is very rapid, being substantial within 24h of the onset of the light increment used to cause rod damage; it occurs without measurable rod death; and it does not involve the death of cones. In addition, control experiments show that it is not a direct response of cones to the light increment; the light levels used (300 lux) were well within the photopic range. We have further shown that the rod-induced damage to cones involves S-cones, as well as LM-cones.

The form of cone-rod dependence that we show here is distinctive, and contrasts with previous descriptions of cone-rod dependence in the P23H retina. In these earlier studies, of P23H line 3 heterozygotes,[14, 15] and line 1 homozygotes[16] and heterozygotes,[14] cone dysfunction was not detected until there had been a severe loss of rods, amounting to an ONL thinning of approximately 50%. Here, cone OS lengths and ERG responses were reduced by half after 2 days photopic exposure, when rod loss was insufficient to cause a detectable thinning of the ONL. The present findings also contrast with evidence that cones in rhodopsin-mutant degenerative human retinas maintain their function until rod OSs are reduced to 25% of normal length.[27] In the present paradigm, damage to cone OSs was evident when rod OS length was within 30% of normal. The rapid damage to P23H-3 cones reported here cannot be attributed

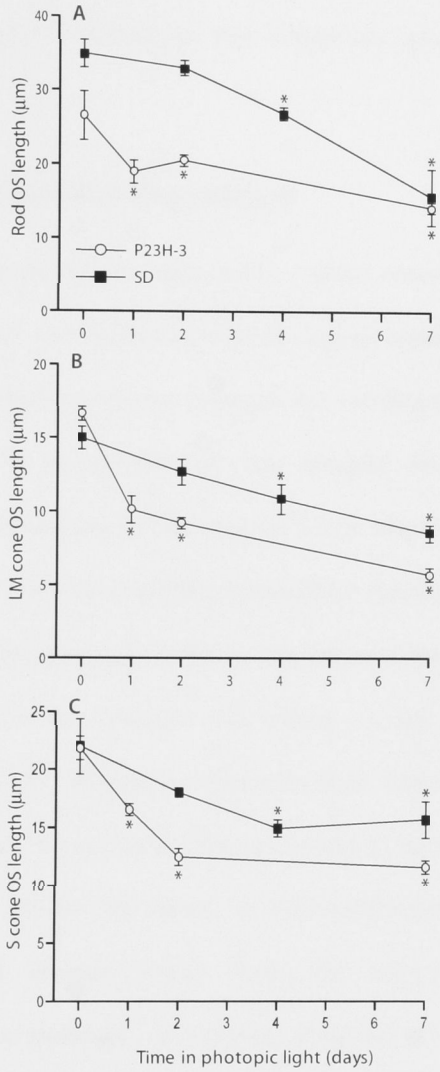

FIGURE 6. Quantitative analysis of rod and cone OS length changes in P23H-3 and SD retinas in response to photopic light exposure. Exposure significantly reduced the length of rod (**A**), LM-cone (**B**) and S-cone (**C**) OSs in both the P23H-3 and SD retina, and this shortening was more rapid in the P23H-3. Data are presented as the mean ±1 SEM for groups of 6 animals at each time point. Asterisks indicate data points that are significantly different from 0d control values using an analysis of variance ($P<0.05$).

to the increase in ambient illumination because cone morphology and function were maintained in the SD retina in response to the same exposure, indicating that cones are not directly damaged by this level of light. The present results suggest that cones are dependent on rod integrity (OS morphology and signalling), even when rod cells are surviving. These features of cone damage raise issues of mechanism and therapeutic opportunity, which are considered below.

The Mechanism of Cone-Rod Dependence

Two of the mechanisms previously proposed to explain cone-rod dependence (a rod-derived cone survival factor [3, 4, 28] and depletion-induced oxygen toxicity [29]) cannot account for rate-dependent manner in which cones are damaged by rod degeneration, without proposing an adaptive mechanism. The preservation of cone integrity when rod loss is slow could be reconciled with these mechanisms if, for example, cones adapt to slow reductions in the levels of a rod-derived trophic factor by amplifying intracellular signalling mechanisms, or to slow rises in oxidative stress by expressing anti-oxidant protective mechanisms. An alternative explanation for this rate dependence is that damaged rods release a toxin, whose concentration reaches a threshold level only when rod damage is sufficiently rapid. The toxin could reach the cytoplasm of cones via gap junctions (the bystander effect proposed by Ripps[13]) or it could be released into the extracellular space around the cones, as rod membranes break down. Examples of substances that could damage cones from the extracellular space are excitatory neurotransmitters such as glutamate, or a purine (reviewed in [30]) such as ATP. Although the latter ideas remain speculative, the present results encourage the search for rate-dependent mechanisms of cone-rod dependence.

Death, Damage and the Capacity for Recovery

The present results provide insight into the mechanisms of rod-cone dystrophies, the forms of human photoreceptor dystrophy in which cone loss is secondary to rod loss. They suggest that, in some forms of the human disease, cone loss may occur when the sufferer experiences a rise

in ambient illumination which occurs suddenly and is maintained for 1-2d. Put more constructively, they indicate that in rod-fragile retinas, cone damage may be minimized by maintaining ambient light exposure both low and constant. The idea that restricting ambient light will slow retinal degenerations has considerable support from the study of animal models and more limited support from human trials (for reviews see [12, 31]). The idea that it is important for cone vision to avoid episodes of high illumination is emphasized by the present study. Further work will be needed to extend these findings, but the technology exists for giving a sufferer real-time measures of ambient light, and for adjusting (say) dark glasses dynamically to counter the changes encountered in daily living.

Still more hopefully, we note that the loss of cone (and rod) function in the acute P23H-3 protocol is largely reversible. Much of the functional (ERG) loss results from a shortening of OSs, rather than photoreceptor death, and will readily reverse in both rods[18] and cones.[19] Light is the stimulus for vision, driving the phototransduction mechanisms of the OS. Light is also a powerful regulator of the cell biology of photoreceptors, and light management seems likely to emerge as an effective tool in the management of photoreceptor stability, whether the instability is caused by genetic mutations, or by environmental factors such as bright light, depletion-induced hyperoxia or age.

Mission and Nemesis: The Paradox of Light-Induced Damage

Most organisms make some investment in light detection, to optimise their behavioural adaptation and individual survival. In higher primates it is often judged that vision is the most powerful of the senses, and has dedicated to it numerous subcortical structures and a large component (the occipital lobe and beyond) of neocortex. Less structurally conspicuous visual pathways control circadian rhythms, eye movements, and pupil size. In plants, light is directly harnessed to create energy rich molecules.

It is an interesting paradox that, although good vision is clearly a major factor in the individual's struggle for survival and quality of life, and photosynthesis is the source of plant life,

the absorption of light – whether by 11-cis retinal in animals or by Photo I in plants – is an intrinsically damaging process. Light-experienced photoreceptors [32-34]and the photosynthetic organelles of plant cells consistently show evidence of damage and an upregulation of protective factors,[35-37] a seemingly unavoidable accompaniment of light absorption.

The paradox is particularly clear in vertebrate photoreceptors. Light decreases dark current, ion pump activity in inner segments, and oxidative phosphorylation (in response to a decrease in ATP turnover). So, light can be expected to decrease the production of reactive oxygen species in photoreceptor mitochondria. Nevertheless, light exposure causes severe damage to OSs. It appears possible that the absorption of light is directly damaging to membranes in which the chromophore is embedded. Winkler[38] has recently argued that the rapid turnover of OS membrane is a substitute for membrane repair, evolved because of the magnitude of the repair task in photoreceptors.

The point of this argument is that repair of the OS, by continuous rebuilding of its membranes at the cilial base, is prominent in vertebrate photoreceptors, and can be harnessed to restore vision in human patients where (as in most cases) many photoreceptors survive but are poorly functional.

REFERENCES

1. John SK, Smith JE, Aguirre GD, Milam AH. Loss of cone molecular markers in rhodopsin-mutant human retinas with retinitis pigmentosa. *Mol Vis* 2000;6:204-215.

2. Mohand-Said S, Deudon-Combe A, Hicks D, et al. Normal retina releases a diffusible factor stimulating cone survival in the retinal degeneration mouse. *Proc Natl Acad Sci USA* 1998;95:8357-8362.

3. Hicks D, Sahel J. The implications of rod-dependent cone survival for basic and clinical research. *Invest Ophthalmol Vis Sci* 1999;40:3071-3074.

4. Leveillard T, Mohand-Said S, Lorentz O, et al. Identification and characterization of rod-derived cone viability factor. *Nat Genet* 2004;36:755-759.

5. Yu DY, Cringle SJ, Su EN, Yu PK. Intraretinal oxygen levels before and after photoreceptor loss in the RCS Rat. *Invest Ophthalmol Vis Sci* 2000;41:3999-4006.

6. Yu DY, Cringle S, Valter K, Walsh N, Lee D, Stone J. Photoreceptor death, trophic factor expression, retinal oxygen status, and photoreceptor function in the P23H rat. *Invest Ophthalmol Vis Sci* 2004;45:2013-2019.

7. Padnick-Silver L, Kang Derwent JJ, Giuliano E, Narfstrom K, Linsenmeier RA. Retinal oxygenation and oxygen metabolism in Abyssinian cats with a hereditary retinal degeneration. *Invest Ophthalmol Vis Sci* 2006;47:3683-3689.

8. Geller S, Krowka R, Valter K, Stone J. Toxicity of hyperoxia to the retina: evidence from the mouse. *Adv Exp Med Biol* 2006;572:425-437.

9. Yamada H, Yamada E, Hackett SF, Ozaki H, Okamoto N, Campochiaro PA. Hyperoxia causes decreased expression of vascular endothelial growth factor and endothelial cell apoptosis in adult retina. *J Cell Physiol* 1999;179:149-156.

10. Wellard J, Lee D, Valter K, Stone J. Photoreceptors in the rat retina are specifically vulnerable to both hypoxia and hyperoxia. *Vis Neurosci* 2005;22:501-507.

11. Shen J, Yang X, Dong A, et al. Oxidative Damage is a Potential Cause of Cone Cell Death in Retinitis Pigmentosa. *J Cell Physiol* 2005;203:457-464.

12. Stone J, Maslim J, Valter-Kocsi K, et al. Mechanisms of photoreceptor death and survival in mammalian retina. *Prog Ret Eye Res* 1999;18:689-735.

13. Ripps H. Cell Death in Retinitis Pigmentosa: Gap Junctions and the `Bystander' Effect. *Exp Eye Res* 2002;74:327-336.

14. Machida S, Kondo M, Jamison JA, et al. P23H rhodopsin transgenic rat: correlation of retinal function with histopathology. *Invest Ophthalmol Vis Sci* 2000;41:3200-3209.

15. Chrysostomou V, Stone J, Valter K. Life History of Cones in the Rhodopsin-Mutant P23H-3 Rat: Evidence of Long Term Survival. *Invest Ophthal Vis Sci* 2009;InPress.

16. Pinilla I, Lund RD, Sauve Y. Enhanced cone dysfunction in rats homozygous for the P23H rhodopsin mutation. *Neuroscience Letters* 2005;382:16-21.

17. Walsh N, Van Driel D, Lee D, J. S. Multiple vulnerability of photoreceptors to mesopic ambient light in the P23H transgenic rat. *Brain Res* 2004;1013:197-203.

18. Jozwick C, Valter K, Stone J. Reversal of functional loss in the P23H-3 rat retina by management of ambient light. *Exp Eye Res* 2006;83:1074-1080.

19. Chrysostomou V, Stone J, Stowe S, Barnett NL, Valter K. The Status of Cones in the Rhodopsin Mutant P23H-3 Retina: Light-Regulated Damage and Repair in Parallel with Rods. *Invest Ophthalmol Vis Sci* 2008;49:1116-1125.

20. Maslim J, Valter K, Egensperger R, Hollander H, Stone J. Tissue oxygen during a critical developmental period controls the death and survival of photoreceptors. *Invest Ophthal Vis Sci* 1997;38:1667-1677.

21. Nixon PJ, Bui BV, Armitage JA, A.J. V. The contribution of cone responses to rat electroretinograms. *Clin Experiment Ophthalmol* 2001;29:193-196.

22. Bowers F, Valter K, Chan S, Walsh N, Maslim J, Stone J. Effects of Oxygen and bFGF on the Vulnerability of Photoreceptors to Light Damage. *Invest Ophthalmol Vis Sci* 2001;42:804-815.

23. Stone J, Mervin K, Walsh N, Valter K, Provis J, Penfold P. Photoreceptor stability and degeneration in mammalian retina: lessons from the edge. In: Penfold P, Provis J (eds), *Macular Degeneration: Science and Medicine in Practice*. Springer Verlag; 2005:149-165.

24. Machida S, Kondo M, Jamison JA, et al. P23H rhodopsin transgenic rat: correlation of retinal function with histopathology. *Invest Ophthalmol Vis Sci* 2000;41:3200-3209.

25. Cicerone C. Cones survive rods in the light-damaged eye of the albino rat. *Science* 1976;194:1183-1185.

26. LaVail MM. Survival of some photoreceptor cells in albino rats following long-term exposure to continuous light. *Invest Ophthalmol* 1976;15:64-70.

27. Cideciyan AV, Hood DC, Huang Y, et al. Disease sequence from mutant rhodopsin allele to rod and cone photoreceptor degeneration in man. *Proc Natl Acad Sci USA* 1998;95:7103-7108.

28. Mohand-Said S, Hicks D, Simonutti M, et al. Photoreceptor transplants increase host cone survival in the retinal degeneration (rd) mouse. *Ophthal Res* 1997;29:290-297.

29. Stone J, Maslim J, Valter-Kocsi K, et al. Mechanisms of photoreceptor death and survival in mammalian retina. *Prog Ret Eye Res* 1999;18:689-735.

30. Burnstock G. Purinergic signalling and disorders of the central nervous system. *Nat Rev Drug Discov* 2008;7:575-590.

31. Paskowitz DM, LaVail MM, Duncan JL. Light and inherited retinal degeneration. *Br J Ophthalmol* 2006;90:1060-1066.

32. Penn J, Anderson R. Effects of light history on the rat retina. *Prog Ret Res* 1991;11:75-98.

33. Penn J, Naash M, Anderson R. Effect of light history on retinal antioxidants and light damage susceptibility in the rat. *Exp Eye Res* 1987;44:779-788.

34. Penn JS, Anderson RE. Effect of light history on rod outer-segment membrane composition in the rat. *Exp Eye Res* 1987;44:767-778.

35. Iverson T. Evolution and unique bioenergetic mechanisms in oxygenic photosynthesis. *Curr Opin Chem Biol* 2006;10:91-100.

36. Kruse O. Light-induced short-term adaptation mechanisms under redox control in the PS II-LHCII supercomplex? LHC II state transitions and PS II repair cycle. *Naturwissenschaften* 2001;88:284-292.

37. Aro E, Virgin I, Andersson BE. Photoinhibition of PhotosystemII. Inactivation, protein damage and turnover. *Biochim Biophys Acta* 1993;1143:113-134.

38. Winkler BS. An hypothesis to account for the renewal of outer segments in rod and cone photoreceptor cells: renewal as a surrogate antioxidant. *Invest Ophthalmol Vis Sci* 2008;49:3259-3261.

CHAPTER 6

Conclusions

When considered together, the studies presented in this thesis give new insights into the cell biology of mechanisms of cone-rod dependence, and explore therapeutic approaches to the management of retinal degeneration.

The current studies have assessed the integrity of cones in two patterns of rod damage. First, the slow and steady loss of rods in the dim-reared P23H-3 retina as a function of age (Chapter 3). Second, the rapid loss of rods in the P23H-3 retina in response to photopic light exposure (Chapter 5). The results show that cone morphology and function is maintained for long periods when rod loss is slow, as when the P23H-3 rat ages. In contrast, cone integrity fails rapidly when rod damage is rapid, accelerated by a rise in ambient illumination. These findings raise the novel concept of a rate-dependent vulnerability of cones on rods. Previous ideas of cone-rod dependence have not considered the rate of rod damage as a relevant factor.

Issues of clinical importance are also raised. The work presented has shown that in response to either an autosomal dominant pattern of rod degeneration (Chapter 3), or photopic light exposure (Chapters 4 and 5), cone damage and dysfunction occur in the absence of cone cell death. Additionally, it is shown in Chapter 4 that this damage and dysfunction is largely reversible. The robust survival of cones combined with their capacity to self-repair suggests that partial recovery of vision loss may be a realistic goal for human patients suffering retinal degeneration from comparable causes. Specifically, recovery of central and high acuity vision that is mediated by the cone system may be achievable.

The demonstration of cone recovery in response to light restriction, presented in Chapter 4, reinforces recent calls for the trial of light deprivation in selected human cases. Additionally, the demonstration that cones are sensitive to acute rod damage, presented in Chapter 5, suggests that, when using light as a therapy, it is not only important to keep ambient light levels low, but also constant. This dual approach (low and constant illumination) will provide conditions optimal for cone repair, in addition to minimising acute rod damage that compromises cone integrity.

Bibliography

Acland GM, Aguirre GD, Ray J, Zhang Q, Aleman TS, Cideciyan AV, Pearce-Kelling SE, Anand V, Zeng Y, Maguire AM, Jacobson SG, Hauswirth WW, Bennett J (2001) Gene therapy restores vision in a canine model of childhood blindness. Nat Genet 28:92-95.

Ahmed J, Braun RD, Dunn RJ, Linsenmeier RA (1993) Oxygen distribution in the macaque retina. Invest Ophthalmol Vis Sci 34:516-521.

Akimoto M, Miyatake S, Kogishi J, Hangai M, Okazaki K, Takahashi JC, Saiki M, Iwaki M, Honda Y (1999) Adenovirally expressed basic fibroblast growth factor rescues photoreceptor cells in RCS rats. Invest Ophthalmol Vis Sci 40:273-279.

Alder V, Ben-Nun J, Cringle S (1990) PO2 profiles and oxygen consumption in cat retina with an occluded retinal circulation. Invest Ophthalmol Vis Sci 31:1029-1034.

Ali RR, Sarra GM, Stephens C, Alwis MD, Bainbridge JW, Munro PM, Fauser S, Reichel MB, Kinnon C, Hunt DM, Bhattacharya SS, Thrasher AJ (2000) Restoration of photoreceptor ultrastructure and function in retinal degeneration slow mice by gene therapy. Nat Genet 25:306-310.

Alm A, Bill A (1972) The oxygen supply to the retina. II. Effects of high intraocular pressure and of increased arterial carbon dioxide tension on uveal and retinal blood flow in cats. A study with radioactively labelled microspheres including flow determinations in brain and some other tissues. Acta Physiol Scand 84:306-319.

Ames A, Li Y-Y, Heher E, Kimble C (1992) Energy metabolism of rabbit retina as related to function: high cost of Na+ transport. J Neurosci 12:840-853.

Arai S, Thomas BB, Seiler MJ, Aramant RB, Qiu G, Mui C, de Juan E, Sadda SR (2004) Restoration of visual responses following transplantation of intact retinal sheets in rd mice. Exp Eye Res 79:331-341.

Arden GB (2001) The absence of diabetic retinopathy in patients with retinitis pigmentosa: implications for pathophysiology and possible treatment. Br J Ophthalmol 85:366-370.

Arshavsky VY, Lamb TD, Pugh EN, Jr. (2002) G proteins and phototransduction. Annu Rev Physiol 64:153-187.

Bahrami H, Melia M, Dagnelie G (2006) Lutein supplementation in retinitis pigmentosa: PC-based vision assessment in a randomized double-masked placebo-controlled clinical trial [NCT00029289]. BMC Ophthalmol 6:23.

Baylor D (1996) How photons start vision. Proc Natl Acad Sci USA 93:560-565.

Bennett J, Tanabe T, Sun D, Zeng Y, Kjeldbye H, Gouras P, Maguire AM (1996) Photoreceptor cell rescue in retinal degeneration (rd) mice by in vivo gene therapy. Nat Med 2:649-654.

Bentmann A, Schmidt M, Reuss S, Wolfrum U, Hankeln T, Burmester T (2005) Divergent Distribution in Vascular and Avascular Mammalian Retinae Links Neuroglobin to Cellular Respiration. J Biol Chem 280:20660-20665.

Berson EL (1971) Light deprivation for early retinitis pigmentosa. A hypothesis. Arch Ophthalmol 85:521-529.

Berson EL (1980) Light deprivation and retinitis pigmentosa. Vision Res 20:1179-1184.

Berson EL (1993) Retinitis pigmentosa. The Friedenwald Lecture. Invest Ophthalmol Vis Sci 34:1659-1676.

Berson EL, Rosner B, Sandberg MA, Hayes KC, Nicholson BW, Weigel-DiFrano C, Willett W (1993) Vitamin A supplementation for retinitis pigmentosa. Arch Ophthalmol 111:1456-1459.

Berson EL, Rosner B, Sandberg MA, Weigel-DiFranco C, Moser A, Brockhurst RJ, Hayes KC, Johnson CA, Anderson EJ, Gaudio AR, Willett WC, Schaefer EJ (2004a) Clinical trial of docosahexaenoic acid in patients with retinitis pigmentosa receiving vitamin A treatment. Arch Ophthalmol 122:1297-1305.

Berson EL, Rosner B, Sandberg MA, Weigel-DiFranco C, Moser A, Brockhurst RJ, Hayes KC, Johnson CA, Anderson EJ, Gaudio AR, Willett WC, Schaefer EJ (2004b) Further evaluation of docosahexaenoic acid in patients with retinitis pigmentosa receiving vitamin A treatment: subgroup analyses. Arch Ophthalmol 122:1306-1314.

Bicknell IR, Darrow R, Barsalou L, Fliesler SJ, Organisciak DT (2002) Alterations in retinal rod outer segment fatty acids and light-damage susceptibility in P23H rats. Mol Vis 8:333-340.

Bill A, Sperber GO (1990) Control of retinal and choroidal blood flow. Eye 4 (Pt 2):319-325.

Bill A, Tornquist P, Alm A (1980) Permeability of the intraocular blood vessels. Trans Ophthalmol Soc UK 100:332-336.

Bok D, Yasumura D, Matthes MT, Ruiz A, Duncan JL, Chappelow AV, Zolutukhin S, Hauswirth W, LaVail MM (2002) Effects of adeno-associated virus-vectored ciliary neurotrophic factor on retinal structure and function in mice with a P216L rds/peripherin mutation. Exp Eye Res 74:719-735.

Braun RD, Linsenmeier RA, Goldstick TK (1995) Oxygen consumption in the inner and outer retina of the cat. Invest Ophthalmol Vis Sci 36:542-554.

Bunge S, Wedemann H, David D, Terwilliger DJ, van den Born LI, Aulehla-Scholz C, Samanns C, Horn M, Ott J, Schwinger E, et al. (1993) Molecular analysis and genetic mapping of the rhodopsin gene in families with autosomal dominant retinitis pigmentosa. Genomics 17:230-233.

Carter-Dawson LD, LaVail MM, Sidman RL (1978) Differential effect of the rd mutation on rods and cones in the mouse retina. Invest Ophthalmol Vis Sci 17:489-498.

Cayouette M, Gravel C (1997) Adenovirus-mediated gene transfer of ciliary neurotrophic factor can prevent photoreceptor degeneration in the retinal degeneration (rd) mouse. Hum Gene Ther 8:423-430.

Cayouette M, Behn D, Sendtner M, Lachapelle P, Gravel C (1998) Intraocular gene transfer of ciliary neurotrophic factor prevents death and increases responsiveness of rod photoreceptors in the retinal degeneration slow mouse. J Neurosci 18:9282-9293.

Chang GQ, Hao Y, Wong F (1993) Apoptosis: final common pathway of photoreceptor death in rd, rds, and rhodopsin mutant mice. Neuron 11:595-605.

Check E (2003) Second cancer case halts gene-therapy trials. Nature 421:305-305.

Chen CK (2005) The vertebrate phototransduction cascade: amplification and termination mechanisms. Rev Physiol Biochem Pharmacol 154:101-121.

Chen CK, Burns ME, Spencer M, Niemi GA, Chen J, Hurley JB, Baylor DA, Simon MI (1999) Abnormal photoresponses and light-induced apoptosis in rods lacking rhodopsin kinase. Proc Natl Acad Sci USA 96:3718-3722.

Chen J, Simon MI, Matthes MT, Yasumura D, LaVail MM (1999) Increased susceptibility to light damage in an arrestin knockout mouse model of Oguchi disease (stationary night blindness). Invest Ophthalmol Vis Sci 40:2978-2982.

Chen J, Flannery JG, LaVail MM, Steinberg RH, Xu J, Simon MI (1996) bcl-2 overexpression reduces apoptotic photoreceptor cell death in three different retinal degenerations. Proc Natl Acad Sci USA 93:7042-7047.

Chong NH, Alexander RA, Waters L, Barnett KC, Bird AC, Luthert PJ (1999) Repeated injections of a ciliary neurotrophic factor analogue leading to long-term photoreceptor survival in hereditary retinal degeneration. Invest Ophthalmol Vis Sci 40:1298-1305.

Cideciyan AV, Jacobson SG, Aleman TS, Gu D, Pearce-Kelling SE, Sumaroka A, Acland GM, Aguirre GD (2005) In vivo dynamics of retinal injury and repair in the rhodopsin mutant dog model of human retinitis pigmentosa. Proc Natl Acad Sci USA 102:5233-5238.

Cohen AI (1972) Rods and cones. In: Handbook of Sensory Physiology (Fuortes MGF, ed). Berlin: Springer.

Coulombre JL, Coulombre AJ (1965) Regeneration of neural retina from the pigmented epithelium in the chick embryo. Dev Biol 12:79-92.

Cringle SJ, Yu D-Y (2002) A multi-layer model of retinal oxygen supply and consumption helps explain the muted rise in inner retinal PO2 during systemic hyperoxia. Comp Biochem Physiol A Mol Integr Physiol 132:61-66.

Curcio CA, Millican CL, Allen KA, Kalina RE (1993) Aging of the human photoreceptor mosaic: evidence for selective vulnerability of rods in central retina. Invest Ophthalmol Vis Sci 34:3278-3296.

Demontis GC, Longoni B, Gargini C, Cervetto L (1997) The energetic cost of photoreception in retinal rods of mammals. Arch Ital Biol 135:95-109.

Dowling JE, Sidman RL (1962) Inherited retinal dystrophy in the rat. J Cell Biol 14:73-109.

Drasdo N, Chiti Z, Owens DR, North RV (2002) Effect of darkness on inner retinal hypoxia in diabetes. Lancet 359:2251-2253.

Drechsler M, Aehnelt C, Hofmann KP (1987) Electron spectroscopic imaging (ESI) of bovine photoreceptor. Eur J Cell Biol 44:174-179.

Dryja TP, Hahn LB, Cowley GS, McGee TL, Berson EL (1991) Mutation spectrum of the rhodopsin gene among patients with autosomal dominant retinitis pigmentosa. Proc Natl Acad Sci USA 88:9370-9374.

Dryja TP, McGee TL, Hahn LB, Cowley GS, Olsson JE, Reichel E, Sandberg MA, Berson EL (1990a) Mutations within the rhodopsin gene in patients with autosomal dominant retinitis pigmentosa. N Engl J Med 323:1302-1307.

Dryja TP, McGee TL, Reichel E, Hahn LB, Cowley GS, Yandell DW, Sandberg MA, Berson EL (1990b) A point mutation of the rhodopsin gene in one form of retinitis pigmentosa. Nature 343:364-366.

Faktorovich EG, Steinberg RH, Yasumura D, Matthes MT, LaVail MM (1990) Photoreceptor degeneration in inherited retinal dystrophy delayed by basic fibroblast growth factor. Nature 347:83-86.

Fan J, Woodruff ML, Cilluffo MC, Crouch RK, Fain GL (2005) Opsin activation of transduction in the rods of dark-reared Rpe65 knockout mice. J Physiol 568:83-95.

Fischer AJ (2005) Neural regeneration in the chick retina. Prog Retin Eye Res 24:161-182.

Frasson M, Picaud S, Leveillard T, Simonutti M, Mohand-Said S, Dreyfus H, Hicks D, Sabel J (1999) Glial cell line-derived neurotrophic factor induces histologic and functional protection of rod photoreceptors in the rd/rd mouse. Invest Ophthalmol Vis Sci 40:2724-2734.

Gao H, Hollyfield JG (1992) Aging of the human retina. Differential loss of neurons and retinal pigment epithelial cells. Invest Ophthalmol Vis Sci 33:1-17.

Gargini C, Belfiore MS, Bisti S, Cervetto L, Valter K, Stone J (1999) The impact of basic fibroblast growth factor on photoreceptor function and morphology. Invest Ophthalmol Vis Sci 40:2088-2099.

Geller S, Krowka R, Valter K, Stone J (2006) Toxicity of hyperoxia to the retina: evidence from the mouse. Adv Exp Med Biol 572:425-437.

Goldman AI, Teirstein PS, O'Brien PJ (1980) The role of ambient lighting in circadian disc shedding in the rod outer segment of the rat retina. Invest Ophthalmol Vis Sci 19:1257-1267.

Goto Y, Peachey NS, Ripps H, Naash MI (1995) Functional abnormalities in transgenic mice expressing a mutant rhodopsin gene. Invest Ophthalmol Vis Sci 36:62-71.

Graymore C (1959) Metabolism of the developing retina: aerobic and anaerobic glycolysis in the developing rat retina. Brit J Ophthal 43:34-39.

Graymore C (1960) Metabolism of the developing retina: respiration in the developing normal rat retina and the effect of an inherited degeneration of the retinal neuro-epithelium. Brit J Ophthal 44:363-369.

Graymore C, Tansley K (1959) Iodoacetate poisoning of the rat retina. Brit J Ophthal 43:486-493.

Green ES, Menz MD, LaVail MM, Flannery JG (2000) Characterization of rhodopsin mis-sorting and constitutive activation in a transgenic rat model of retinitis pigmentosa. Invest Ophthalmol Vis Sci 41:1546-1553.

Hacein-Bey-Abina S, Von Kalle C, Schmidt M, McCormack MP, Wulffraat N, Leboulch P, Lim A, Osborne CS, Pawliuk R, Morillon E, Sorensen R, Forster A, Fraser P, Cohen JI, de Saint Basile G, Alexander I, Wintergerst U, Frebourg T, Aurias A, Stoppa-Lyonnet D, Romana S, Radford-Weiss I, Gross F, Valensi F, Delabesse E, Macintyre E, Sigaux F, Soulier J, Leiva LE, Wissler M, Prinz C, Rabbitts TH, Le Deist F, Fischer A, Cavazzana-Calvo M (2003) LMO2-Associated clonal T cell proliferation in two patients after gene therapy for SCID-X1. Science 302:415-419.

Haim M (1993) Retinitis pigmentosa: problems associated with genetic classification. Clin Genet 44:62-70.

Hao W, Wenzel A, Obin MS, Chen CK, Brill E, Krasnoperova NV, Eversole-Cire P, Kleyner Y, Taylor A, Simon MI, Grimm C, Reme CE, Lem J (2002) Evidence for two apoptotic pathways in light-induced retinal degeneration. Nat Genet 32:254-260.

Harris A, Arend O, Danis RP, Evans D, Wolf S, Martin BJ (1996) Hyperoxia improves contrast sensitivity in early diabetic retinopathy. Brit J Ophthal 80:209-213.

Heckenlively JR, Rodriguez JA, Daiger SP (1991) Autosomal dominant sectoral retinitis pigmentosa. Two families with transversion mutation in codon 23 of rhodopsin. Arch Ophthalmol 109:84-91.

Hoffman DR, Locke KG, Wheaton DH, Fish GE, Spencer R, Birch DG (2004) A randomized, placebo-controlled clinical trial of docosahexaenoic acid supplementation for X-linked retinitis pigmentosa. Am J Ophthalmol 137:704-718.

Hopkinson L, Kerly M (1959) The effect of monoiodoacetate on the aerobic metabolism of ox retina in vitro. Biochem J 72:22-27.

Hotta N, Nakamura J, Sakakibara F, Hamada Y, Hara T, Mori K, Nakashima E, Sasaki H, Kasama N, Inukai S, Koh N (1997) Electroretinogram in sucrose-fed diabetic rats

treated with an aldose reductase inhibitor or an anticoagulant. Am J Physiol Endocrinol Metab 273:E965-E971.

Illing ME, Rajan RS, Bence NF, Kopito RR (2002) A rhodopsin mutant linked to autosomal dominant retinitis pigmentosa is prone to aggregate and interacts with the ubiquitin proteasome system. J Biol Chem 277:34150-34160.

Inglehearn CF, Keen TJ, Bashir R, Jay M, Fitzke F, Bird AC, Crombie A, Bhattacharya S (1992) A completed screen for mutations of the rhodopsin gene in a panel of patients with autosomal dominant retinitis pigmentosa. Hum Mol Genet 1:41-45.

Jay M (1982) Figures and fantasies: the frequencies of the different genetic forms of retinitis pigmentosa. Birth Defects Orig Artic Ser 18:167-173.

Johnson G (1901) Contributions to the comparative anatomy of the mammalian eye chiefly based on ophthalmoscopic examination. Phil Trans Roy Soc London 194.

Jomary C, Vincent KA, Grist J, Neal MJ, Jones SE (1997) Rescue of photoreceptor function by AAV-mediated gene transfer in a mouse model of inherited retinal degeneration. Gene Ther 4:683-690.

Jozwick C, Valter K, Stone J (2006) Reversal of functional loss in the P23H-3 rat retina by management of ambient light. Exp Eye Res 83:1074-1080.

Kaitz M, Auerbach E (1979a) Retinal degeneration in RCS rats raised under ambient light levels. Vision Res 19:79-81.

Kaitz M, Auerbach E (1979b) Action spectrum for light-induced retinal degeneration in dystrophic rats. Vision Res 19:1041-1044.

Kedzierski W, Bok D, Travis GH (1998) Non-cell-autonomous photoreceptor degeneration in rds mutant mice mosaic for expression of a rescue transgene. J Neurosci 18:4076-4082.

Kremmer S, Eckstein A, Gal A, Apfelstedt-Sylla E, Wedemann H, Ruther K, Zrenner E (1997) Ocular findings in patients with autosomal dominant retinitis pigmentosa and Cys110Phe, Arg135Gly, and Gln344stop mutations of rhodopsin. Graefes Arch Clin Exp Ophthalmol 235:575-583.

Kumar-Singh R, Farber DB (1998) Encapsidated adenovirus mini-chromosome-mediated delivery of genes to the retina: application to the rescue of photoreceptor degeneration. Hum Mol Genet 7:1893-1900.

Kwan AS, Wang S, Lund RD (1999) Photoreceptor layer reconstruction in a rodent model of retinal degeneration. Exp Neurol 159:21-33.

Lau D, McGee LH, Zhou S, Rendahl KG, Manning WC, Escobedo JA, Flannery JG (2000) Retinal degeneration is slowed in transgenic rats by AAV-mediated delivery of FGF-2. Invest Ophthalmol Vis Sci 41:3622-3633.

LaVail MM (1973) Kinetics of rod outer segment renewal in the developing mouse retina. J Cell Biol 58:650-661.

LaVail MM (1980) Circadian nature of rod outer segment disc shedding in the rat. Invest Ophthalmol Vis Sci 19:407-411.

LaVail MM, Battelle BA (1975) Influence of eye pigmentation and light deprivation on inherited retinal dystrophy in the rat. Exp Eye Res 21:167-192.

LaVail MM, Gorrin GM, Yasumura D, Matthes MT (1999) Increased susceptibility to constant light in nr and pcd mice with inherited retinal degenerations. Invest Ophthalmol Vis Sci 40:1020-1024.

LaVail MM, Yasumura D, Matthes MT, Lau-Villacorta C, Unoki K, Sung CH, Steinberg RH (1998) Protection of mouse photoreceptors by survival factors in retinal degenerations. Invest Ophthalmol Vis Sci 39:592-602.

LaVail MM, Yasumura D, Matthes MT, Drenser KA, Flannery JG, Lewin AS, Hauswirth WW (2000) Ribozyme rescue of photoreceptor cells in P23H transgenic rats: long-term survival and late-stage therapy. Proc Natl Acad Sci USA 97:11488-11493.

Leveillard T, Mohand-Said S, Lorentz O, Hicks D, Fintz AC, Clerin E, Simonutti M, Forster V, Cavusoglu N, Chalmel F, Dolle P, Poch O, Lambrou G, Sahel JA (2004) Identification and characterization of rod-derived cone viability factor. Nat Genet 36:755-759.

Lewin AS, Drenser KA, Hauswirth WW, Nishikawa S, Yasumura D, Flannery JG, LaVail MM (1998) Ribozyme rescue of photoreceptor cells in a transgenic rat model of autosomal dominant retinitis pigmentosa. Nat Med 4:967-971.

Li T, Franson WK, Gordon JW, Berson EL, Dryja TP (1995) Constitutive activation of phototransduction by K296E opsin is not a cause of photoreceptor degeneration. Proc Natl Acad Sci USA 92:3551-3555.

Li T, Sandberg MA, Pawlyk BS, Rosner B, Hayes KC, Dryja TP, Berson EL (1998) Effect of vitamin A supplementation on rhodopsin mutants threonine-17 --> methionine and proline-347 --> serine in transgenic mice and in cell cultures. Proc Natl Acad Sci USA 95:11933-11938.

Linsenmeier RA (1986) Effects of light and darkness on oxygen distribution and consumption in the cat retina. J Gen Physiol 88:521-542.

Linsenmeier RA, Braun RD (1992) Oxygen distribution and consumption in the cat retina during normoxia and hypoxemia. J Gen Physiol 99:177-197.

Linsenmeier RA, Braun RD, McRipley MA, Padnick LB, Ahmed J, Hatchell DL, McLeod DS, Lutty GA (1998) Retinal hypoxia in long-term diabetic cats. Invest Ophthalmol Vis Sci 39:1647-1657.

Liu C, Li Y, Peng M, Laties AM, Wen R (1999) Activation of caspase-3 in the retina of transgenic rats with the rhodopsin mutation s334ter during photoreceptor degeneration. J Neurosci 19:4778-4785.

Lolley RN, Lee RH (1990) Cyclic GMP and photoreceptor function. Faseb J 4:3001-3008.

Lolley RN, Rong H, Craft CM (1994) Linkage of photoreceptor degeneration by apoptosis with inherited defect in phototransduction. Invest Ophthalmol Vis Sci 35:358-362.

Lowitt S, Malone JI, Salem A, Kozak WM, Orfalian Z (1993) Acetyl-L-carnitine corrects electroretinographic deficits in experimental diabetes. Diabetes 42:1115-1118.

Lucas DR, Newhouse JP (1957) The toxic effect of sodium L-glutamate on the inner layers of the retina. AMA Arch Ophthalmol 58:193-201.

Machida S, Kondo M, Jamison JA, Khan NW, Kononen LT, Sugawara T, Bush RA, Sieving PA (2000) P23H rhodopsin transgenic rat: correlation of retinal function with histopathology. Invest Ophthalmol Vis Sci 41:3200-3209.

Miyake Y, Sugita S, Horiguchi M, Yagasaki K (1990) Light deprivation and retinitis pigmentosa. Am J Ophthalmol 110:305-306.

Mohand-Said S, Hicks D, Dreyfus H, Sahel JA (2000) Selective transplantation of rods delays cone loss in a retinitis pigmentosa model. Arch Ophthalmol 118:807-811.

Mohand-Said S, Deudon-Combe A, Hicks D, Simonutti M, Forster V, Fintz AC, Leveillard T, Dreyfus H, Sahel JA (1998) Normal retina releases a diffusible factor stimulating cone survival in the retinal degeneration mouse. Proc Natl Acad Sci USA 95:8357-8362.

Naash MI, Hollyfield JG, al-Ubaidi MR, Baehr W (1993) Simulation of human autosomal dominant retinitis pigmentosa in transgenic mice expressing a mutated murine opsin gene. Proc Natl Acad Sci USA 90:5499-5503.

Naash ML, Peachey NS, Li ZY, Gryczan CC, Goto Y, Blanks J, Milam AH, Ripps H (1996) Light-induced acceleration of photoreceptor degeneration in transgenic mice expressing mutant rhodopsin. Invest Ophthalmol Vis Sci 37:775-782.

Nathans J, Thomas D, Hogness DS (1986) Molecular genetics of human color vision: the genes encoding blue, green, and red pigments. Science 232:193-202.

Natoli R, Provis J, Valter K, Stone J (2008) Expression and role of the early-response gene Oxr1 in the hyperoxia-challenged mouse retina. Invest Ophthalmol Vis Sci 49:4561-4567.

Neitz M, Neitz J, Jacobs GH (1991) Spectral tuning of pigments underlying red-green color vision. Science 252:971-974.

Nir I, Kedzierski W, Chen J, Travis GH (2000) Expression of Bcl-2 protects against photoreceptor degeneration in retinal degeneration slow (rds) mice. J Neurosci 20:2150-2154.

Nixon PJ, Bui BV, Armitage JA, A.J. V (2001) The contribution of cone responses to rat electroretinograms. Clin Exp Ophthalmol 29:193-196.

Noell WK (1955) Visual cell effects of high oxygen pressures. Fed Proc 14:107-108.

Noell WK, Walker VS, Kang BS, Berman S (1966) Retinal damage by light in rats. Invest Ophthalmol 5:450-473.

Ogilvie JM, Tenkova T, Lett JM, Speck J, Landgraf M, Silverman MS (1997) Age-related distribution of cones and ON-bipolar cells in the rd mouse retina. Curr Eye Res 16:244-251.

Okoye G, Zimmer J, Sung J, Gehlbach P, Deering T, Nambu H, Hackett S, Melia M, Esumi N, Zack DJ, Campochiaro PA (2003) Increased expression of brain-derived neurotrophic factor preserves retinal function and slows cell death from rhodopsin mutation or oxidative damage. J Neurosci 23:4164-4172.

Olsson JE, Gordon JW, Pawlyk BS, Roof D, Hayes A, Molday RS, Mukai S, Cowley GS, Berson EL, Dryja TP (1992) Transgenic mice with a rhodopsin mutation (Pro23His): a mouse model of autosomal dominant retinitis pigmentosa. Neuron 9:815-830.

Organisciak DT, Li M, Darrow RM, Farber DB (1999) Photoreceptor cell damage by light in young Royal College of Surgeons rats. Curr Eye Res 19:188-196.

Organisciak DT, Darrow RM, Barsalou L, Kutty RK, Wiggert B (2003) Susceptibility to retinal light damage in transgenic rats with rhodopsin mutations. Invest Ophthalmol Vis Sci 44:486-492.

Padnick-Silver L, Kang Derwent JJ, Giuliano E, Narfstrom K, Linsenmeier RA (2006) Retinal oxygenation and oxygen metabolism in Abyssinian cats with a hereditary retinal degeneration. Invest Ophthalmol Vis Sci 47:3683-3689.

Panda-Jonas S, Jonas JB, Jakobczyk-Zmija M (1995) Retinal photoreceptor density decreases with age. Ophthalmology 102:1853-1859.

Paskowitz DM, LaVail MM, Duncan JL (2006) Light and inherited retinal degeneration. Br J Ophthalmol 90:1060-1066.

Penn JS, Williams TP (1986) Photostasis: regulation of daily photon-catch by rat retinas in response to various cyclic illuminances. Exp Eye Res 43:915-928.

Perry J, Du J, Kjeldbye H, Gouras P (1995) The effects of bFGF on RCS rat eyes. Curr Eye Res 14:585-592.

Portera-Cailliau C, Sung CH, Nathans J, Adler R (1994) Apoptotic photoreceptor cell death in mouse models of retinitis pigmentosa. Proc Natl Acad Sci USA 91:974-978.

Potts AM, Modrell RW, Kingsbury C (1960) Permanent fractionation of the electroretinogram by sodium glutamate. Am J Ophthalmol 50:900-907.

Punzo C, Cepko C (2007) Cellular responses to photoreceptor death in the rd1 mouse model of retinal degeneration. Invest Ophthalmol Vis Sci 48:849-857.

Punzo C, Kornacker K, Cepko CL (2009) Stimulation of the insulin/mTOR pathway delays cone death in a mouse model of retinitis pigmentosa. Nat Neurosci 12:44-52.

Raper SE, Chirmule N, Lee FS, Wivel NA, Bagg A, Gao GP, Wilson JM, Batshaw ML (2003) Fatal systemic inflammatory response syndrome in a ornithine transcarbamylase deficient patient following adenoviral gene transfer. Mol Genet Metab 80:148-158.

Richer S, Stiles W, Statkute L, Pulido J, Frankowski J, Rudy D, Pei K, Tsipursky M, Nyland J (2004) Double-masked, placebo-controlled, randomized trial of lutein and antioxidant supplementation in the intervention of atrophic age-related macular degeneration: the Veterans LAST study (Lutein Antioxidant Supplementation Trial). Optometry 75:216-230.

Ripps H (2002) Cell death in retinitis pigmentosa: gap junctions and the `Bystander' Effect. Exp Eye Res 74:327-336.

Roof DJ, Adamian M, Hayes A (1994) Rhodopsin accumulation at abnormal sites in retinas of mice with a human P23H rhodopsin transgene. Invest Ophthalmol Vis Sci 35:4049-4062.

Sagdullaev BT, Aramant RB, Seiler MJ, Woch G, McCall MA (2003) Retinal transplantation-induced recovery of retinotectal visual function in a rodent model of retinitis pigmentosa. Invest Ophthalmol Vis Sci 44:1686-1695.

Sanyal S, Hawkins RK (1986) Development and degeneration of retina in rds mutant mice: effects of light on the rate of degeneration in albino and pigmented homozygous and heterozygous mutant and normal mice. Vision Res 26:1177-1185.

Sarantis M, Attwell D (1990) Glutamate uptake in mammalian retinal glia is voltage- and potassium-dependent. Brain Res 516:322-325.

Schlichtenbrede FC, MacNeil A, Bainbridge JW, Tschernutter M, Thrasher AJ, Smith AJ, Ali RR (2003) Intraocular gene delivery of ciliary neurotrophic factor results in significant loss of retinal function in normal mice and in the Prph2Rd2/Rd2 model of retinal degeneration. Gene Ther 10:523-527.

Schremser JL, Williams TP (1995) Rod outer segment (ROS) renewal as a mechanism for adaptation to a new intensity environment. I. Rhodopsin levels and ROS length. Exp Eye Res 61:17-23.

Seiler MJ, Thomas BB, Chen Z, Wu R, Sadda SR, Aramant RB (2008) Retinal transplants restore visual responses: trans-synaptic tracing from visually responsive sites labels transplant neurons. Eur J Neurosci 28:208-220.

Shen J, Yang X, Dong A, Petters RM, Peng YW, Wong F, Campochiaro PA (2005) Oxidative damage is a potential cause of cone cell death in retinitis pigmentosa. J Cell Physiol 203:457-464.

Sisk DR, Kuwabara T (1985) Histologic changes in the inner retina of albino rats following intravitreal injection of monosodium L-glutamate. Graefes Arch Clin Exp Ophthalmol 223:250-258.

Skogstad M, Bast-Pettersen R, Tynes T, Bjornsen D, Aaserud O (1994) Treatment with hyperbaric oxygen. Illustrated by the treatment of a patient with retinitis pigmentosa. Tidsskr Nor Laegeforen 114:2480-2483.

Steinberg RH (1985) Interactions between the retinal pigment epithelium and the neural retina. Doc Ophthalmol 60:327-346.

Steinberg RH (1987) Monitoring communications between photoreceptors and pigment epithelial cells: effects of "mild" systemic hypoxia. Friedenwald Lecture. Invest Ophthalmol Vis Sci 28:1888-1904.

Stone J, Maslim J, Valter-Kocsi K, Kyle Mervin, Bowers F, Chu Y, Barnett N, Provis J, Lewis G, Fisher SK (1999) Mechanisms of photoreceptor death and survival in mammalian retina. Prog Ret Eye Res 18:689-735.

Streichert LC, Birnbach CD, Reh TA (1999) A diffusible factor from normal retinal cells promotes rod photoreceptor survival in an in vitro model of retinitis pigmentosa. J Neurobiol 39:475-490.

Sung CH, Makino C, Baylor D, Nathans J (1994) A rhodopsin gene mutation responsible for autosomal dominant retinitis pigmentosa results in a protein that is defective in localization to the photoreceptor outer segment. J Neurosci 14:5818-5833.

Sung CH, Schneider BG, Agarwal N, Papermaster DS, Nathans J (1991) Functional heterogeneity of mutant rhodopsins responsible for autosomal dominant retinitis pigmentosa. Proc Natl Acad Sci USA 88:8840-8844.

Takahashi M, Miyoshi H, Verma IM, Gage FH (1999) Rescue from photoreceptor degeneration in the rd mouse by human immunodeficiency virus vector-mediated gene transfer. J Virol 73:7812-7816.

Tam BM, Moritz OL, Hurd LB, Papermaster DS (2000) Identification of an outer segment targeting signal in the COOH terminus of rhodopsin using transgenic Xenopus laevis. J Cell Biol 151:1369-1380.

Thomas BB, Seiler MJ, Sadda SR, Aramant RB (2004) Superior colliculus responses to light - preserved by transplantation in a slow degeneration rat model. Exp Eye Res 79:29-39.

Thomas BB, Seiler MJ, Aramant RB, Samant D, Qiu G, Vyas N, Arai S, Chen Z, Sadda SR (2007) Visual functional effects of constant blue light in a retinal degenerate rat model. Photochem Photobiol 83:759-765.

Tso MO, Zhang C, Abler AS, Chang CJ, Wong F, Chang GQ, Lam TT (1994) Apoptosis leads to photoreceptor degeneration in inherited retinal dystrophy of RCS rats. Invest Ophthalmol Vis Sci 35:2693-2699.

Ulshafer RJ, Sherry DM, Dawson R, Jr., Wallace DR (1990) Excitatory amino acid involvement in retinal degeneration. Brain Res 531:350-354.

Uteza Y, Rouillot JS, Kobetz A, Marchant D, Pecqueur S, Arnaud E, Prats H, Honiger J, Dufier JL, Abitbol M, Neuner-Jehle M (1999) Intravitreous transplantation of encapsulated fibroblasts secreting the human fibroblast growth factor 2 delays photoreceptor cell degeneration in Royal College of Surgeons rats. Proc Natl Acad Sci USA 96:3126-3131.

Valter K, Bisti S, Stone J (2003) Location of CNTFR-alpha on outer segments: evidence of the site of action of CNTF in rat retina. Brain Res 985:169-175.

Valter K, Kirk DK, Stone J (2008) The potential of ambient light restriction to restore function to the degenerating P23H-3 rat retina. Adv Exp Med Biol 613:193-199.

van de Pavert SA, Kantardzhieva A, Malysheva A, Meuleman J, Versteeg I, Levelt C, Klooster J, Geiger S, Seeliger MW, Rashbass P, Le Bivic A, Wijnholds J (2004) Crumbs homologue 1 is required for maintenance of photoreceptor cell polarization and adhesion during light exposure. J Cell Sci 117:4169-4177.

Vaughan DK, Coulibaly SF, Darrow RM, Organisciak DT (2003) A morphometric study of light-induced damage in transgenic rat models of retinitis pigmentosa. Invest Ophthalmol Vis Sci 44:848-855.

Vingolo EM, Rocco M, Grenga P, Salvatore S, Pelaia P (2008) Slowing the degenerative process, long lasting effect of hyperbaric oxygen therapy in retinitis pigmentosa. Graefes Arch Clin Exp Ophthalmol 246:93-98.

Vingolo EM, Pelaia P, Forte R, Rocco M, Giusti C, Rispoli E (1998) Does hyperbaric oxygen (HBO) delivery rescue retinal photoreceptors in retinitis pigmentosa? Doc Ophthalmol 97:33-39.

Vollrath D, Feng W, Duncan JL, Yasumura D, D'Cruz PM, Chappelow A, Matthes MT, Kay MA, LaVail MM (2001) Correction of the retinal dystrophy phenotype of the RCS rat by viral gene transfer of Mertk. Proc Natl Acad Sci USA 98:12584-12589.

Wald G (1969) The molecular basis of human vision. UCLA Forum Med Sci 8:281-295.

Walsh N, van Driel D, Lee D, Stone J (2004) Multiple vulnerability of photoreceptors to mesopic ambient light in the P23H transgenic rat. Brain Res 1013:194-203.

Wang M, Lam TT, Tso MO, Naash MI (1997) Expression of a mutant opsin gene increases the susceptibility of the retina to light damage. Vis Neurosci 14:55-62.

Wellard J, Lee D, Valter K, Stone J (2005) Photoreceptors in the rat retina are specifically vulnerable to both hypoxia and hyperoxia. Vis Neurosci 22:222-229.

Williams TP, Squitieri A, Henderson RP, Webbers JP (1999) Reciprocity between light intensity and rhodopsin concentration across the rat retina. J Physiol 516 (Pt 3):869-874.

Winkler B (1995) A quantitative assessment of glucose metabolism in the isolated rat retina. In: Les Seminaires Ophthalmologiques d'IPSEN: Vision et Adaptation (Doly CY, Droy-LeFaix MT, eds), pp 78-96. Amsterdam: Elsevier.

Winkler BS (2008) An hypothesis to account for the renewal of outer segments in rod and cone photoreceptor cells: renewal as a surrogate antioxidant. Invest Ophthalmol Vis Sci 49:3259-3261.

Winkler BS, Dang L, Malinoski C, Easter SS, Jr. (1997) An assessment of rat photoreceptor sensitivity to mitochondrial blockade. Invest Ophthalmol Vis Sci 38:1569-1577.

Yamada H, Yamada E, Hackett SF, Ozaki H, Okamoto N, Campochiaro PA (1999) Hyperoxia causes decreased expression of vascular endothelial growth factor and endothelial cell apoptosis in adult retina. J Cell Physiol 179:149-156.

Yau KW, Nakatani K (1984) Cation selectivity of light-sensitive conductance in retinal rods. Nature 309:352-354.

Young RW (1967) The renewal of photoreceptor cell outer segments. J Cell Biol 33:61-72.

Young RW (1971) An hypothesis to account for a basic distinction between rods and cones. Vision Res 11:1-5.

Young RW (1982) The Bowman Lecture, 1982. Biological Renewal. Applications to the eye. Trans Ophthalmol Soc UK 102 (Pt 1):42-75.

Yu D-Y, Cringle SJ (2001) Oxygen distribution and consumption within the retina in vascularised and avascular retinas and in animal models of retinal disease. Prog Retin Eye Res 20:175-208.

Yu D-Y, Cringle SJ, Alder VA, Su EN (1994) Intraretinal oxygen distribution in rats as a function of systemic blood pressure. Am J Physiol 267:H2498-2507.

Yu D-Y, Cringle SJ, Su E-N, Yu PK (2000) Intraretinal oxygen levels before and after photoreceptor loss in the RCS rat. Invest Ophthalmol Vis Sci 41:3999-4006.

Yu D-Y, Cringle S, Valter K, Walsh N, Lee D, Stone J (2004) Photoreceptor death, trophic factor expression, retinal oxygen status, and photoreceptor function in the P23H rat. Invest Ophthalmol Vis Sci 45:2013-2019.

Zhao S, Rizzolo LJ, Barnstable CJ (1997) Differentiation and transdifferentiation of the retinal pigment epithelium. Int Rev Cytol 171:225-266.

APPENDIX

Conference Proceedings

ABSTRACTS

Chrysostomou V, Stone J, Stowe S and Valter K (2009) Self-Repair of Cones in the Rhodopsin-Mutant Rat Retina by Management of Ambient Light. *Australian Neuroscience Society 29th Annual Meeting.* Canberra, Australia.

Chrysostomou V, Valter K and Stone J (2008) Cones in the rhodopsin-mutant P23H-3 retina: evidence of long term survival. *Australasian Ophthalmic and Visual Science Meeting.* Canberra, Australia.

Chrysostomou V, Stone J and Valter K (2008) Strain-dependent differences in photoreceptor vulnerability to hyperoxia in the rat. *XIIIth International Symposium on Retinal Degeneration.* Emeishan, Sichuan, China.

Chrysostomou V, Stone J, Stowe S, Barnett NL and Valter K (2007). Light-regulated damage and repair of cones in the rhodopsin-mutant P23H-3 rat retina. *Australasian Ophthalmic and Visual Science Meeting.* Canberra, Australia.

Chrysostomou V, Stowe S, Valter K, Barnett NL and Stone J (2007). Light restriction induces recovery of cone structure and function in the P23H-3 retina. *Vision Down Under.* Palm Cove, Australia.

Chrysostomou V, Valter K and Stone S (2007). Reversal of cone functional loss in the P23H-3 retina by management of ambient light. *Asia ARVO Meeting on Research in Vision and Ophthalmology.* Singapore.

Chrysostomou V, Valter K and Stone S (2006). Reversal of cone structural and functional loss in the P23H-3 retina by management of ambient light. *Australasian Ophthalmic and Visual Science Meeting.* Canberra, Australia.

Chrysostomou V, Valter K and Stone S (2006). Reversal of cone structural and functional loss in the P23H-3 retina by management of ambient light. *Bringing Science Together: ANU College of Science.* Canberra, Australia.

Chrysostomou V, Valter K and Stone S (2006). Early signs of oxygen stress in the P23H-3 retina. *XIIth International Symposium on Retinal Degeneration.* San Carlos de Bariloche, Argentina.

SELF-REPAIR OF CONES IN THE RHODOPSIN-MUTANT RAT RETINA BY MANAGEMENT OF AMBIENT LIGHT

Vicki Chrysostomou [1,2], Jonathan Stone [1,2,3], Sally Stowe [1,2] and Krisztina Valter [1,2]

[1] ARC Centre of Excellence in Vision Science
[2] Research School of Biological Sciences, The Australian National University, Canberra, ACT, Australia
[3] Save Sight Institute and Discipline of Physiology, University of Sydney, NSW, Australia

INTRODUCTION

The idea that limiting the exposure of the retina to light might slow the progression of retinal disease goes back over 100 years.[1] In most animal models of retinal degeneration, whose human counterparts include retinitis pigmentosa,[2-14] and Oguchi disease,[15,16] the disease progression is slowed by darkness and accelerated by light. In humans suffering retinal degeneration, however, attempts to slow the progression of the disease by light restriction have reported mixed success.[17,18]

Recently, it has been shown that rods in the rhodopsin-mutant transgenic P23H-3 retina, a model of autosomal dominant retinitis pigmentosa, can recover structure and function when ambient light levels are reduced. Here, we test whether cones in the P23H-3 retina are damaged by ambient light, and whether subsequent light restriction can repair any damage.

CONCLUSIONS

Modest increases in ambient light cause rapid loss of cone structure and function in the P23H-3 retina, in the absence of cone cell death.

Light restriction induces self-repair of cone structure and function.

These results suggest that partial recovery of vision loss may be a realistic goal in comparable human degenerations through the use of simple non-invasive interventions such as light restriction. Specifically, recovery of central and high acuity vision that is

RESULTS

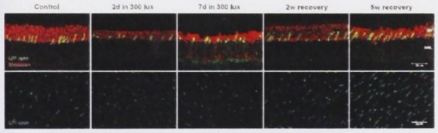

FIGURE 1: The outer segments of cones (green) were markedly reduced in length after 2-7 days exposure to photopic (300 lux) light. After 2-5 weeks recovery in dim (5 lux) light, cone outer segments regrew substantially. The density of cone outer segments remained constant at ~2000/mm² throughout, indicating that there was no cone cell death.

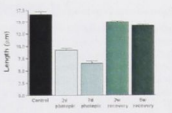

FIGURE 2: Quantitatively, exposure to photopic light resulted in shortening of cone outer segments to 55% of control lengths within 2 days, and 39% by 7 days. After 5 weeks recovery in dim conditions, cone outer segments regrew to 85% of control values.

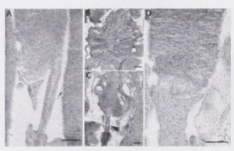

FIGURE 3: Exposure to photopic ambient light for 7 days had a devastating effect on the ultrastructural organisation of outer segments (B-C). All were shortened, and in some (B) disc stacking was severely distorted and vesiculated, while in others (C) the outer segment could be recognised only by its attachment to a ciliary process (arrow). After 5 weeks recovery in dim light, almost all outer segments present were well organised (D). Scale bars = 0.5 μm.

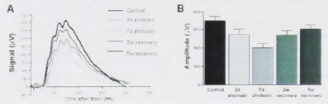

FIGURE 4: (A) Photopic light exposure had a major impact on cone function, as measured by the electroretinogram. (B) Quantitatively, the cone b-wave was reduced to, on average, 79% of control values after 2 days exposure and 58% after 7 days. From this, it recovered to 87% of the control value after 5 weeks in scotopic conditions.

METHODS

All experiments were conducted in accordance with the ARVO Statement for the Use of Animals in Ophthalmic and Vision Research. Observations were made in heterozygous P23H-3 transgenic rats aged from postnatal day 100-155. Animals were born and raised in scotopic conditions (12 hr 5 lx/12 hr dark). The brightness of the day part of the cycle was increased to 300 lx (photopic conditions) for 2-7 days and then returned to scotopic conditions for up to 5 weeks. Photoreceptor function was assessed by the dark-adapted flash-evoked electroretinogram (ERG), using a two-flash paradigm to isolate the cone response. Immunohistochemical staining of retinal cryosections was performed using antibodies specific for rhodopsin and long/medium wavelength-sensitive (LM) opsin. Immunolabeling for LM opsin was also performed on flat-mounted retinas. Using labeled flatmounts, cone outer segments were assessed for both density and length. For transmission electron microscopy (TEM), samples were dissected into Karnovsky's fixative, postfixed in osmium tetroxide, dehydrated through ethanol and acetone and embedded in Araldite/Epon resin. Images were taken with a Soft Imaging Systems Megaview III camera on a Hitachi 7100 TEM.

REFERENCES

CONES IN THE RHODOPSIN MUTANT P23H-3 RETINA: EVIDENCE OF LONG-TERM SURVIVAL

Vicki Chrysostomou [1,2], Krisztina Valter [1,2] and Jonathan Stone [1,2,3]

[1] ARC Centre of Excellence in Vision Science

[2] Research School of Biological Sciences, The Australian National University, Canberra, ACT, Australia

[3] Save Sight Institute and School of Medical Sciences, University of Sydney, NSW, Australia

PURPOSE

The loss of cone vision is a progressive, debilitating and currently untreatable feature of many retinal dystrophies. In many forms of human retinal disease, cones degenerate despite the causal mutation being in a protein expressed specifically in rods.

To understand and test therapeutic interventions aimed at cones, a careful and detailed description of their life history is necessary. To date, the study of cones in rodent models of retinal degeneration has been largely restricted to assessment by the photopic electroretinogram (ERG). In addition, data have not been collected in the rat beyond 200 days of age.[1,2] Because cone pathology in human disease may begin relatively late, it is important to understand the status of cones in the aging and aged retina.

The current study comprehensively assesses the life history of cones in the heterozygous rhodopsin-mutant P23H-3 rat retina, from before eye opening until the late stages of the rodent's lifespan.

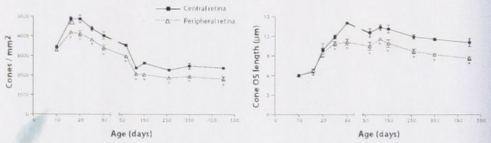

FIGURE 2:

Cone density in the P23H-3 retina increased from P10 until P20, a time during which the eyes of the rat open and terminal photoreceptor differentiation is occurring. Between P30 and P115, as the rat reached adulthood, the population of LM cones declined steadily. This fall in density is likely to be due to growth in the area of retina rather than the death of cones. At all ages studied over the next 13 months, from P115 to P500, cone density in the P23H-3 retina remained steady at approximately 2000/mm^2.

Cone density was significantly higher in the central retina at all ages above P16 compared to the peripheral retina.

FIGURE 3:

At the earliest age studied (P10) and before eye opening, LM cone OSs were less than 8 µm in length. From P16-P30, cone OSs elongated to 12 µm. From P30 until adulthood (P150), the OSs of the cone population remained stable at an average length of 16 µm. During late adulthood (P150-P500), OSs steadily shortened and by P500, were 11 µm in length.

Cones in the central retina had significantly longer OSs than those in the retinal periphery at every age above P20.

RESULTS

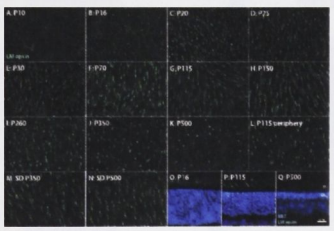

FIGURE 1:

The relatively low number of cones in the rat retina (1% of the total photoreceptor population[3,4]) meant that individual outer segments (*green*) could be clearly distinguished in LM opsin-labeled wholemounts. This form of preparation allowed us to quantify cone density, distribution and outer segment (OS) length across the entire retinal surface at 11 ages during the life of the P23H-3 rat (A-K), from before eye opening (P10) until the late stages of the rodent's lifespan (P500). (L) Anterior edge of the young adult P23H-3 retina. (M-N) Age-matched SD controls for the two oldest ages studied (P360 and P500). (O-Q) LM opsin-labeled retinal sections, used to confirm the OS length seen in wholemount preparations.

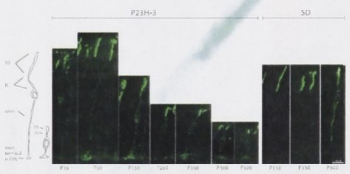

FIGURE 4:

We used the tendency of LM opsin to accumulate in the membrane of stressed cones to demonstrate the morphology of the somas and axons of cones in the P23H-3 retina (*left*), and in the aged SD retina (*right*). Soma morphology in the P23H-3 retina appeared constant during adulthood, but the length of the axon was steadily reduced after P30. This shortened the cone cell in a striking way, but may be an adaptive change (to the thinning of the outer nuclear layer), rather than a degenerative change. In the SD retina by contrast, whole-cell opsin labeling was rare before P500 and the length of the cone cell was maintained.

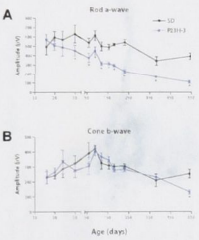

FIGURE 5:

Rod-mediated responses (A) were significantly lower in the P23H-3 retina than the SD retina at all ages above P30. By contrast, cone-mediated responses (B) in the P23H-3 retina maintained amplitude at SD levels until P380.

CONCLUSIONS

Despite the ongoing loss of rod function and numbers, cone numbers in the P23H-3 retina were maintained to the oldest age examined, and cone function and morphology were maintained for approximately 1 year, indicating a long period of cone independence.

The long period of cone survival in the P23H-3 degenerative retina creates an opportunity to induce self-repair, if the stress causing their dysfunction can be reduced.

METHODS

All experiments were conducted in accordance with the ARVO Statement for the Use of Animals in Ophthalmic and Vision Research and with the requirements of the Australian National University Animal Experimentation Ethics Committee. Observations were made in P23H-3 heterozygous transgenic rats and Sprague-Dawley controls aged from postnatal day (P) 10 to P540. All animals were born and raised in dim cyclic light (12 h 5 lux, 12 h dark). Retinal wholemounts and retinal cryosections were immunolabeled for the long-medium wavelength-sensitive (LM) cone outer segment opsin. LM opsin-labeled wholemounts were used to assess the density, distribution and outer segment length of LM cones. Photoreceptor function was assessed by the dark-adapted flash-evoked electroretinogram (ERG), using a two-flash paradigm to isolate the cone response.

REFERENCES

1. Machida S, Kondo M, Jamison JA, et al. P23H Rhodopsin Transgenic Rat: Correlation of Retinal Function with Histopathology. Invest Ophthalmol Vis Sci 2000;41:3200-3209.

2. Yu D-Y, Cringle S, Valter K, Walsh N, Lee D, Stone J. Photoreceptor Death, Trophic Factor Expression, Retinal Oxygen Status, and Photoreceptor Function in the P23H Rat. Invest Ophthalmol Vis Sci 2004;45:2013-2019.

3. Lavail MM. Survival of some photoreceptor cells in albino rats following long-term exposure to continuous light. Invest Ophthalmol 1976;15:64-70.

4. Szél A, Röhlich P. Two cone types of rat retina detected by anti-visual pigment antibodies. Exp Eye Res 1992;55:47-52.

STRAIN-DEPENDENT DIFFERENCES IN PHOTORECEPTOR VULNERABILITY TO HYPEROXIA IN THE RAT

Vicki Chrysostomou [1,2], Jonathan Stone [1,2,3] and Krisztina Valter [1,2]

[1] ARC Centre of Excellence in Vision Science
[2] Research School of Biological Sciences, The Australian National University, Canberra, ACT, Australia
[3] Save Sight Institute and Department of Physiology, University of Sydney, NSW, Australia

PURPOSE

It has long[1] been known that hyperoxia is selectively toxic to photoreceptors.

In the mouse, strain-dependent differences in photoreceptor vulnerability to oxygen stress have been described. Photoreceptors in the adult pigmented C57BL/6J mouse strain are vulnerable to hyperoxia, while those in the albino BALB/cJ, C57BL/6-c2J and A/J strains are relatively resistant[2-4]. Recently, the genetic basis for the C57BL/6J - A/J difference has been localized to chromosome 6[2].

The vulnerability of adult rat strains to hyperoxia has not been explored but studies of the neonatal rat retina suggest that, like the mouse, there are strain-dependent differences in responses to oxygen stress. Pigmented Dark Agouti, Hooded Wistar and Brown Norway rat strains are more vulnerable to oxygen-induced retinopathy than albino Sprague-Dawley, Fischer 344, Wistar-Furth and Lewis strains[5, 6].

Here, we test the vulnerability of photoreceptors to hyperoxic stress in the adult retina of two rat strains: the pigmented Long-Evans (LE) and the albino Sprague-Dawley (SD).

RESULTS

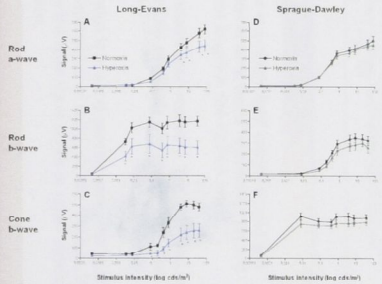

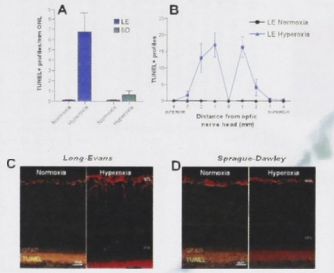

FIGURE 1:

In the pigmented LE strain, exposure to hyperoxia for 14 days resulted in a 55-fold increase in the frequency of TUNEL+ (dying) cells in the outer nuclear layer (A). In the albino SD strain, the same hyperoxic exposure resulted in a much smaller (5-fold) increase in TUNEL-labeling of photoreceptors.

Hyperoxia-induced DNA damage to LE photoreceptors was most prominent in central retina (B).

TUNEL labelling in the central LE retina co-localized with areas of raised GFAP immunoreactivity (C), a well known indicator of retinal stress. In the SD retina, hyperoxic exposure had no effect on GFAP expression (D).

FIGURE 2:

In the LE strain, exposure to hyperoxia for 14 days significantly (asterisks) reduced the amplitude of rod a-wave (A), rod b-wave (B) and cone b-wave (C) components of the ERG. At the brightest flash intensity, which was sufficient to elicit saturated responses, amplitudes of the rod a-wave, rod b-wave and cone b-wave were reduced by 29%, 46% and 49% respectively.

In the SD strain, the effect of hyperoxic exposure on the ERG was much less marked, and did not reach statistical significance for rod (D-E) or cone (F) ERG components.

METHODS

All experiments were conducted in accordance with the ARVO Statement for the Use of Animals in Ophthalmic and Vision Research and with the requirements of the Australian National University Animal Experimentation Ethics Committee. Pigmented Long-Evans (LE) and albino Sprague-Dawley (SD) rats aged 90-150 days were used. All animals were born, raised, and exposed to hyperoxia under dim cyclic illumination (12 h 5 lux/12 h dark). Animals were exposed to hyperoxia (75% oxygen) for 14 days by placing litter boxes inside a plexiglass chamber in which the oxygen concentration was controlled by a feed-back system (OxyCycler, Biospherix Biosystems Co). Photoreceptor function was assessed by the dark-adapted flash-evoked electroretinogram (ERG), using a two-flash paradigm to isolate the cone response. Immunohistochemical labeling of retinal cryosections was performed using antibodies specific for rhodopsin, long/medium wavelength-sensitive (L/M) opsin, and glial fibrillary acidic protein (GFAP). Retinal cryosections were labeled using the TUNEL technique to identify the fragmentation of DNA characteristic of apoptotic cells.

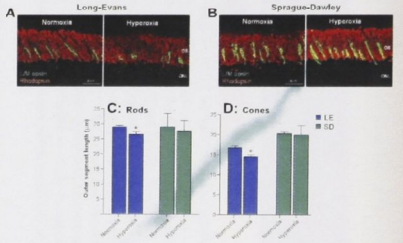

FIGURE 3:

Rod and cone outer segments, identified by opsin immunolabeling, appeared reduced in length by 14 days hyperoxic exposure in the LE (A), but not the SD (B), retina.

Quantitatively, hyperoxia in the LE retina resulted in statistically significant (asterisks) reductions of 10% in rod outer segment length (C) and 14% in cone outer segment length (D). Hyperoxia-induced changes of SD rod and cone outer segment lengths were much smaller (5% and 1% respectively) and not statistically significant.

CONCLUSIONS

In the retinas of the LE and SD strains of rat, hyperoxia induces cell death specific to photoreceptors. In the LE strain, photoreceptor death induced by hyperoxia is an order of magnitude higher, and hyperoxia also shortens outer segments of rods and cones, reduces rod and cone components of the ERG and upregulates the expression of a stress-inducible protein (GFAP).

The regulation of oxygen vulnerability has been localized to chromosome 6 in the mouse, using the C57BL/6 (vulnerable) and A/J (resistant) phenotypes[2]. The present results show that genetically-determined variations in oxygen susceptibility are not unique to the mouse.

'Oxygen phenotypes', such as that described here for the rat, may provide a useful basis for identification of the genes that determine photoreceptor vulnerability to oxygen stress, and of the *mechanisms involved*.

REFERENCES

1. Noell WK. Visual cell effects of high oxygen pressures. Fed Proc 1953;14:107-108.

2. Smith RS,Sidman Z, Gilger SL, Lavail MM, Hollenhorst JM. A strong genetic determinant of hyperoxia-induced retinal degeneration in mouse chimaeras. Invest Ophthalmol Vis Sci 2007;48:419-411.

3. Wikler N, Breen-Nunez A, Gallo S, Shaw J. Resistance of photoreceptors in the C57BL/6-Cr, C57BL/6J, and BALB/cJ mouse strains to oxygen stress: Evidence of an oxygen phenotype. Current Eye Research. 2004;29:441-448.

4. Yamada H, Yamada E, Hackett SF, Ozaki H, Okamoto N, Campochiaro PA. Hyperoxia causes decreased expression of vascular endothelial growth factor and endothelial cell apoptosis in adult retina. J Cell Physiol 1999;179:179-190.

5. Gao G, Li Y, Peet J, Crosson CE, Bowers SW, Ma JX. Difference in ischemic regulation of vascular endothelial growth factor and pigment epithelium-derived factor in Brown Norway and Sprague Dawley rats contributing to different susceptibilities to retinal neovascularization. Diabetes 2002;51:1218-1225.

6. van Wijngaarden P, Coster DJ, Beaulieu MM, Chisholm S, Williams KA. Strain-dependent differences in oxygen-induced retinopathy in the adult rat. Invest Ophthalmol Vis Sci 2005;46:1445-1452.

LIGHT-REGULATED DAMAGE AND REPAIR OF CONES IN THE RHODOPSIN-MUTANT P23H-3 RAT RETINA

Vicki Chrysostomou,[1] Jonathan Stone[1], Sally Stowe[1], Nigel L. Barnett[2] and Krisztina Valter[1]
ARC Centre of Excellence in Vision Science
[1] Research School of Biological Sciences, The Australian National University, Canberra, ACT, Australia
[2] Vision, Touch and Hearing Research Centre, School of Biomedical Sciences, University of Queensland, Brisbane, QLD, Australia

PURPOSE

The degenerative retina is more sensitive to light than the normal retina. Increases in ambient light levels have a severe effect on photoreceptors in genetically engineered rhodopsin mutants, such as the P23H-3[1] and S334ter rat,[2] and naturally occurring rhodopsin mutants such as the T4R dog.[3] In the P23H rat, mesopic light exposure sharply accelerates photoreceptor death rates and reduces outer segment length and ERG amplitude.[1] Our group has recently reported evidence of partial recovery of light-induced photoreceptor changes in the P23H retina.[4] Here, we extend the study to specifically examine the effect of light restriction on cone photoreceptors in the degenerative retina.

RESULTS

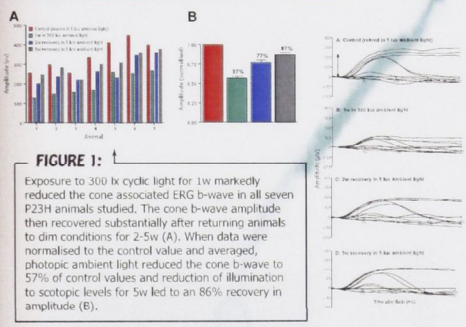

FIGURE 1:
Exposure to 300 lx cyclic light for 1w markedly reduced the cone associated ERG b-wave in all seven P23H animals studied. The cone b-wave amplitude then recovered substantially after returning animals to dim conditions for 2-5w (A). When data were normalised to the control value and averaged, photopic ambient light reduced the cone b-wave to 57% of control values and reduction of illumination to scotopic levels for 5w led to an 86% recovery in amplitude (B).

FIGURE 2:
Double-flash-isolated cone ERG responses recorded from a representative P23H animal show recovery of the cone b-wave amplitude in response to light restriction. Each of A-D shows 10 responses to a series of flashes of increasing intensity from 0.00004 to 3.8 cd/s/m^2.

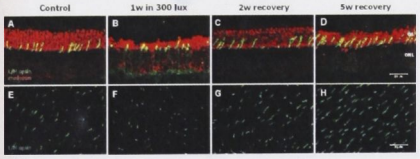

FIGURE 3:
The outer segment (OS) of rods and cones was markedly reduced in length by 1w exposure to photopic ambient illumination and regrew significantly over the recovery period (A-D). In wholemount preparations (E-H), again, cone OS length was reduced sharply by 1w exposure to photopic ambient conditions and, by 5w recovery, appeared normal in length.

METHODS

All experiments were conducted in accordance with the ARVO Statement for the Use of Animals in Ophthalmic and Vision Research. Observations were made in heterozygous P23H-3 transgenic rats aged from postnatal day 100-155. Animals were born and raised in scotopic conditions (12 hr 5 lx/12 hr dark). The brightness of the day part of the cycle was increased to 300 lx (photopic conditions) for 1 week and then returned to scotopic conditions for up to 5 weeks. Photoreceptor function was assessed by the dark-adapted flash-evoked electroretinogram (ERG), using a two-flash paradigm to isolate the cone response. Immunohistochemical staining of retinal cryosections was performed using antibodies specific for rhodopsin and long/medium wavelength-sensitive (L/M) opsin. Immunolabelling for L/M opsin was also done on flat-mounted retinas. Counts of L/M-opsin-labelled cones were made across the flat-mounted retina and cone outer segment (OS) length in each region of counting was noted. For transmission electron microscopy (TEM), samples were dissected into Karnovsky's fixative, microwaved, post-fixed in osmium tetroxide, dehydratec through ethanol and acetone, and embedded in Araldite/Epon resin. Images were taken with a Soft Imaging Systems Megaview III camera on a Hitachi 7100 TEM.

REFERENCES
1. Wekh N, van Driel D, Lee D, Stone J (2004) Nubble-vulnerability of photoreceptors to mesopic ambient light in the P23H transgenic rat. Brain Research 1012:194-203.
2. Chrysostomou DT, Darrow KN, Bonelli L, Rady KE, Wiggert B (2005) Susceptibility to Retinal Light Damage in Transgenic Rats with Rhodopsin Mutations. Invest Ophthalmol Vis Sci 46:486-492.
3. Cideciyan AV, Aleman TS, Gu D, Pearce-Kelling SE, Sumaroka A, Acland GM, Aguirre GD (2005) In vivo dynamics of retinal injury and repair in the rhodopsin mutant dog model of human retinitis pigmentosa. Proc Natl Acad Sci USA 102:5233-5238.
4. Animal K C, Valter K, Stone J (2006) Reversal of functional loss in the P23H-3 rat retina by management of ambient light. Experimental Eye Research 83:1074-1083.

Fig 4: L/M Cone Density

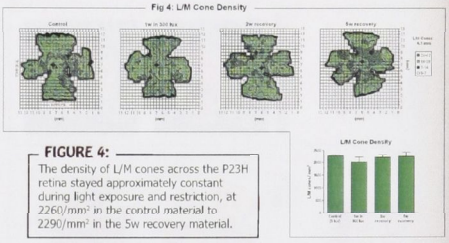

FIGURE 4:
The density of L/M cones across the P23H retina stayed approximately constant during light exposure and restriction, at 2260/mm^2 in the control material to 2290/mm^2 in the 5w recovery material.

Fig 5: L/M Cone OS Length

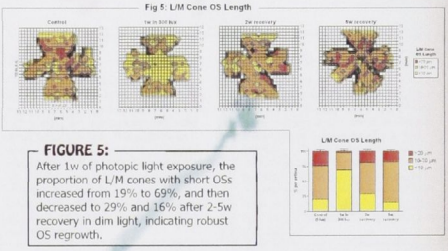

FIGURE 5:
After 1w of photopic light exposure, the proportion of L/M cones with short OSs increased from 19% to 69%, and then decreased to 29% and 16% after 2-5w recovery in dim light, indicating robust OS regrowth.

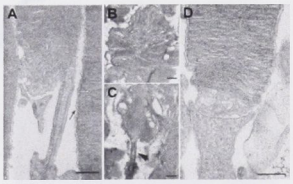

FIGURE 6:
Electron micrographs of P23H-3 photoreceptor OSs. (A) Ciliary connection from inner segment to OS of a control dim-reared animal. (B-C) Exposure to 300 lux cyclic ambient light for 1w had a devastating effect on the organisation of most OSs. All were shortened, and in some (B) disc stacking was severely distorted and vesiculated, while in others (C) the OS could be recognized only by its attachment to a ciliary process (arrow). (D) After 5w recovery in 5 lux ambient conditions, almost all OSs present were well organised. Scale bars = 0.5 µm.

CONCLUSIONS

A modest increase in ambient light causes a rapid and significant reduction in cone visual responsiveness and cone outer segment length in the P23H-3 retina.

Light restriction induces cone recovery. This was seen as an increase in the ERG amplitude and regrowth of cone outer segments.

As the P23H mutation is in a rod-specific gene, this study emphasises the dependence of cones on rod function. It also demonstrates the capacity of cones to repair structure and resume function.

REVERSAL OF CONE STRUCTURAL AND FUNCTIONAL LOSS IN THE P23H-3 RETINA BY MANAGEMENT OF AMBIENT LIGHT

Vicki Chrysostomou,[1] Nigel Barnett,[2] Krisztina Valter[1] and Jonathan Stone[1]
ARC Centre of Excellence in Vision Science
[1] Research School of Biological Sciences, The Australian National University, Canberra, ACT, Australia
[2] Vision, Touch and Hearing Research Centre, School of Biomedical Sciences, University of Queensland, Brisbane, QLD, Australia

PURPOSE

The degenerative retina is more sensitive to light than the normal retina. Increases in ambient light levels have a severe effect on photoreceptors in genetically engineered rhodopsin mutants, such as the P23H-3[1] and S334ter rat,[2] and naturally occurring rhodopsin mutants such as the T4R dog.[3] In the P23H rat, mesopic light exposure sharply accelerates photoreceptor death rates and reduces outer segment length and ERG amplitude.[1] Our group has recently reported evidence of partial recovery of light-induced photoreceptor changes in the P23H retina.[4] Here, we extend the study to specifically examine the effect of light restriction on cone photoreceptors in the degenerative retina.

RESULTS

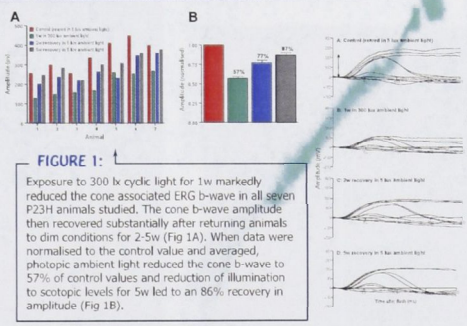

FIGURE 1:
Exposure to 300 lx cyclic light for 1w markedly reduced the cone associated ERG b-wave in all seven P23H animals studied. The cone b-wave amplitude then recovered substantially after returning animals to dim conditions for 2-5w (Fig 1A). When data were normalised to the control value and averaged, photopic ambient light reduced the cone b-wave to 57% of control values and reduction of illumination to scotopic levels for 5w led to an 86% recovery in amplitude (Fig 1B).

FIGURE 2:
Double-flash-isolated cone ERG responses recorded from a representative P23H animal show recovery of the cone b-wave amplitude in response to light restriction. Each of A-D shows 10 responses to a series of flashes of increasing intensity from 0.00004 to 3.8 cd/s/m².

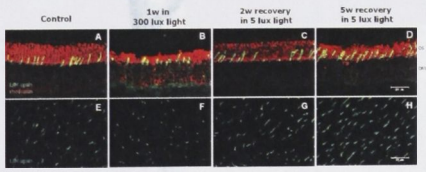

FIGURE 3:
The outer segment (OS) of rods and cones was markedly reduced in length by 1w exposure to photopic ambient illumination and regrew significantly over the recovery period (Fig 3A-D). In wholemount preparations (Fig 3E-H), again, cone OS length was reduced sharply by 1w exposure to photopic ambient conditions and, by 5w recovery, appeared normal in length.

METHODS

All experiments were conducted in accordance with the ARVO Statement for the Use of Animals in Ophthalmic and Vision Research. Observations were made in heterozygous P23H-3 transgenic rats aged from postnatal day 100-155. Animals were born and raised in scotopic conditions (12 hr 5 lx/12 hr dark). The brightness of the day part of the cycle was increased to 300 lx (photopic conditions) for 1 week and then returned to scotopic conditions for up to 5 weeks. Photoreceptor function was assessed by the dark-adapted flash-evoked electroretinogram (ERG), using a two-flash paradigm to isolate the cone response. Immunohistochemical staining of retinal cryosections was performed using antibodies specific for rhodopsin, long/medium wavelength-sensitive (L/M) opsin, protein kinase C (PKC), synaptophysin and bassoon. Immunolabelling for L/M opsin was also done on flat-mounted retinas. Counts of L/M-opsin-labelled cones were made across the flat-mounted retina and cone outer segment (OS) length in each region of counting was noted.

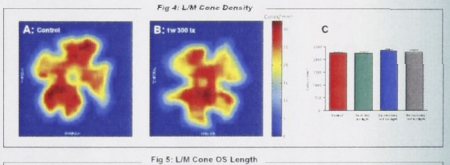

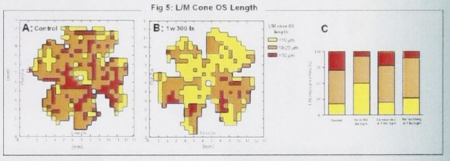

FIGURE 4:
L/M cones were distributed uniformly across the majority of the control retina. Areas of lowest density were seen at the retinal edge and surrounding the optic nerve head (Fig 4A). This pattern appeared unchanged by photopic light exposure (Fig 4B). Quantitatively, the density of L/M cones stayed approximately constant during light exposure and restriction, at 2260/mm² in the control material to 2290/mm² in the 5w recovery material (Fig 4C).

FIGURE 5:
In control retinas, 19% of the L/M cone population was classed as having short (<10 mm) OSs and these cones were predominantly restricted to the retinal edge and optic nerve head (Fig 5A), co-localising with the areas of low cone density shown in Fig 4A. After 1w of photopic light exposure, the proportion of L/M cones with short OSs increased from 19% to 50%, and the shortening was most dramatic in the superior retina (Fig 4B-C).

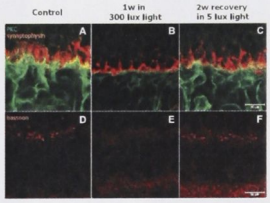

FIGURE 6:
Immunoreactivity of two markers of photoreceptor synaptic structure was clearly diminished after 1w exposure to photopic ambient light:
- a presynaptic vesicle glycoprotein (synaptophysin, Fig 4A-C)
- a synaptic ribbon protein (bassoon, Fig 4D-F)

After 2w recovery in scotopic conditions, this synaptic disruption appeared reversed and labelling returned to levels similar to controls.

CONCLUSIONS

A modest increase in ambient light causes a rapid and significant reduction in cone visual responsiveness, cone outer segment length, and photoreceptor synaptic protein density in the P23H-3 retina.

Light restriction induces cone recovery. This was seen as an increase in the ERG amplitude, regrowth of cone outer segments, and an increase in photoreceptor synaptic protein density.

As the P23H mutation is in a rod-specific gene, this study emphasises the dependence of cones on rod function. It also demonstrates the capacity of cones to repair structure and resume function.

REFERENCES
1. Wilsh R, ver. Dilel D, Lee D, Stone J (2004) Mutable vulnerability of photoreceptors to mesopic ambient light in the P23H transgenic rat. Brain Research 1015:194-202.
2. Organisciak DT, Darrow RM, Barsalou L, Kutty RK, Wiggert B (2003) Susceptibility to Retinal Light Damage in Transgenic Rats with Rhodopsin Mutations. Invest Ophthalmol Vis Sci 44:486-481.
3. Petersen A.C., Jacobsen SG, Aleman TS, Cu D, Intveldt GJ, Surowiak A, Jolent AM, Aguirre GD (2007) In vivo dynamics of retinal injury and repair in the rhodopsin mutant dog model of human retinitis pigmentosa. Prog. Ret Mol Sci 26:1-21-2259236.
4. Stone J C, Valter K, Stone J (2004) Reversal of functional loss in the P23H rat retina by management of ambient light. Experimental Eye Research 83:1074-1081.

REVERSAL OF CONE STRUCTURAL AND FUNCTIONAL LOSS IN THE P23H-3 RETINA BY MANAGEMENT OF AMBIENT LIGHT

P234

Vicki Chrysostomou, Sally Stowe, Krisztina Valter and Jonathan Stone
ARC Centre of Excellence in Vision Science
Research School of Biological Sciences, The Australian National University, Canberra, ACT, Australia

PURPOSE

The degenerative retina is more sensitive to light than the normal retina. Increases in ambient light levels have a severe effect on photoreceptors in genetically engineered rhodopsin mutants, such as the P23H-3[1] and S334ter rat,[2] and naturally occurring rhodopsin mutants such as the T4R dog.[3] In the P23H rat, mesopic light exposure sharply accelerates photoreceptor death rates and reduces outer segment length and electroretinogram amplitude.[1] Our group has recently reported evidence of partial recovery of light-induced photoreceptor changes in the P23H retina. These studies have demonstrated a significant recovery of ERG amplitude and regrowth of photoreceptor outer segments in response to a reduction in ambient light.[4] Here, we extend the study to specifically examine the effect of light restriction on cone photoreceptors in the degenerative retina.

METHODS

All experiments were conducted in accordance with the ARVO Statement for the Use of Animals in Ophthalmic and Vision Research. Observations were made in heterozygous P23H-3 transgenic rats aged from postnatal day 100-155. Animals were born and raised in dim cyclic light conditions (12 hr 5 lx/12 hr dark). The brightness of the day part of the cycle was increased to 300 lx (low end of the daylight range) for 1 week and then reduced to 5 lx for 5 weeks. Using a double flash protocol, the electroretinogram (ERG) was used to record the cone associated b-wave in dark-adapted, anaesthetised animals. Immunohistochemical staining of retinal cryosections was performed using antibodies specific for long/medium wavelength-sensitive (L/M) opsin, protein kinase C (PKC) and synaptophysin. Immunolabelling for L/M opsin was also done on flat-mounted retinas. For transmission electron microscopy (TEM), samples were dissected into Karnovsky's fixative, microwaved (5 x 10 sec on ice), postfixed in osmium tetroxide, dehydrated through ethanol and acetone and embedded in Araldite/Epon resin. Images were taken with a Soft Imaging Systems Megaview III camera on a Hitachi 7100 TEM. For scanning electron microscopy (SEM), samples were treated after the initial fixation with a modification of Tanaka's osmium-tannic acid-osmium technique[5] and viewed with a Hitachi 4300 SE/N FESEM.

RESULTS

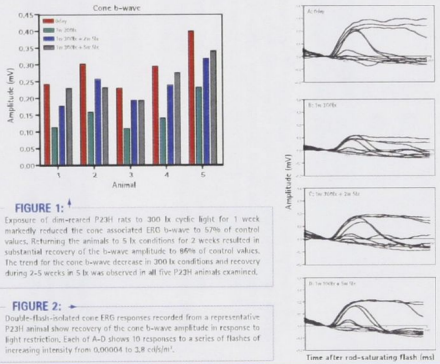

FIGURE 1: [4]
Exposure of dim-reared P23H rats to 300 lx cyclic light for 1 week markedly reduced the cone associated ERG b-wave to 57% of control values. Returning the animals to 5 lx conditions for 2 weeks resulted in substantial recovery of the b-wave amplitude to 86% of control values. The trend for the cone b-wave decrease in 300 lx conditions and recovery during 2-5 weeks in 5 lx was observed in all five P23H animals examined.

FIGURE 2:
Double-flash-isolated cone ERG responses recorded from a representative P23H animal show recovery of the cone b-wave amplitude in response to light restriction. Each of A–D shows 10 responses to a series of flashes of increasing intensity from 0.00004 to 2.8 cd·s/m².

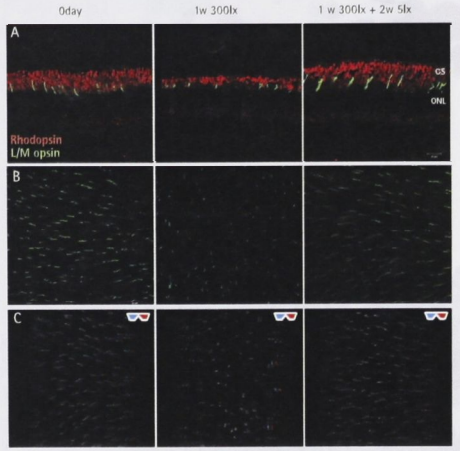

FIGURE 3:
The normal concentration of L/M opsin in cone outer segments was disrupted by 1 week 300 lx light exposure, as indicated by immunolabelling of retinal cryosections (A) and flat-mounted retinas (B,C). Cone outer segments appeared shortened and disorganised immediately after 300 lx exposure but these changes were reversed after recovery in dim light. In animals returned to 5 lx conditions for 2 weeks, opsin-bearing cone outer segments regrew substantially and became reorganised. Figure 3C shows a stereoscopic image of L/M opsin-labelled flat-mounted retinas in which the shortening and restoration of cone outer segment structure can be observed using the red/green glasses provided.

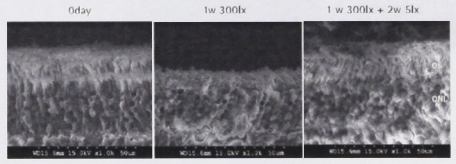

FIGURE 4:
Fluorescent microscopy results (Figure 3) that demonstrated changes in photoreceptor outer segment length in response to light restriction were confirmed at the SEM level. Scanning electron micrographs reveal long organised photoreceptor outer segments in control retinas, shortening after 1 week 300 lx light exposure and regrowth after 2 weeks recovery in dim light conditions.

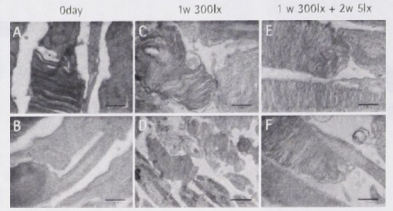

FIGURE 5:
Transmission electron micrographs of the basal region of photoreceptor outer segments revealed extensive disruption of outer segment structure in response to 1 week 300 lx light exposure, including disconnection of outer segments from connecting cilia (CDL. Outer segment integrity appeared to be restored after 2 weeks recovery in dim light (E,F). Based on outer segment morphology, we identified what we believe to be rods (A,E) and cones (B,F) and note that recovery of outer segment ultrastructure by light management is seen in both types of photoreceptor.

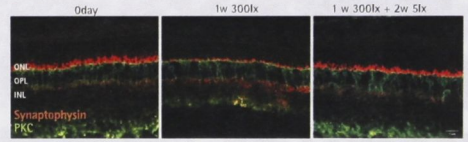

FIGURE 6:
Synaptophysin immunoreactivity in photoreceptor terminals of the outer plexiform layer (OPL) decreased substantially in response to 1 week 300 lx light exposure. After returning animals to dim light for 2 weeks, the disruption of photoreceptor synaptic terminals appeared to be reversed and the density of synaptophysin labelling in the OPL increased, reaching levels similar to the control.

CONCLUSIONS

Previous studies have described the hypersensitivity of photoreceptors in the P23H retina to low levels of ambient light. Such results indicate a dual source of vision loss in the P23H retina: photoreceptor death and photoreceptor damage. While photoreceptor death remains largely irreversible, present results suggest that the damage component of vision loss is reversible. In response to a reduction in ambient light, the P23H retina showed:

1) Recovery of the cone b-wave
2) Regrowth and reorganisation of cone outer segments
3) Reorganisation of photoreceptor synaptic terminals

Improvement in these three key parameters of retinal performance suggest that partial recovery of vision loss may be a realistic goal in comparable human degenerations through the use of simple non-invasive interventions such as light restriction. Specifically, recovery of central and high acuity vision that is mediated by the cone system may be achievable.

REFERENCES

1. Vidal M, Lee NY, Lo R, Shaw I (2004) Multiple vulnerability of photoreceptors to hereditary retinal light in the P23H transgenic rat. *Brain Research* 1033:114-121.
2. Organisciak DT, Darrow RM, Barsalou L, Kutty RK, Wiggert B (2000) Susceptibility to Retinal Light Damage in Transgenic Rats with Rhodopsin Mutations. *Invest Ophthalmol Vis Sci* 41:4149-4157.
3. Goldstein EB, Sandmeyer SV, Nguyen TJ, Cia D, Fuerst-Buckley SK, Sarmiento A, Acland GM, Aguirre GD (2000) In vivo dynamics of retinal injury and repair in the rhodopsin mutant dog model of human retinitis pigmentosa. *Proc Natl Acad Sci USA* 97(26):14315-14318.
4. Chrysostomou V, Valter K, Stowe S (2007) Reversal of functional loss in the P23H-3 rat retina by management of ambient light. *Experimental Eye Research* 83:1184-1193.
5. Tanaka K and Nakata T (1983) High resolution scanning electron microscopy of cells osmicated by a new specimen preparation method. *Biomed Res (Suppl)* 3:43-55.

REVERSAL OF CONE STRUCTURAL AND FUNCTIONAL LOSS IN THE P23H-3 RETINA BY MANAGEMENT OF AMBIENT LIGHT

Vicki Chrysostomou, Krisztina Valter and Jonathan Stone

ARC Centre of Excellence in Vision Science
The Australian National University, Canberra, ACT, Australia

INTRODUCTION

The degenerative retina is more sensitive to light than thez normal retina. Increases in ambient light levels have a severe effect on photoreceptors in genetically engineered rhodopsin mutants, such as the P23H-3[1] and S334ter rat,[2] and naturally occurring rhodopsin mutants such as the T4R dog.[3] In the P23H rat, mesopic light exposure sharply accelerates photoreceptor death rates and reduces outer segment length and ERG amplitude.[1] Our group has recently reported evidence of partial recovery of light-induced photoreceptor changes in the P23H retina. These studies have demonstrated a significant recovery of ERG amplitude and regrowth of photoreceptor outer segments in response to a reduction in ambient light.[4] Here, we extend the study to specifically examine the effect of light restriction on cone photoreceptors in the degenerative retina.

METHODS

Observations were made in heterozygous P23H-3 transgenic rats aged from postnatal day 155-200. Animals were born and raised in dim cyclic light conditions (12 hr 5 lx/12 hr dark). The brightness of the day part of the cycle was increased to 300 lx (low end of the daylight range) for 1 week and then reduced to 5 lx for 5 weeks. Using a double flash protocol, the electroretinogram (ERG) was used to assess cone function before and after 1 week of 300 lx light exposure and after 2 and 5 weeks recovery in dim light. Cone structure was assessed by immunohistochemical staining of retinal cryosections with antibodies specific for long/medium wavelength-sensitive (L/M) opsin.

RESULTS

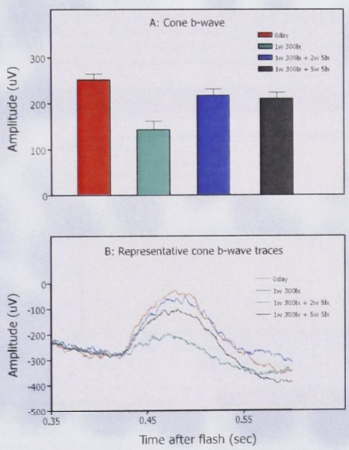

FIGURE 1:

Exposure of dim-reared P23H rats to 300 lx cyclic light for 1 week markedly reduced the cone associated ERG b-wave to 57% of control values. Returning the animals to 5 lx conditions for 2 weeks resulted in substantial recovery of the b-wave amplitude to 86% of control values. Data in Figure 1A is represented as the mean ± SEM of 5 animals.

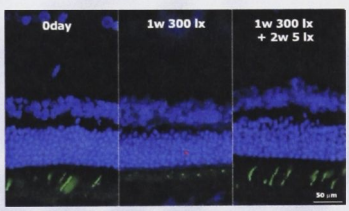

FIGURE 2:

The normal concentration of L/M opsin in cone outer segments was disrupted by 1 week 300 lx light exposure. Cone outer segments appeared shortened and disorganised and opsin became prominent in somas in the ONL. In animals returned to ambient light conditions for 2 weeks, cone outer segment structure appeared to be restored to normal. Opsin-bearing cone outer segments regrew substantially and became reorganised.

DISCUSSION & CONCLUSIONS

Previous results have described the hypersensitivity of photoreceptors in the P23H retina to low levels of ambient light.[1] Such results indicate a dual source of vision loss in the P23H retina; photoreceptor death and photoreceptor damage. While photoreceptor death remains largely irreversible, Jozwick et al. (2006) have shown that the damage component of rod vision loss is reversible. Here we extend the concept, showing that damage to cone photoreceptors is also reversible. In response to a reduction in ambient light, cones in the P23H retina showed:

1) regrowth of outer segments and;
2) recovery of the ERG b-wave

Improvement in these two key parameters of retinal performance suggest that, in humans suffering vision loss due to comparable genetic mutations, light management should improve retinal function. Specifically, improvement should be seen in central and high acuity vision that is mediated by the cone system.

REFERENCES

1. Wekin N, van Driel D, Lee D, Stone J (2004) Multiple vulnerability of photoreceptors to mesopic ambient light in the P23H transgenic rat. **Brain Research 1013**: 194-213.

2. Organisciak DT, Darrow RM, Barsalou L, Kutty RK, Wiggert B (2003) Susceptibility to Retinal Light Damage in Transgenic Rats with Rhodopsin Mutations. **Invest Ophthalmol Vis Sci** 44:486-492.

3. Cideciyan AV, Jacobson SG, Aleman TS, Gu D, Pearce-Kelling SE, Sumaroka A, Acland GM, Aguirre GD (2005) In vivo dynamics of retinal injury and repair in the rhodopsin mutant dog model of human retinitis pigmentosa. **Proc Natl Acad Sci USA 102**:5233-5238.

4. Jozwick C, Valter K, Stone J (2006) Reversal of functional loss in the P23H-3 rat retina by management of ambient light.

EARLY SIGNS OF OXYGEN STRESS IN THE P23H RETINA

Vicki Chrysostomou, Krisztina Valter and Jonathan Stone
ARC Centre of Excellence in Vision Science
The Australian National University, Canberra, ACT, Australia

INTRODUCTION

Our group has described earlier a critical period in the second week of retinal development in the rodent, during which the photoreceptor population undergoes a wave of naturally occurring cell death. This death appears to be a normal part of development, thought to cull the photoreceptor population from an initial excess to a level appropriate for adult life. These earlier studies demonstrated that the rate of photoreceptor death can be modulated by oxygen (O_2) in the normal (SD) rat, the degenerative (RCS) rat and the normal (C57BL) mouse. By changing ambient O_2 levels, we were able to slow (10% O_2) or accelerate (70% O_2) the rate of photoreceptor culling during development. Here, we test the role of O_2 in the early stages of photoreceptor death in the P23H transgenic rat, a model of retinitis pigmentosa. The transgene in this model (a proline for histidine substitution at position 23 of the rhodopsin protein) was engineered to mimic a rhodopsin mutation which causes an autosomal dominant degeneration of photoreceptors in humans. The mutation causes a similar autosomal dominant degeneration in the transgenic rat.

METHODS

Heterozygous P23H-3 rats were used. Pups were split into three experimental groups (n=5) and exposed to normoxia (21% O_2), hypoxia (10% O_2) or hyperoxia (70% O_2) from postnatal (P) day 16 to 24, the time of peak developmental photoreceptor culling. O_2 exposure was managed by placing litter boxes inside a plexiglass chamber in which the O_2 concentration was controlled by a computer system (OxyCycler, Reming Bioinstruments). After 0, 4, 8 and 14 days, eyes were collected, fixed in 4% paraformaldehyde and cryosectioned at 12 µm. TUNEL labeling was performed to detect apoptotic cell death. Photoreceptor function in the normoxic retina at P16, P20, P24 and P30 (n=3) was assessed by the flash-evoked, dark-adapted electroretinogram (ERG), recorded in anaesthetised animals. A double flash paradigm was used to record cone responses.

RESULTS

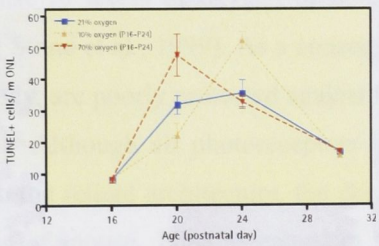

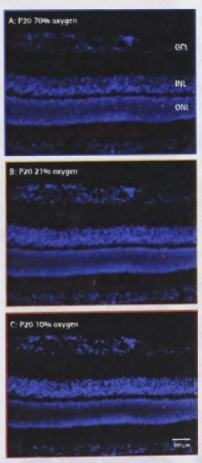

FIGURE 1:
In agreement with previous data, a wave of photoreceptor death was seen between P16 and P30 in the normoxic (control) P23H retina, as detected by TUNEL+ profiles in the ONL. This death is similar in duration to the naturally occurring culling that has previously been described in the non-degenerative SD rat, but much greater in magnitude.

Exposure to hypoxia reduced the rate of photoreceptor death in the P23H retina at P20 but this effect was reversed at P24, when hypoxia significantly accelerated cell death in the ONL.

Hyperoxic exposure greatly increased the rate of photoreceptor death at P20 but this effect was diminished by P24.

Photoreceptor vulnerability to both hypoxia and hyperoxia was lost by P30, at which point cell death rates fell to low levels, similar to controls. Data in graphs is represented as the mean ± SEM of 5 animals.

CONCLUSIONS

The regulatory effect of O_2 on photoreceptor death in the developing P23H retina is different from that previously described in the normal rat, RCS rat and normal mouse.

Hyperoxia was never protective during the critical period in the P23H rat. Hypoxia was protective during the early stages of the critical period. Consistent with previous findings in the adult, present results indicate that there is an excess of O_2 throughout the developing P23H retina. The protective effect of hypoxia at P20 confirms that the developing P23H retina is hyperoxic but later, due to unknown mechanisms, hypoxia becomes damaging.

Rod and cone function in the P23H retina steadily improves between P16 and P30, despite the abnormally high photoreceptor loss during this time.

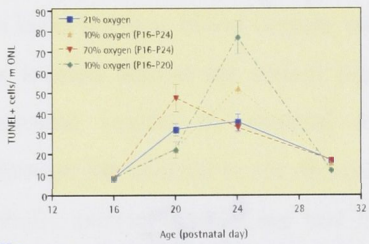

FIGURE 2:
In an attempt to maintain the protective effect of hypoxia on photoreceptor survival at P20 (without causing damage at P24), we shortened the hypoxic exposure from 8 days (P16–P24) to 4 days (P16–P20). Surprisingly, this short period of hypoxia was severely damaging to the photoreceptor population, accelerating cell death at P24 more than two-fold compared to normoxic controls and more than 1.5-fold compared to 8 day hypoxic exposure. Consistent with all other O_2 conditions, the influence of short hypoxic exposure on photoreceptor death rates was lost by P30, at which point photoreceptor death dropped to control levels.

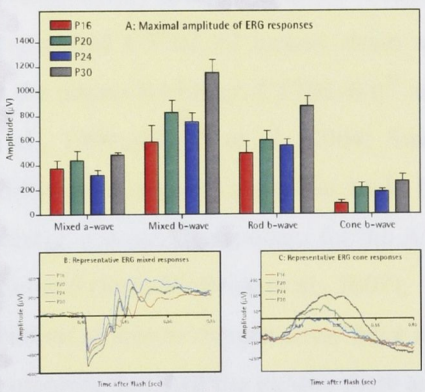

FIGURE 3:
The ERG was used to assess retinal function before (P16), during (P20, P24) and after (P30) the wave of critical period photoreceptor death. The maximal amplitude of all four ERG parameters (mixed a-wave, mixed b-wave, rod b-wave and cone b-wave) increased between P16 and P20 before decreasing slightly at P24, the time of peak photoreceptor death. This was followed by a larger increase in amplitude at P30, correlating with a drop in photoreceptor death rate. Data is represented as the mean ± SEM of 3 animals.

Differences in Photoreceptor Sensitivity to Oxygen Stress between Long Evans and Sprague-Dawley Rats

Vicki Chrysostomou, Jonathan Stone, and Krisztina Valter

1 Introduction

It has long been known that hyperoxia is specifically toxic to photoreceptors (Noell, 1955). Elevation of the partial pressure of oxygen in the retina results in photoreceptor degeneration that increases as a function of time (Yamada et al., 1999; Okoye et al., 2003; Geller et al., 2006) and oxygen concentration (Wellard et al., 2005). The vulnerability of photoreceptors to hyperoxia is a result of the unique architecture of oxygen delivery to the outer retina. The outer retina lacks intrinsic blood vessels; oxygen diffuses to photoreceptors from choroidal vessels located behind the retinal pigment epithelium (RPE). Presumably because the choroidal vessels lie external to the photoreceptors that they serve, the flow of blood through the choroid is not regulated in response to levels of oxygen or other local metabolic factors (Chan-Ling and Stone, 1993; Stone et al., 1999). As a consequence, photoreceptors, unlike most other tissues in the body, are poorly protected against fluctuations of oxygen.

Although all photoreceptors have a pre-determined vulnerability to hyperoxia due to the retinal architecture, the degree of this vulnerability appears to differ between strains of mouse. Photoreceptors in the adult pigmented C57BL/6J mouse strain are relatively vulnerable to hyperoxia, while those in the albino BALB/cJ, C57BL/6-c^{2J} and A/J strains are relatively resistant (Yamada et al., 1999; Walsh et al., 2004; Smit-McBride et al., 2007). These strain-dependent differences suggest a genetic basis for photoreceptor sensitivity to oxygen stress and, recently, a strong determinant for the A/J-C57BL/6 difference has been localised to chromosome 6 (Smit-McBride et al., 2007).

To date, the vulnerabilities of different adult rat strains to oxygen stress have not been explored. However, work in the neonatal rat suggests that, like the mouse, there are

V. Chrysostomou
Research School of Biological Sciences and ARC Centre of Excellence in Vision Science, The Australian National University, Tel: 61 2 6125 4489, Fax: 61 2 6125 8294
E-mail: vicki.chrysostomou@anu.edu.au

R.E. Anderson et al. (eds.), Recent Advances in Retinal Degenerations

strain-dependent differences to oxygen stress. Pigmented Dark Agouti, Hooded Wistar and Brown Norway rats are more vulnerable to oxygen-induced retinopathy than albino Sprague-Dawley, Fischer 344, Wistar-Furth and Lewis rats (Gao et al., 2002; van Wijngaarden et al., 2005). Using formal backcross analysis, the genetic basis of the Dark Agouti-Fischer 344 difference has been modeled using an autosomal dominant pattern of inheritance (van Wijngaarden et al., 2007).

Here, we test the impact of hyperoxia on photoreceptors in the mature retina of two rat strains; the pigmented Long Evans (LE) and the albino Sprague-Dawley (SD).

2 Methods

2.1 Animal Strains and Oxygen Exposure

All procedures were in accordance with the ARVO Statement for the Use of Animals in Ophthalmic and Vision Research. Pigmented Long Evans (LE) and albino Sprague-Dawley (SD) rats aged 90-150 days were used. All animals were born, raised and exposed to hyperoxia in dim cyclic illumination (12 h 5 lux/12 h dark). Animals were exposed to hyperoxia (75% oxygen) for 14 days by placing litter boxes inside a plexiglass chamber in which the oxygen concentration was controlled by a feedback system (OxyCycler, Biospherix).

2.2 Electroretinography

Animals were dark-adapted overnight and prepared for recording in dim red illumination as described previously (Chrysostomou et al., 2008). Following previous reports, (Nixon et al., 2001), responses to a standard test flash (44.5 cds/m^2) were considered to be 'mixed' with contributions from rods and cones. Responses to the test flash preceded, by 400 msec, by a conditioning flash (12 cds/m^2) were considered those of cones. By subtracting the cone response from the 'mixed' response, the rod response was isolated. The standard flash stimulus was sufficient to elicit saturated a-wave and b-wave responses.

2.3 Immunohistochemistry and TUNEL Labeling

Enucleated eyes were fixed, processed, cryoembedded and cryosectioned as described previously (Chrysostomou et al., 2008). Immunohistochemical labelling of retinal cryosections was performed using antibodies specific for glial fibrillary acidic protein (GFAP). Retinal cryosections were labeled using the TUNEL technique to identify the fragmentation of DNA characteristic of apoptosis.

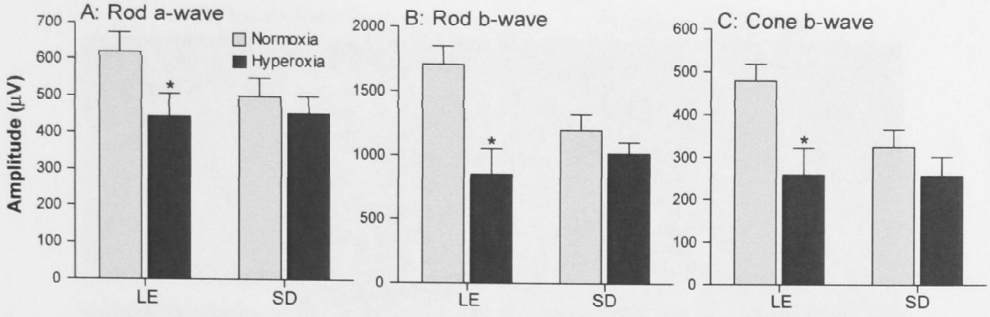

Fig. 1 ERG responses were recorded in LE and SD rats before (normoxia) and immediately after (hyperoxia) 14 days exposure to 75% oxygen. Exposure to hyperoxia significantly reduced the amplitudes of rod (A,B) and cone (C) components of the ERG in the LE but not the SD strain of rat. Histograms show mean ± SEM (n=7). * $P<0.05$ using a student's t-test.

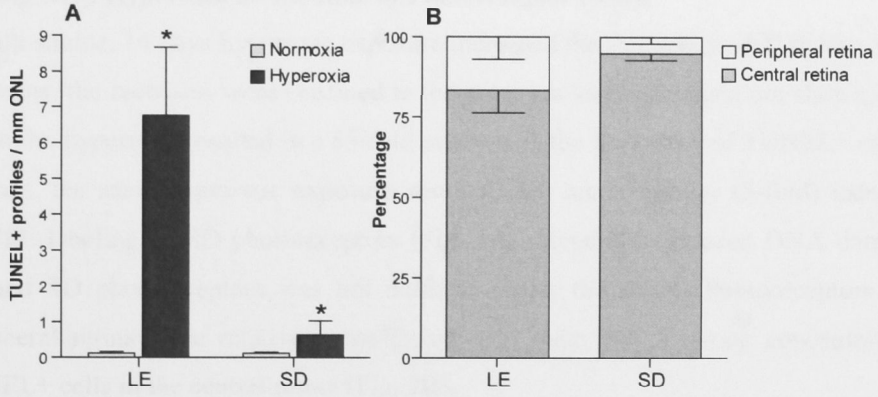

Fig. 2 Frequency and distribution of TUNEL+ profiles in LE and SD retinas after hyperoxic exposure. (A) Hyperoxia-induced increases in TUNEL+ profiles were much greater in the LE retina than the SD retina. (B) In both strains, TUNEL+ profiles were more common in the central retina than the peripheral retina (200 μm from the retinal edge) after hyperoxia. Histograms show mean ± SEM (n=5). * $P<0.01$ using a student's t-test.

3 Results

3.1 Rod and Cone Components of the ERG after Hyperoxia

Full field ERG responses were recorded in LE and SD adult rats before and after 14 days exposure to hyperoxia. In the pigmented LE strain, exposure to hyperoxia for 14 days significantly ($P<0.05$) reduced the amplitude of rod a-wave (Fig. 1A), rod b-wave (Fig. 1B) and cone b-wave (Fig. 1C) components of the ERG, by 29%, 46% and 49% respectively. In the albino SD strain the effect of hyperoxic exposure on the ERG was much less marked, and did not reach statistical significance for any of these three ERG components (Figs. 1A-C).

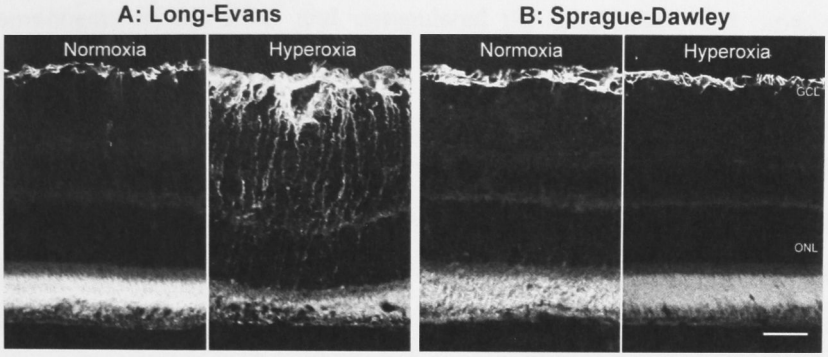

Fig. 3 Expression of the stress-inducible factor GFAP in LE and SD retinas after hyperoxic exposure. Immunoreactivity for GFAP was markedly upregulated in the LE (A) but not the SD (B) retina after 14 days hyperoxic exposure. All images are taken from the central retina. GCL, ganglion cell layer; ONL, outer nuclear layer. Scale bar = 20 μm.

3.2 Impact of Hyperoxia on the Rate of Photoreceptor Death

In both strains, 14 days hyperoxic exposure increased the frequency of TUNEL+ cells in the retina; the increases were confined to the outer nuclear layer (data not shown). In the LE strain, hyperoxia resulted in a 55-fold increase in the frequency of TUNEL+ cells. By contrast, the same hyperoxic exposure resulted in a much smaller (5-fold) increase in TUNEL labeling of SD photoreceptors (Fig. 2A). Hyperoxia-induced DNA damage to LE and SD photoreceptors was not uniform across the retina. Photoreceptors in the peripheral retina were relatively unaffected, and there was a strong concentration of TUNEL+ cells in the central retina (Fig. 2B).

3.3 Impact of Hyperoxia on GFAP Expression

In normoxic LE and SD retinas, GFAP expression was confined to astrocyte cell bodies and processes at the inner surface of the retina (left panels of Figs. 3A, 3B). After 14 days hyperoxic exposure, GFAP was prominent in radially-oriented Müller cell processes in the LE retina (right panel of Fig. 3A). Raised GFAP expression was most prominent in the central LE retina, co-localising with areas of high TUNEL labelling. In the SD retina, hyperoxic exposure had no effect on GFAP expression (right panel of Fig. 3B).

4 Discussion

In the retinas of both LE and SD strains of rat, hyperoxia induced cell death specific to photoreceptors. Quantitatively, the photoreceptor death induced by hyperoxia was an order of magnitude higher in the LE strain, in which hyperoxia also reduced rod and

cone components of the ERG and upregulated the expression of a stress-inducible protein (GFAP) by Müller cells.

'Oxygen phenotypes', such as that described here for the rat, may provide a useful basis for identification of the genes that determine photoreceptor vulnerability to oxygen stress, and of the mechanisms involved. The regulation of oxygen vulnerability has been localised to chromosome 6 in the mouse, using the C57BL/6 (vulnerable) and A/J (resistant) phenotypes (Smit-McBride et al., 2007). The present results show that genetically-determined variations in oxygen susceptibility are not unique to the mouse. They may therefore play a role in human retinal dystrophies, since the partial depletion of photoreceptors is known to cause irreversible and progressive hyperoxia of the outer layers of the retina. This rise has been demonstrated in three models of retinal degeneration; the RCS rat (Yu et al., 2000), the P23H-3 rat (Yu et al., 2004) and the Abyssinian cat (Padnick-Silver et al., 2006).

There may be an association between ocular pigmentation and susceptibility of photoreceptors to oxygen stress. Using a backcross analysis, van Wijngaarden and colleagues (2007) found that the trait for susceptibility to oxygen-induced retinopathy in Dark Agouti and Fischer 334 rats was associated with pigmentation. Other studies that have exposed either the neonatal (Gao et al., 2002; van Wijngaarden et al., 2005) or adult (Yamada et al., 1999; Walsh et al., 2004; Smit-McBride et al., 2007) rodent retina to hyperoxia, show a similar trend: albino mice (BALB/cJ, C57BL/6-c^{2J}, A/J) and rats (SD, Fischer 344, Wistar-Furth, Lewis) are more resistant to oxygen stress than pigmented mice (C57BL/6J) and rats (Dark Agouti, Hooded Wistar, Brown Norway). The current findings from LE and SD retinas also fit this pattern.

Ocular pigmentation includes high concentrations of melanin within melanosomes of RPE cells. The biological effect of RPE melanin is not completely understood; both protective and cytotoxic roles have been described. Melanins are efficient antioxidants, able to scavenge free radicals, quench electronically excited states, inhibit lipid peroxidation and chelate metal ions (Dunford et al., 1995; Rozanowska et al., 1999; Zhang et al., 2000; Ye et al., 2003). However, aged, photolysed or oxidized melanosomes lose their antioxidant properties and become increasingly able to generate reactive oxygen species (Burke et al., 2007; Zadlo et al., 2007; Zareba et al., 2007). High oxygen levels may also trigger the conversion of melanin from antioxidant to pro-oxidant thus making photoreceptors in pigmented retinas more vulnerable to oxygen stress than those in albino retinas.

References

Burke JM, Henry MM, Zareba M, Sarna T (2007) Photobleaching of melanosomes from retinal pigment epithelium: I. Effects on protein oxidation. Photochem Photobiol 83:920-924.

Chan-Ling T, Stone J (1993) Retinopathy of prematurity: Origins in the architecture of the retina. Progress in retinal Research 12:155-178.

Chrysostomou V, Stone J, Stowe S, Barnett NL, Valter K (2008) The status of cones in the rhodopsin mutant p23h-3 retina: Light-regulated damage and repair in parallel with rods. Invest Ophthalmol Vis Sci 49:1116-1125.

Dunford R, Land EJ, Rozanowska M, Sarna T, Truscott TG (1995) Interaction of melanin with carbon- and oxygen-centered radicals from methanol and ethanol. Free Radic Biol Med 19:735-740.

Gao G, Li Y, Fant J, Crosson CE, Becerra SP, Ma JX (2002) Difference in ischemic regulation of vascular endothelial growth factor and pigment epithelium--derived factor in brown norway and sprague dawley rats contributing to different susceptibilities to retinal neovascularization. Diabetes 51:1218-1225.

Geller S, Krowka R, Valter K, Stone J (2006) Toxicity of hyperoxia to the retina: Evidence from the mouse. Adv Exp Med Biol 572:425-437.

Nixon PJ, Bui BV, Armitage JA, A.J. V (2001) The contribution of cone responses to rat electroretinograms. Clin Exp Ophthalmol 29:193-196.

Noell WK (1955) Visual cell effects of high oxygen pressures. Fed Proc 14:107-108.

Okoye G, Zimmer J, Sung J, Gehlbach P, Deering T, Nambu H, Hackett S, Melia M, Esumi N, Zack DJ, Campochiaro PA (2003) Increased expression of brain-derived neurotrophic factor preserves retinal function and slows cell death from rhodopsin mutation or oxidative damage. J Neurosci 23:4164-4172.

Padnick-Silver L, Kang Derwent JJ, Giuliano E, Narfstrom K, Linsenmeier RA (2006) Retinal oxygenation and oxygen metabolism in abyssinian cats with a hereditary retinal degeneration. Invest Ophthalmol Vis Sci 47:3683-3689.

Rozanowska M, Sarna T, Land EJ, Truscott TG (1999) Free radical scavenging properties of melanin interaction of eu- and pheo-melanin models with reducing and oxidising radicals. Free Radic Biol Med 26:518-525.

Smit-McBride Z, Oltjen SL, Lavail MM, Hjelmeland LM (2007) A strong genetic determinant of hyperoxia-related retinal degeneration on mouse chromosome 6. Invest Ophthalmol Vis Sci 48:405-411.

Stone J, Maslim J, Valter-Kocsi K, Kyle Mervin, Bowers F, Chu Y, Barnett N, Provis J, Lewis G, Fisher SK (1999) Mechanisms of photoreceptor death and survival in mammalian retina. Prog Ret Eye Res 18:689-735.

van Wijngaarden P, Brereton HM, Coster DJ, Williams KA (2007) Genetic influences on susceptibility to oxygen-induced retinopathy. Invest Ophthalmol Vis Sci 48:1761-1766.

van Wijngaarden P, Coster DJ, Brereton HM, Gibbins IL, Williams KA (2005) Strain-dependent differences in oxygen-induced retinopathy in the inbred rat. Invest Ophthalmol Vis Sci 46:1445-1452.

Walsh N, Bravo-Nuevo A, Geller S, Stone J (2004) Resistance of photoreceptors in the c57bl/6-c2j, c57bl/6j, and balb/cj mouse strains to oxygen stress: Evidence of an oxygen phenotype. Curr Eye Res 29:441-447.

Wellard J, Lee D, Valter K, Stone J (2005) Photoreceptors in the rat retina are specifically vulnerable to both hypoxia and hyperoxia. Visual Neuroscience 22:222-229.

Yamada H, Yamada E, Hackett SF, Ozaki H, Okamoto N, Campochiaro PA (1999) Hyperoxia causes decreased expression of vascular endothelial growth factor and endothelial cell apoptosis in adult retina. J Cell Physiol 179:149-156.

Ye T, Simon JD, Sarna T (2003) Ultrafast energy transfer from bound tetra (4-n,n,n,n-trimethylanilinium) porphyrin to synthetic dopa and cysteinyldopa melanins. Photochem Photobiol 77:1-4.

Yu D-Y, Cringle SJ, Su E-N, Yu PK (2000) Intraretinal oxygen levels before and after photoreceptor loss in the rcs rat. Invest Ophthalmol Vis Sci 41:3999-4006.

Yu D-Y, Cringle S, Valter K, Walsh N, Lee D, Stone J (2004) Photoreceptor death, trophic factor expression, retinal oxygen status, and photoreceptor function in the p23h rat. Invest Ophthalmol Vis Sci 45:2013-2019.

Zadlo A, Rozanowska MB, Burke JM, Sarna TJ (2007) Photobleaching of retinal pigment epithelium melanosomes reduces their ability to inhibit iron-induced peroxidation of lipids. Pigment Cell Res 20:52-60.

Zareba M, Sarna T, Szewczyk G, Burke JM (2007) Photobleaching of melanosomes from retinal pigment epithelium: Ii. Effects on the response of living cells to photic stress. Photochem Photobiol 83:925-930.

Zhang X, Erb C, Flammer J, Nau WM (2000) Absolute rate constants for the quenching of reactive excited states by melanin and related 5,6-dihydroxyindole metabolites: Implications for their antioxidant activity. Photochem Photobiol 71:524-533.